

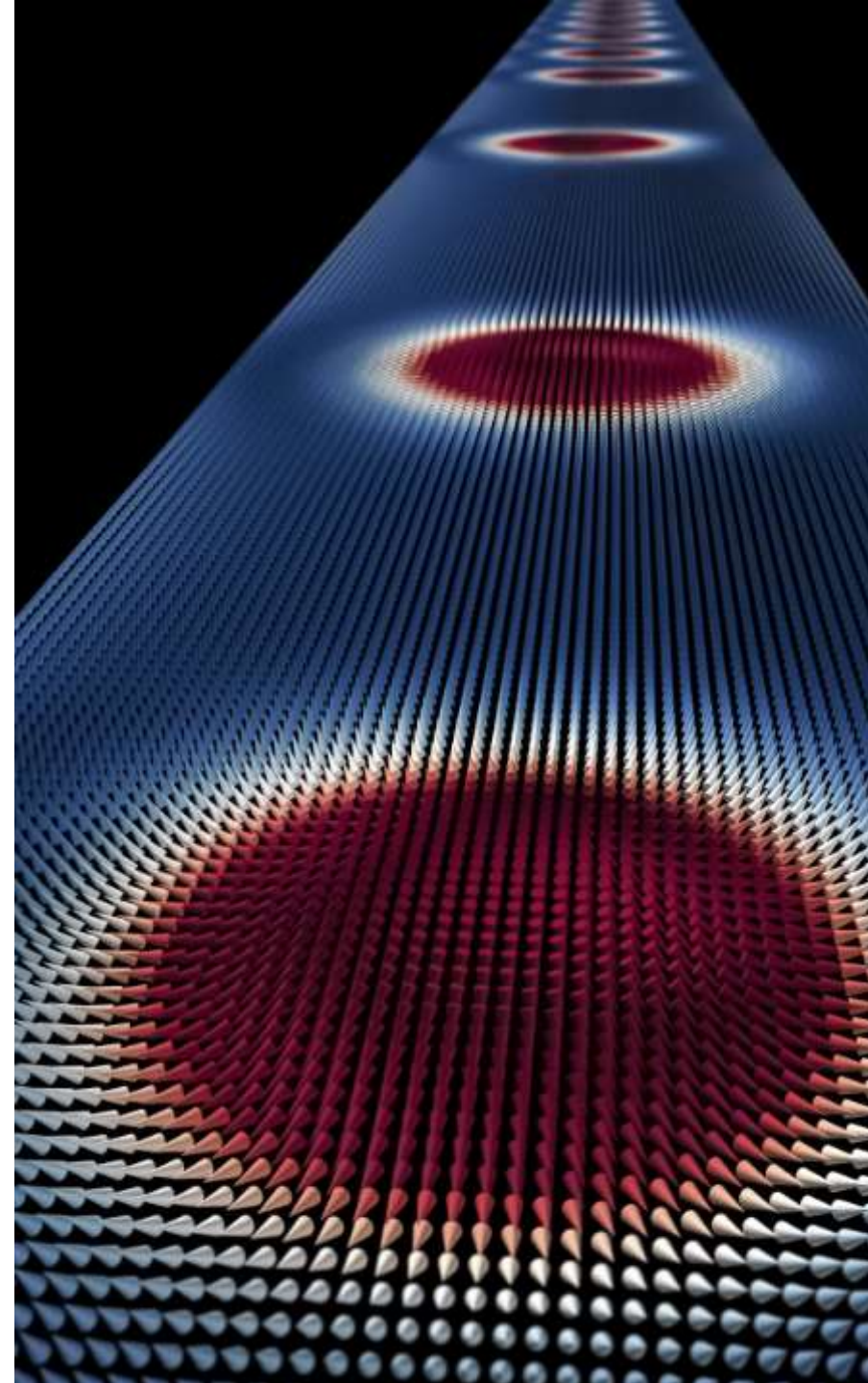


THALES



Magnetic Skyrmions (stabilized by interfacial DMI in thin metallic multilayers)

NICOLAS REYREN



Acknowledgments



Unité Mixte de Physique CNRS/Thales, France

F. Ajejas, **K. Bouzehouane**, **S. Collin**, J.-Y. Chauleau*, **V. Cros**, **A. Fert**,
K. Garcia^o, W. Legrand, D. Maccariello, C. Moreau-Luchaire,
N. Reyren, J. Sampaio^x, Y. Sassi, A. Vecchiola



SOLEIL Synchrotron, France (XRMS)

J.-Y. Chauleau*, **N. Jaouen**, H. Popescu



Swiss Light Source - PSI, Switzerland (STXM)

C. Moutafis⁺, **J. Raabe**, C.A.F. Vaz, P. Warnicke, P. Wohlhütter



University of Glasgow, UK (Lorentz TEM)

S. Hughes, K. Fallon, S. McFadzean, **S. McVitie**



Magnetic skyrmions

- topology and definitions
- Interfacial Dzyaloshinskii-Moriya interaction (DMI) and other energies - *reminders*

QUESTIONS

Technological motivation and technical means

- Skyrmions in metallic multilayers – principles and characterizations
- Means of observations of isolated skyrmions: STXM, L-TEM, MFM, etc.

QUESTIONS

External control of magnetic skyrmions

- Stability and nucleation means
- Skyrmion motion

QUESTIONS

- Skyrmion electrical detection
- Hybrid chirality (XRMS and L-TEM) and consequences

QUESTIONS

- Conclusion

BONUS - Perspectives for SAF systems
Detailed model for better predictions and experimental fit

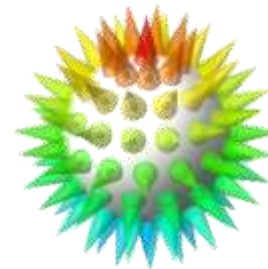
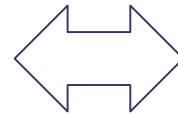
What is a Magnetic Skyrmion?

Remarkable properties:

- Topology different than the ferromagnetic state (“topological protection”):

$$N_{sk} = \frac{1}{4\pi} \int_{uc} \hat{m} \cdot (\partial_x \hat{m} \times \partial_y \hat{m}) dx dy = \pm 1$$

3D spin texture lying in 2D plane

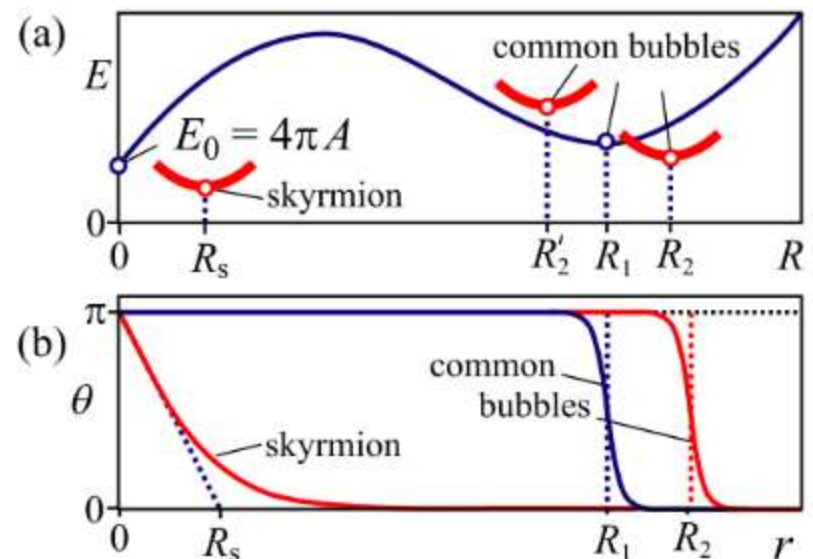


K. Everschor, thesis (2012)

- Behaves like a particle: soliton
- Size as small as a few crystalline lattice parameters

→ “...the smallest conceivable micromagnetic configuration.”

N. S. Kiselev et al, *J. Phys. D: Appl. Phys.* **44**, 392001 (2011)

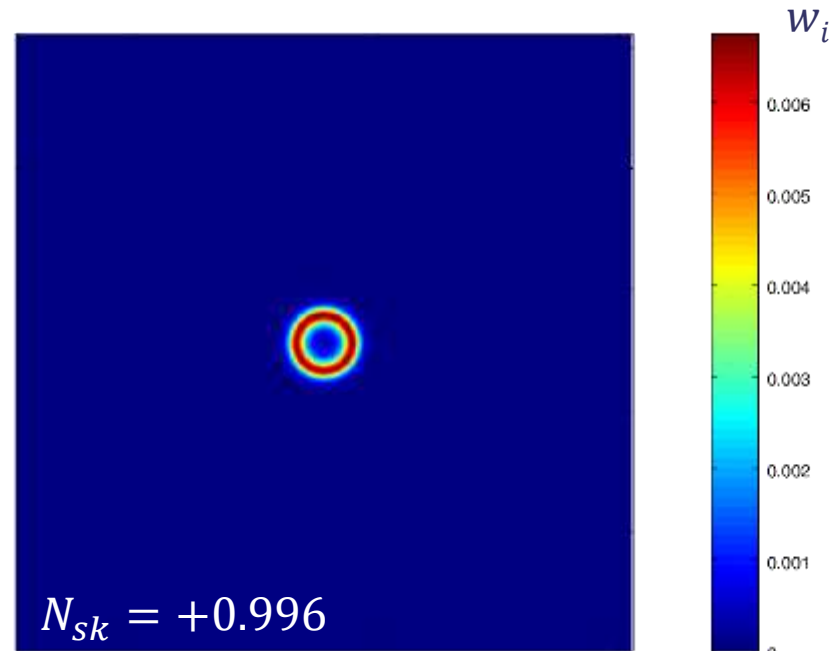
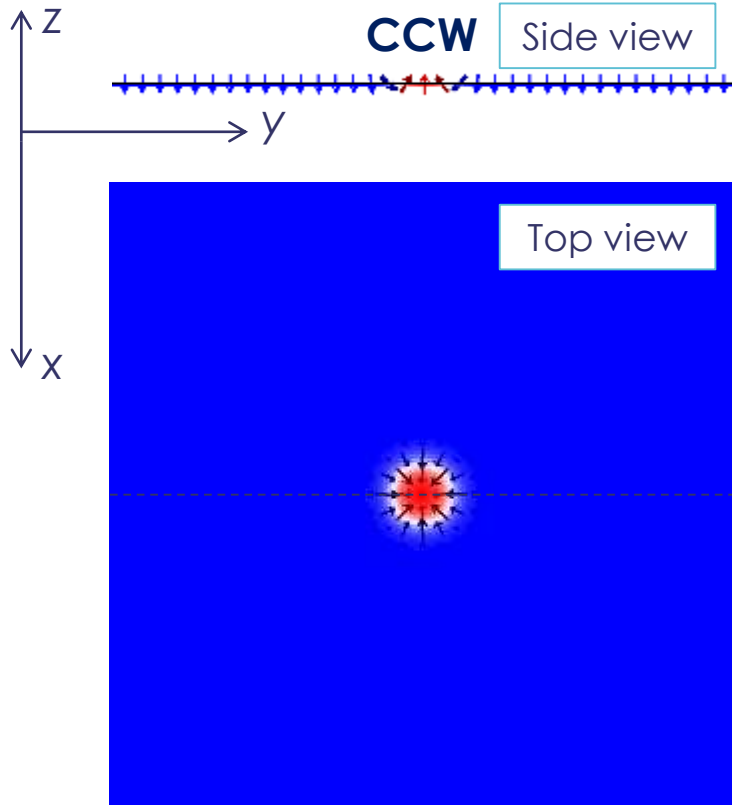


Topology of the Magnetic Skyrmions

The winding or skyrmion number

► Topology different than the ferromagnetic state (“topological protection”):

$$N_{sk} = \frac{1}{4\pi} \int_{uc} \underbrace{\hat{m} \cdot (\partial_x \hat{m} \times \partial_y \hat{m})}_{w_i} dx dy = \pm 1$$



magnetization

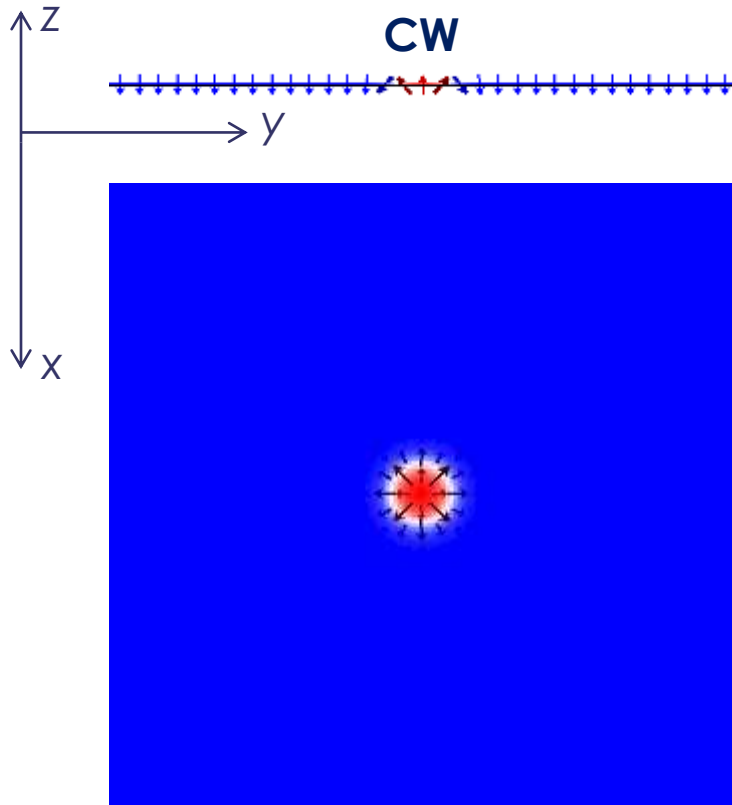
whirling

Topology of the Magnetic Skyrmions

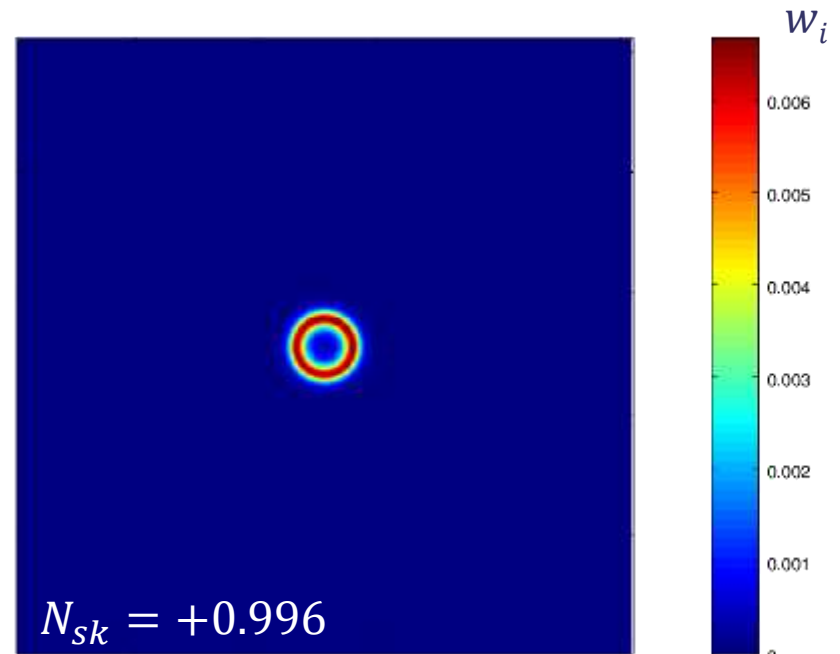
The winding or skyrmion number

► Topology different than the ferromagnetic state (“topological protection”):

$$N_{Sk} = \frac{1}{4\pi} \int_{uc} \underbrace{\hat{m} \cdot (\partial_x \hat{m} \times \partial_y \hat{m})}_{w_i} dx dy = \pm 1$$



magnetization



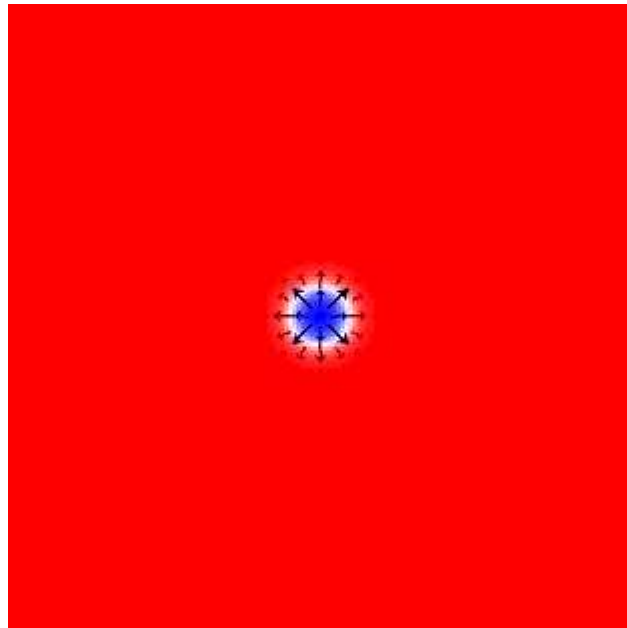
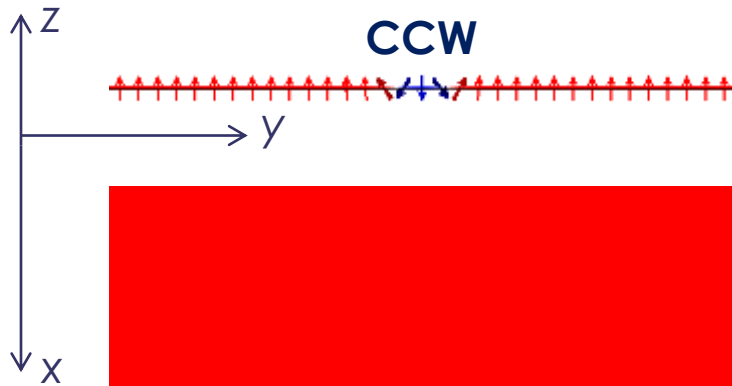
whirling

Topology of the Magnetic Skyrmions

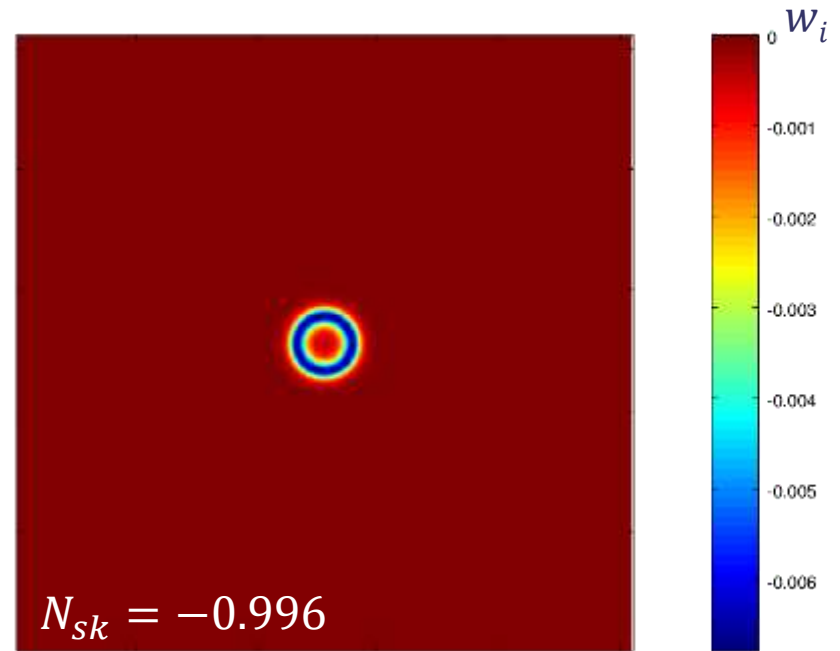
The winding or skyrmion number

► Topology different than the ferromagnetic state (“topological protection”):

$$N_{Sk} = \frac{1}{4\pi} \int_{uc} \underbrace{\hat{m} \cdot (\partial_x \hat{m} \times \partial_y \hat{m})}_{w_i} dx dy = \pm 1$$



magnetization



$$N_{Sk} = -0.996$$

whirling

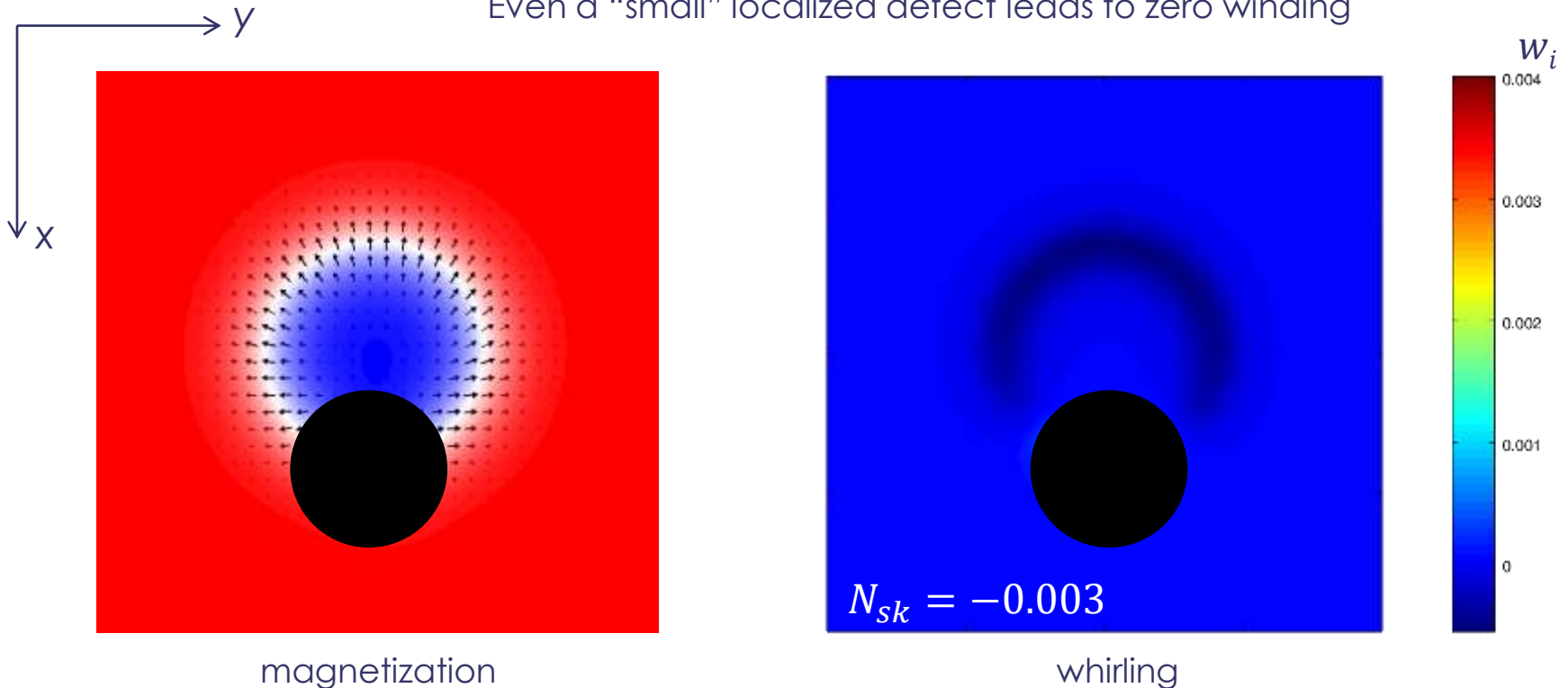
Topology of the Magnetic Skyrmions

The winding or skyrmion number

► Topology different than the ferromagnetic state (“topological protection”):

$$N_{sk} = \frac{1}{4\pi} \int_{uc} \underbrace{\hat{m} \cdot (\partial_x \hat{m} \times \partial_y \hat{m})}_{w_i} dx dy = \pm 1$$

Even a “small” localized defect leads to zero winding



Topology of the Magnetic Skyrmions

Winding number, vorticity, helicity, polarity, etc.

➤ Topology different than the ferromagnetic state (“topological protection”):

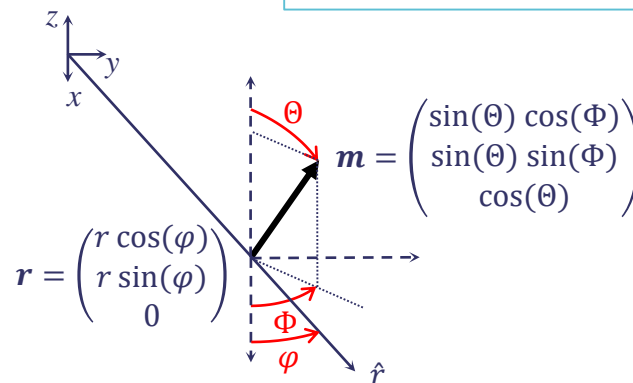
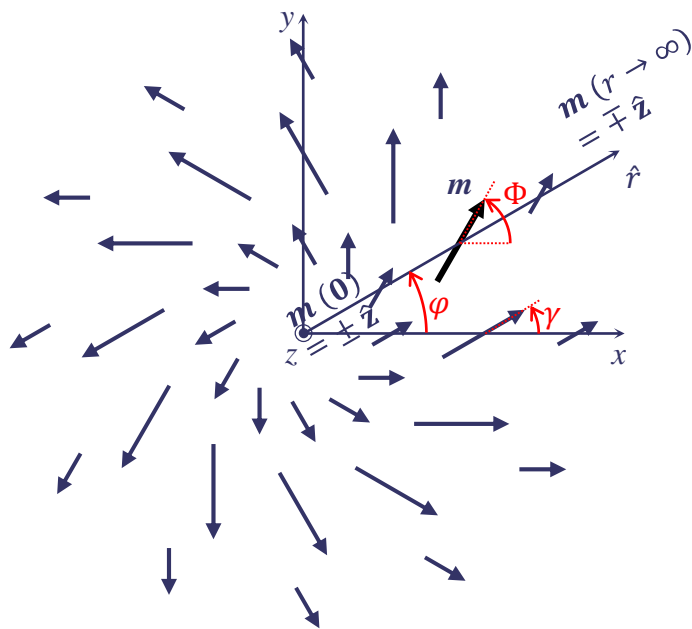
$$N_{Sk} = \frac{1}{4\pi} \int_{uc} \hat{m} \cdot (\partial_x \hat{m} \times \partial_y \hat{m}) dx dy = \pm 1$$

➤ If an axial symmetry (as expected for skyrmions) is considered:

$$N_{Sk} = \frac{1}{4\pi} \int_0^\infty dr \int_0^{2\pi} d\varphi \frac{d\Theta(r)}{dr} \frac{d\Phi(\varphi)}{d\varphi} \sin(\Theta(r)) = \frac{1}{4\pi} \underbrace{[\cos(\Theta(r))]_0^\infty}_{-2P} \underbrace{[\Phi(\varphi)]_0^{2\pi}}_{2\pi V}$$

$\Phi(\varphi) = V\varphi + \gamma$
 “core polarity” “vorticity” “helicity”
 “chirality”

For skyrmions $V = 1$



Topology of the Magnetic Skyrmions

Skymion zoo:

► If an axial symmetry is considered:

$$N_{Sk} = \frac{1}{4\pi} \int_0^\infty dr \int_0^{2\pi} d\varphi \frac{d\Theta(r)}{dr} \frac{d\Phi(\varphi)}{d\varphi} \sin(\Theta(r)) = \frac{1}{4\pi} \overbrace{[\cos(\Theta(r))]_0^\infty}^{-2P} \overbrace{[\Phi(\varphi)]_0^{2\pi}}^{2\pi V} \Phi(\varphi) = V\varphi + \overbrace{\gamma}^{\text{“chirality”}}$$

N. Nagaosa and Y. Tokura, *Nature Nanotechnol.* **8**, 899 (2013)

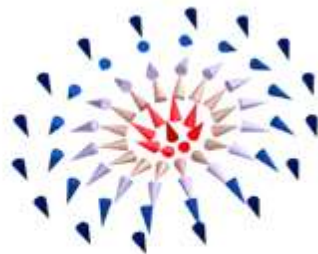
$$\gamma = 0$$

$$\gamma = \frac{\pi}{2}$$

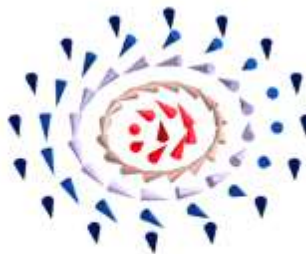
$$\gamma = \pi$$

$$\gamma = \frac{3\pi}{2}$$

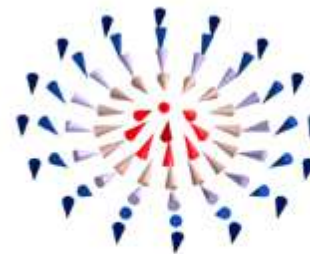
$$P = +1$$



CW Néel



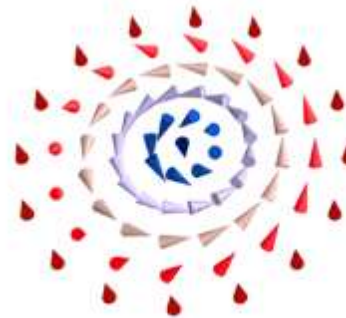
Bloch



$$P = -1$$



CCW Néel



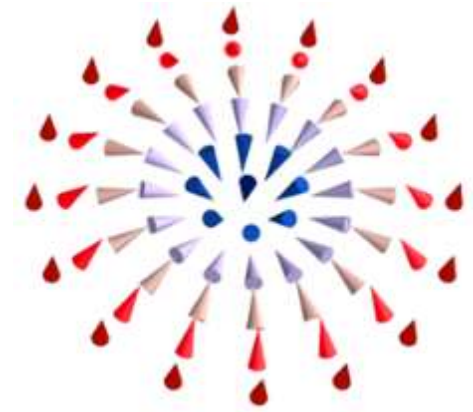
Is topology enough to define a skyrmion?

Remarkable properties:

- Topology different than the ferromagnetic state (“topological protection”):

$$N_{Sk} = \frac{1}{4\pi} \int_{uc} \hat{m} \cdot (\partial_x \hat{m} \times \partial_y \hat{m}) dx dy = \pm 1$$

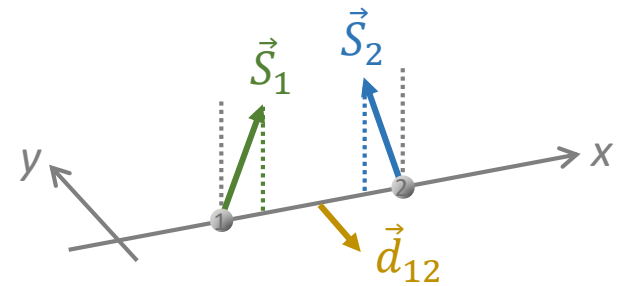
- Behaves like a particle (soliton)
- Size as small as a few crystalline lattice parameters



More stringent definition:

- Not stabilized by dipolar coupling only (unlike classical bubbles)
- Continuous rotation of the magnetization through the core
- Fixed chirality

$$H_{H+DM} = -J \sum (\vec{S}_i \cdot \vec{S}_j) - \sum \vec{d}_{ij} \cdot (\vec{S}_i \times \vec{S}_j)$$



Essential role of Dzyaloshinskii-Moriya interaction

Antisymmetric exchange term:

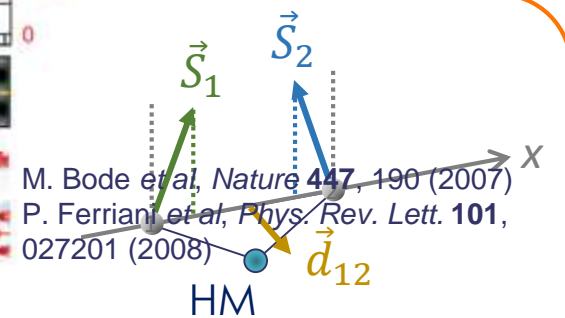
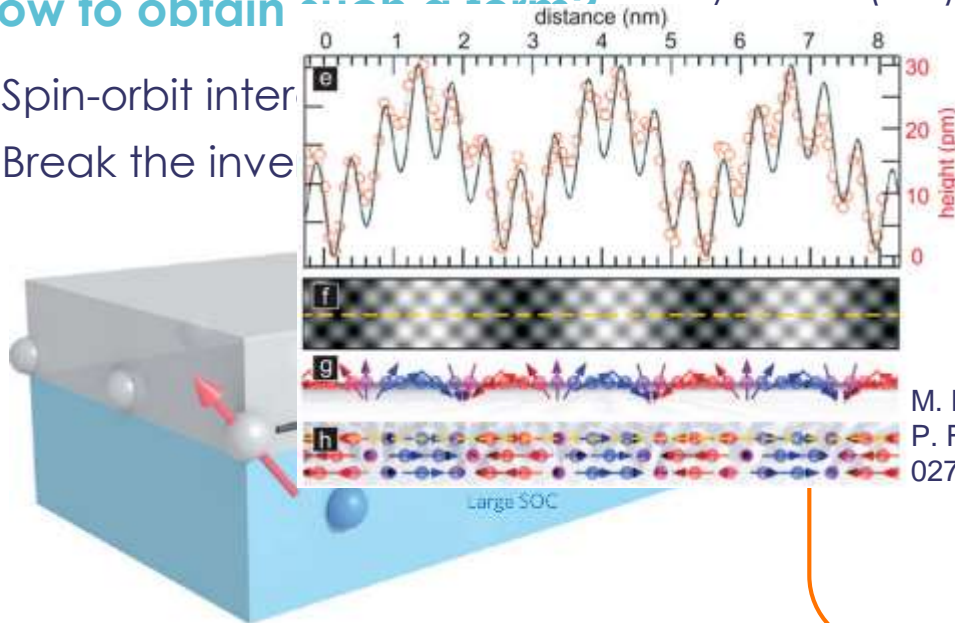
$$H_{H+DM} = \underbrace{-J \sum (\vec{S}_i \cdot \vec{S}_j)}_{\text{Exchange}} - \underbrace{\sum \vec{d}_{ij} \cdot (\vec{S}_i \times \vec{S}_j)}_{\text{DMI}}$$

I. Dzyaloshinskii, *J. Phys. Chem. Solids* **4**, 241 (1958)
 T. Moriya, *Phys. Rev. Lett.* **4**, 228 (1960)

How to obtain

- Spin-orbit inter
- Break the inve

SP-STM of a Mn monolayer on W(110):



Interfacial case

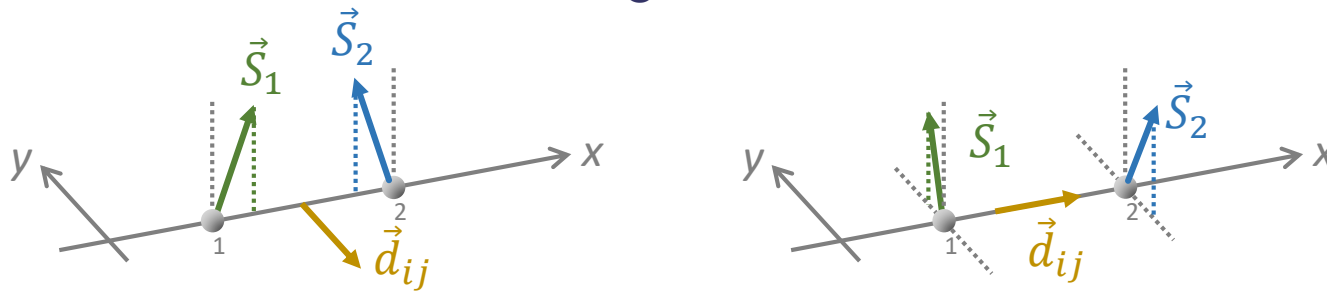
A. Fert *et al*, *Nat. Nanotechnol.* **8**, 152 (2013)

A. Fert, *Mater. Sci. Forum* **59-60**, 439 (1990)

Magnetic Skyrmions stabilized by DMI

Does topology change with DM vector direction?

$$H_{H+DM} = \underbrace{-J \sum (\vec{S}_i \cdot \vec{S}_j)}_{\text{Exchange}} - \underbrace{\sum \vec{d}_{ij} \cdot (\vec{S}_i \times \vec{S}_j)}_{\text{DMI}}$$

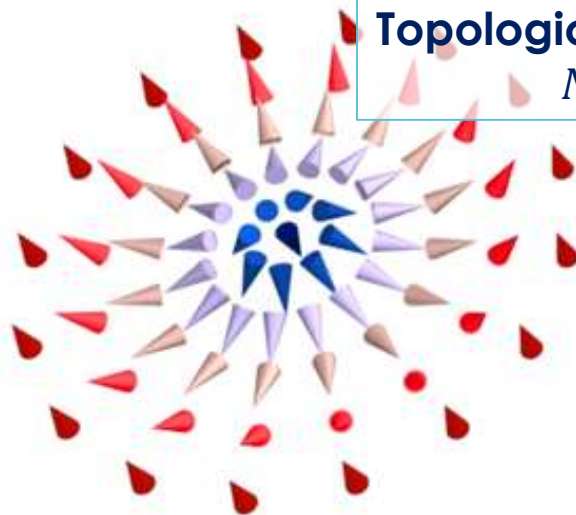


Topologically equivalent:

$$N_{sk} = -1$$

$$P = -1$$

$$\gamma = 0$$

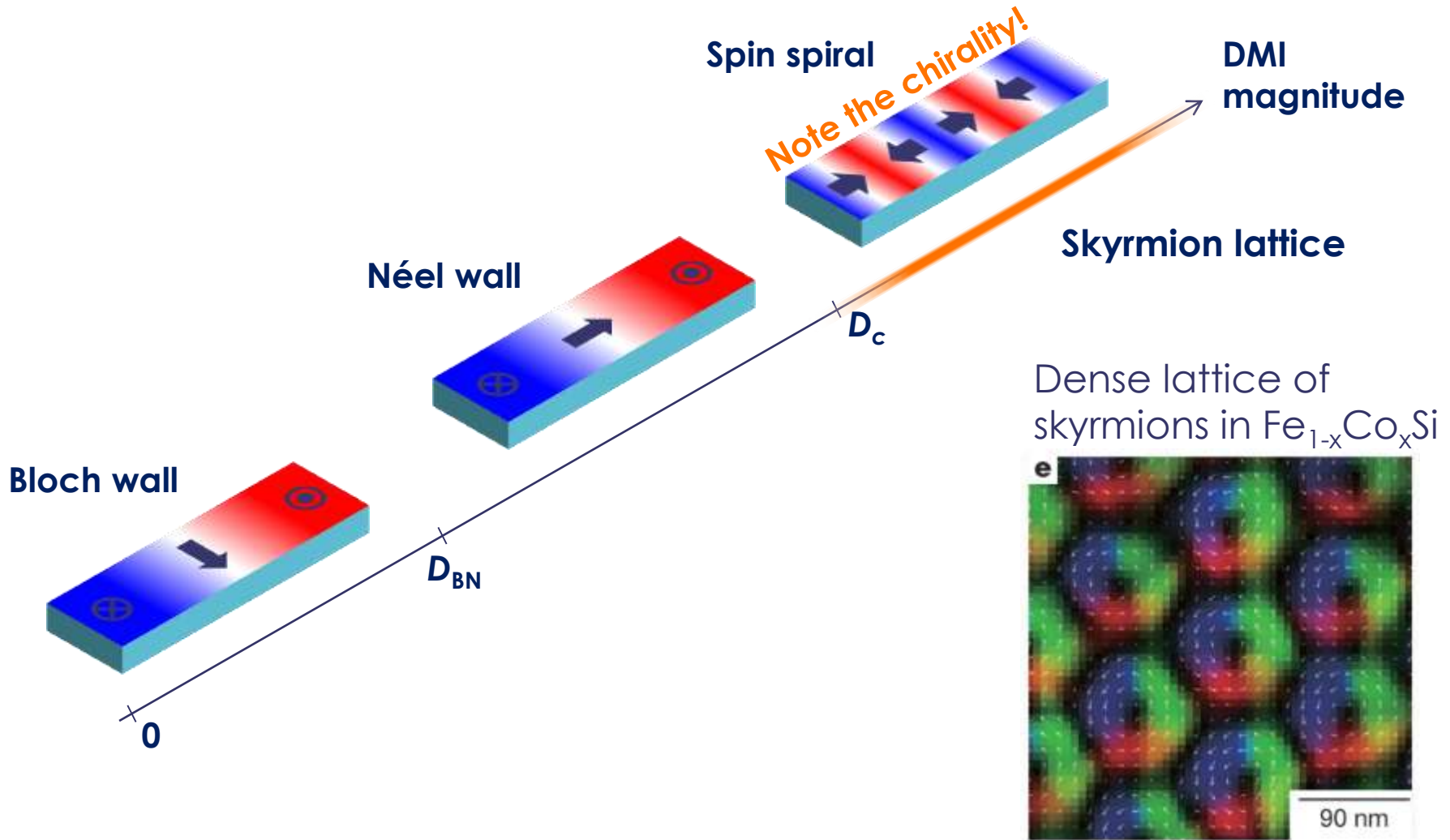


$$P = -1$$

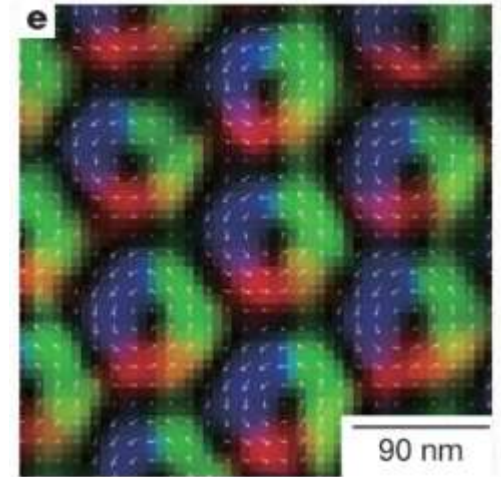
$$\gamma = \frac{\pi}{2}$$



But different exchange DMI energy for a given type of DMI!



Dense lattice of skyrmions in $Fe_{1-x}Co_xSi$

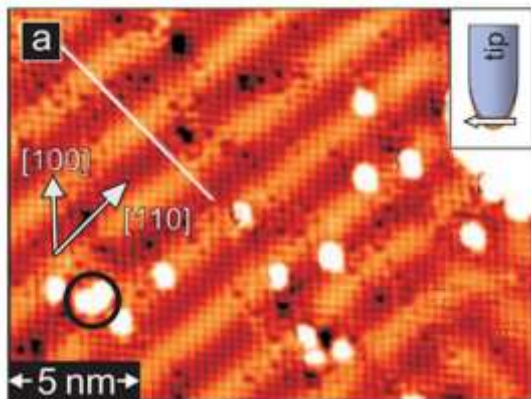


X. Z. Yu et al, *Nature* **465**, 901 (2010)

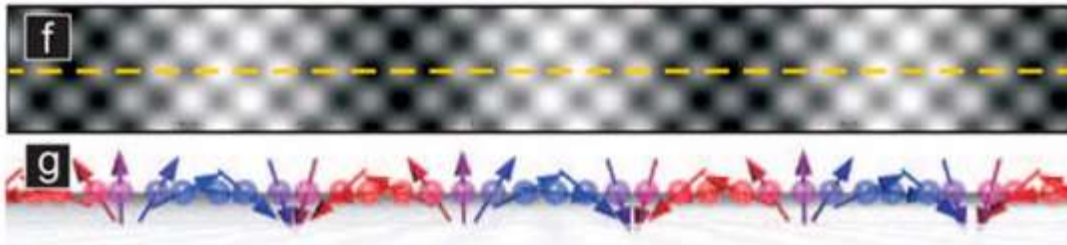
Dzyaloshinskii-Moriya Interaction (Strong Case $D > D_c$)

Consequences of the DMI

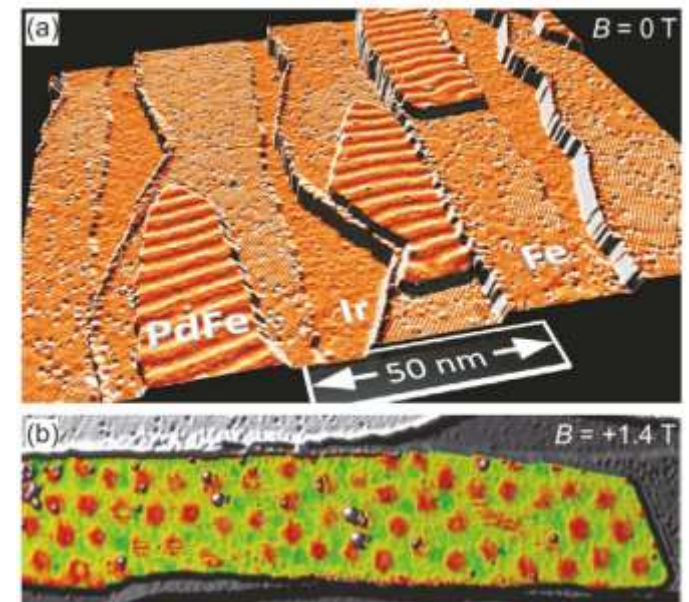
- Very strong DMI: Domain wall energy density ($\sigma_{DW} = 4\sqrt{AK} - \pi D$) is negative
- stabilize spin spirals, skyrmions, etc.



SP-STM observation of spin spirals in a monolayer of Mn on W (001)...



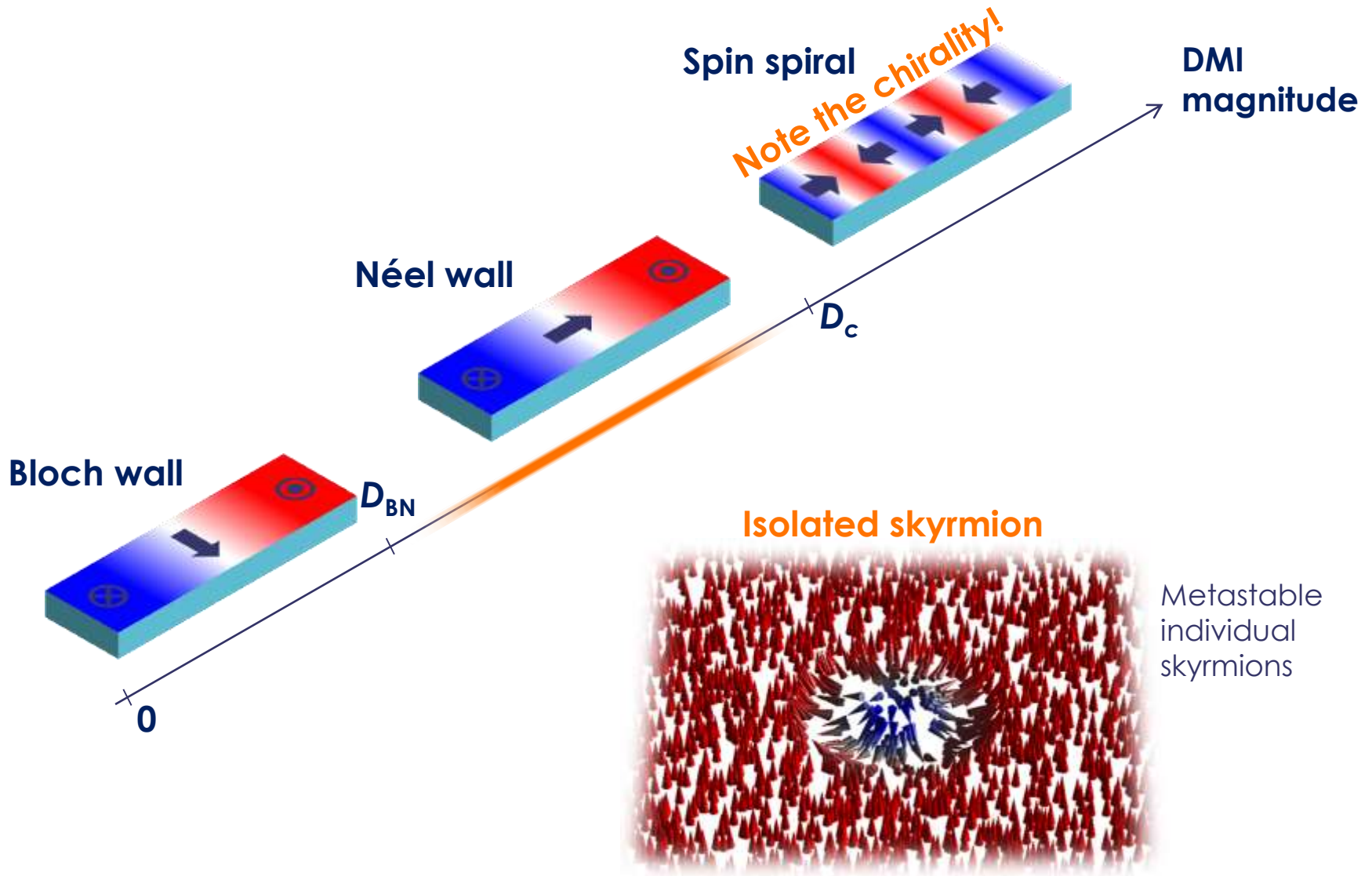
P. Ferrianni *et al*, *Phys. Rev. Lett.* **101**, 027201 (2008)



...and skyrmions in
Ir(111) | Fe (1 ML) | Pd (1 ML)

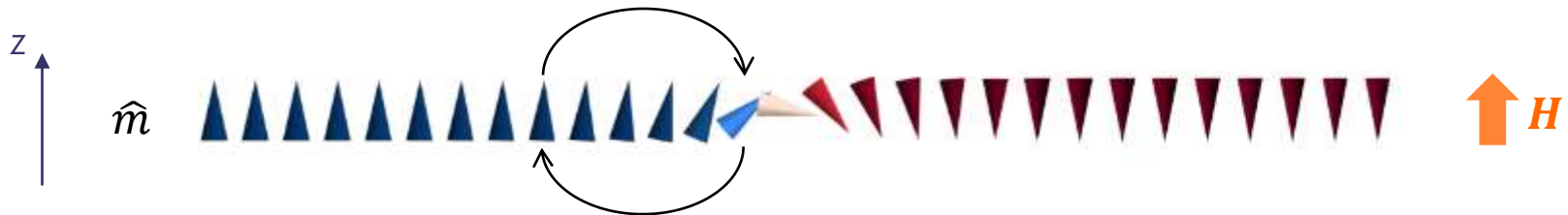
K. von Bergmann *et al*, *J. Phys.: Condens. Matter* **26**, 394002 (2014)

Dzyaloshinskii-Moriya Interaction



Other Energy Terms at Play: Anisotropy and Zeeman Energies

- \hat{m} is continuous in space (micromagnetic approximation):
 - discrete differences turn into derivatives.
- Different interactions favour different magnetic configurations:
 - the magnetic textures result from delicate energy balance.
- The dipolar energy (or demagnetizing “demag” energy) is the tricky one! (Computationally expensive, non-local, ...)

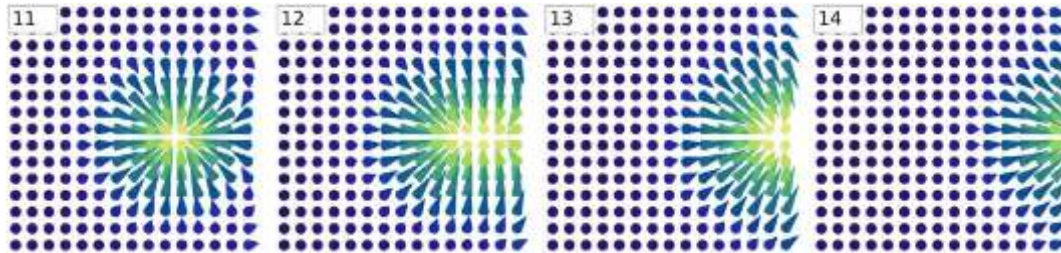


	Heisenberg exchange	Dzyaloshinskii-Moriya interaction	Perp. anisotropy	Zeeman
Atomistic formulation	$J \sum (\vec{S}_i \cdot \vec{S}_j)$	$\sum \vec{d}_{ij} \cdot (\vec{S}_i \times \vec{S}_j)$	$K_u \sum (\hat{z} \cdot \vec{S}_i)^2$	$\mu \sum (\vec{H} \cdot \vec{S}_i)$
Micromagnetic energy density	$E_A = A \left(\frac{\partial m_i}{\partial x_j} \right)^2$	$E_D = D(m_z \text{div } \hat{m} - (\hat{m} \cdot \nabla)m_z)$	$E_K = K_u(m_z)^2$	$E_Z = M_s \mu_0 \vec{H} \cdot \hat{m}$
	$E(\uparrow \uparrow) < E(\uparrow \searrow)$	$E(\uparrow \searrow) < E(\uparrow \uparrow)$	$E(\uparrow) < E(\searrow)$	$E(\uparrow) < E(\downarrow)$

Topological Protection?

Mathematical concept in the continuous magnetization limit

- Impossible to unwind an isolated skyrmion in an infinite film.
- Possibility at edges of magnetic films (1D demo)



In practice, there is a barrier of a few J at the edge.

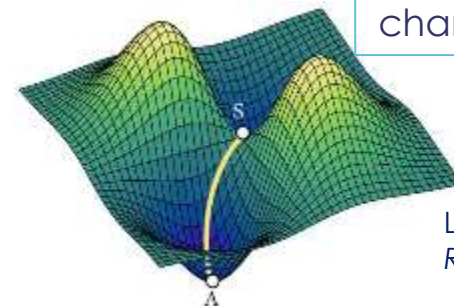
L. Desplat *et al*,
Phys. Rev. B **98**, 134407 (2018)

Real system is “discrete”



Finite exchange energy

- Even in the micromagnetic limit,
the energy barrier is expected to
be finite and approx. equal to $8\pi At$.



“Attempt rate” might
change with topology

L. Desplat *et al*, *Phys.*
Rev. B **98**, 134407 (2018)

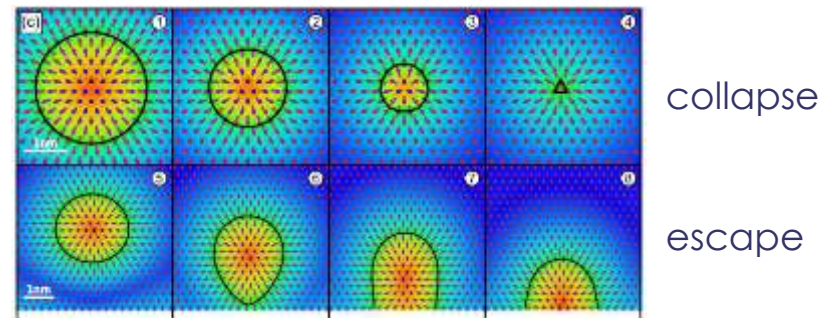
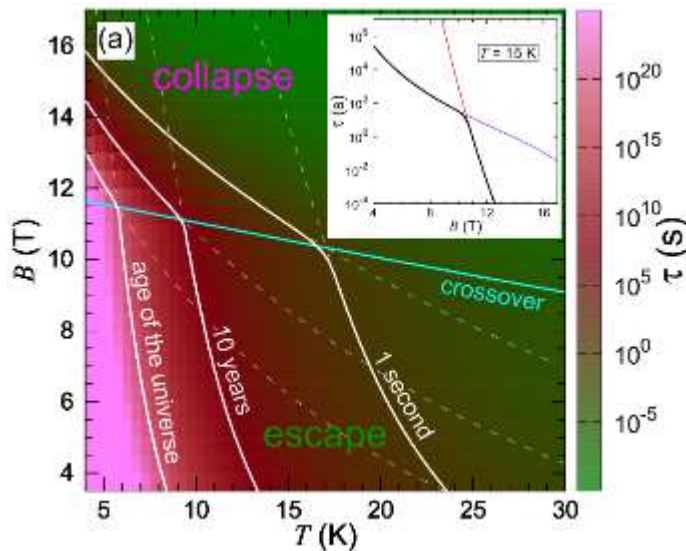
S. Rohart *et al*, *Phys. Rev. B* **93**, 214412 (2016)
F. Büttner *et al*, *Sci. ReP.* **8**, 4464 (2018)

Arrhenius expression for transition rate

$$\frac{1}{\tau} = \underbrace{\nu(T, B, \dots)}_{\text{Attempt frequency}} \exp\left(-\frac{\underbrace{\Delta E}_{\text{Energy barrier}}}{k_B T}\right)$$

What is the attempt frequency?

- It depends on the different annihilation paths (in the energy landscape), and hence on the detailed annihilation conditions (e.g. proximity to the edge in a skyrmion racetrack).



Lifetime of a skyrmion calculated (*ab initio*) in a Pd/Fe/Ir(111) racetrack (atomistic, fcc stacking).

P. S. Bessarab *et al*, *Sci. Rep.* **8**, 3433 (2018)



My Question: "How to distinguish chiral bubble from skyrmions?"

The topology was already discussed at the "magnetic bubble time"

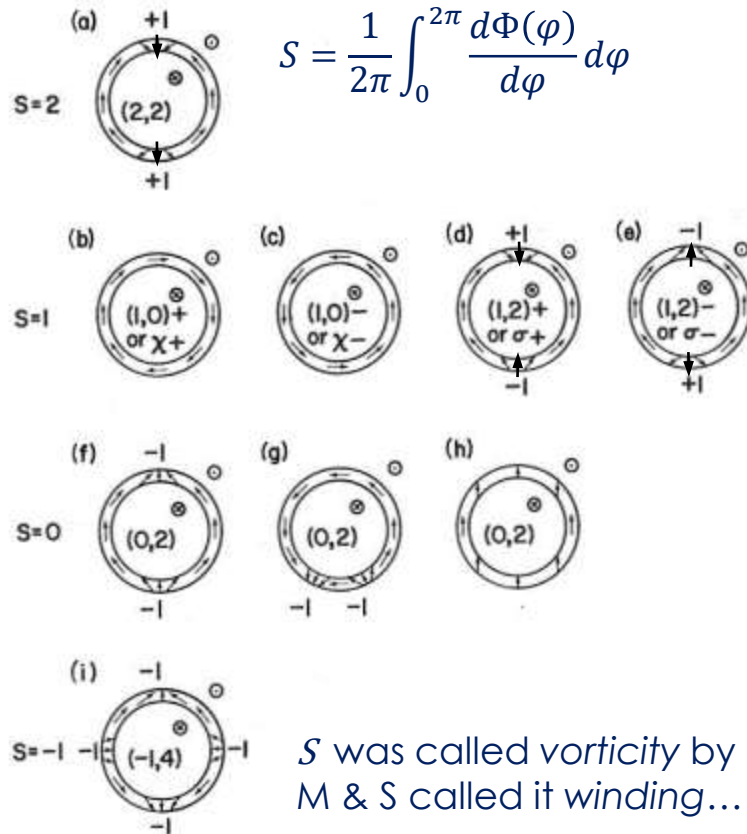
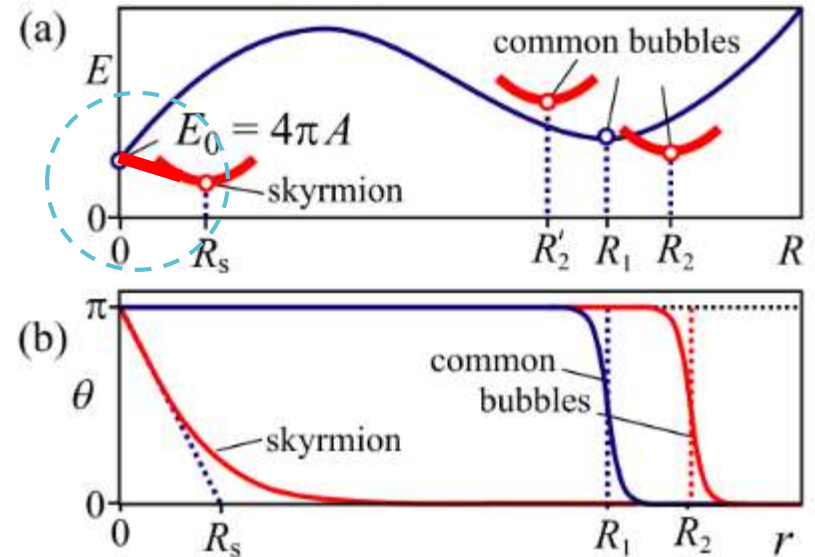


Fig. 8.5. Schematic illustrations of selected bubble wall states viewed from the +z direction (bias-field direction). Conventional state notation is indicated inside the bubble, and the winding number S [Eq. (8.22)] is given on the left. ± 1 beside each Bloch line is the handedness index [Eq. (8.23)].

A. P. Malozemoff & J. C. Slonczewski,

"Magnetic Domain Walls in Bubble Materials", Academic Press, 1979.

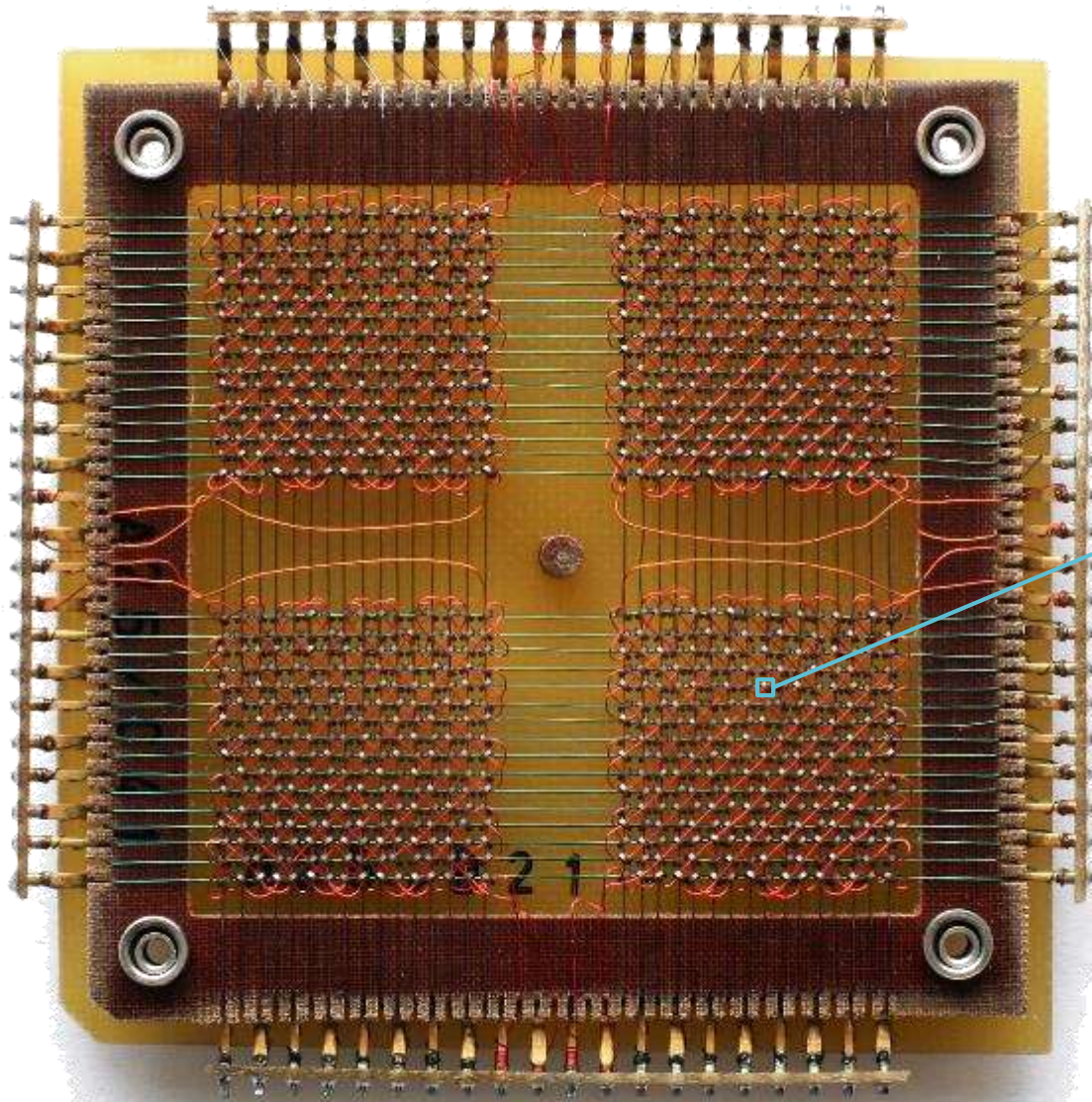


N. S. Kiselev *et al*, *J. Phys. D: Appl. Phys.* **44**, 392001 (2011)

Roughly:
 $dE/dR < 0$ needs an energy
 term that decreases with
 radius for small radius: the DMI!

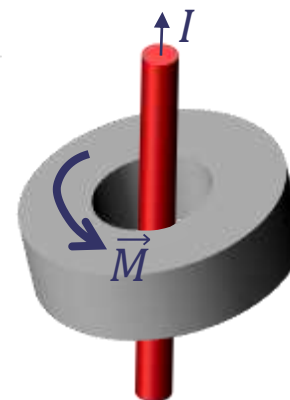
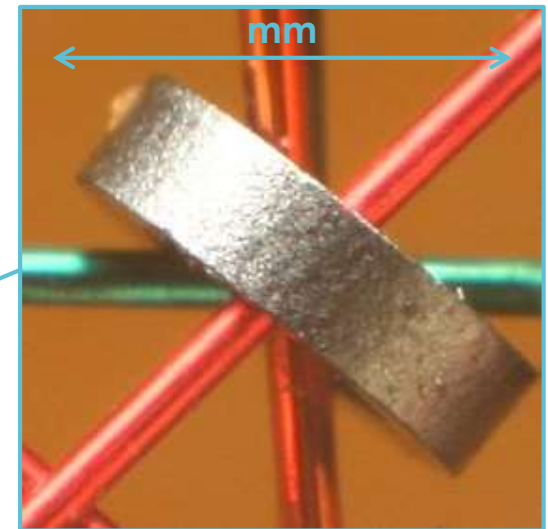
Technological motivation

Magnetic Memories 1955~1975



A 32 x 32 core memory plane storing 1024 bits of data.

Reach 32 kB at 1 MHz in the 70's.



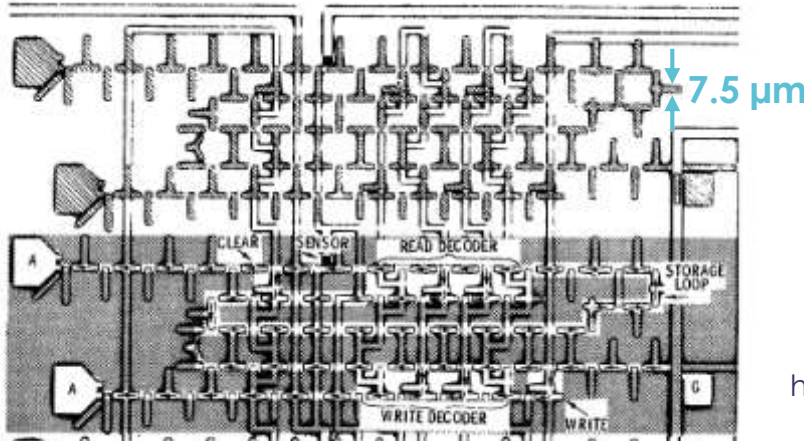
These types of memory were used in place with high level of radiations, e.g. the space shuttle.

Bubble Memories

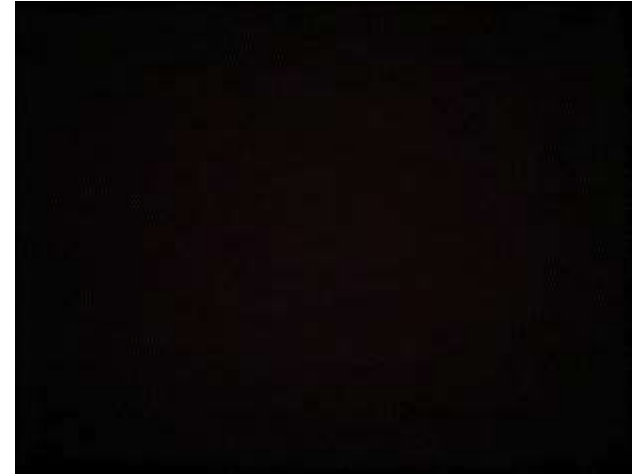
FABRICATION AND OPERATION OF A SELF-CONTAINED BUBBLE DOMAIN MEMORY CHIP*

G.S. Almasi, B.J. Canavello, E.A. Giess, R.J. Hendel, R.E. Horstmann, T.F. Jamba**, G.E. Keefe, J.V. Powers, and L.L. Rosier
IBM Thomas J. Watson Research Center, Yorktown Heights, N.Y. 10598

* Supported in part by NASA contract NAS-8-26671



Demonstration device 1971



<https://www.gsalmasi.com/almasiconsulting/bubbles/chip2.html>



Hitachi 4 Mb
BDN0153
bubble memory
module

Bubble-Memory Board Protects Data In the Face of Adverse Conditions

Magnetic disk media are not designed to operate reliably in many industrial or otherwise-unfriendly work environments. The PCH-3 Bubbl-Board, \$1,257 with 1/2 megabyte of RAM, from the Bubbl-Tec division of PC/M, is aimed at just such difficult applications.

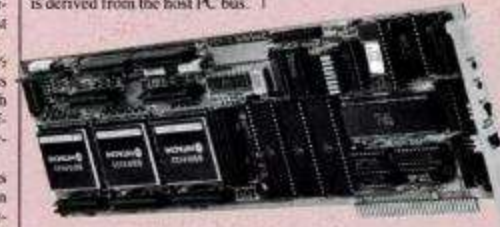
The board provides up to 1 1/2 megabytes of nonvolatile mass storage on a standard full-length PC adapter card, and it is unaffected by dust, smoke, and airborne dirt, Bubbl-Tec says.

Expansion to 6 megabytes is possible with available add-on boards, and removable bubble-cassette capability can be added with Bubbl-Tec's BD-series Bubbl-Dek.

Access time of the PCH-3 system averages below 20 milliseconds, and the effective data transfer rate to and from the bubble device exceeds 190K bits per second. System power is derived from the host PC bus.

List Price: PCH-3 Bubbl-Board, with 1 1/2 Mbytes of on-board storage, \$2,297; with 1 Mbyte, \$1,789; with 1/2 Mbyte, \$1,257. Bubbl-Tec, 6805 Sierra Ct., Dublin, CA 94568, (415) 829-8700.

CIRCLE 429 ON READER SERVICE CARD



Adverse operating conditions that rule out magnetic disk media are less of a problem for the PCH-3 Bubbl Board, from Bubbl-Tec. The board can be configured with up to 1 1/2 megabytes of nonvolatile RAM (\$2,297).

A source of excitement:

Skyrmions on the track

Albert Fert, Vincent Cros and João Sampaio

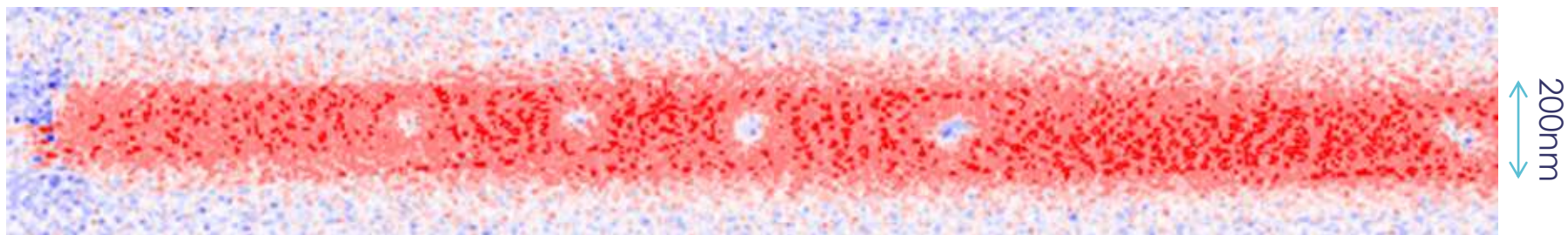
Magnetic skyrmions are nanoscale spin configurations that hold promise as information carriers in ultradense memory and logic devices owing to the extremely low spin-polarized currents needed to move them.

A. Fert *et al*, *Nature Nanotech.* **8**, 152 (2013)



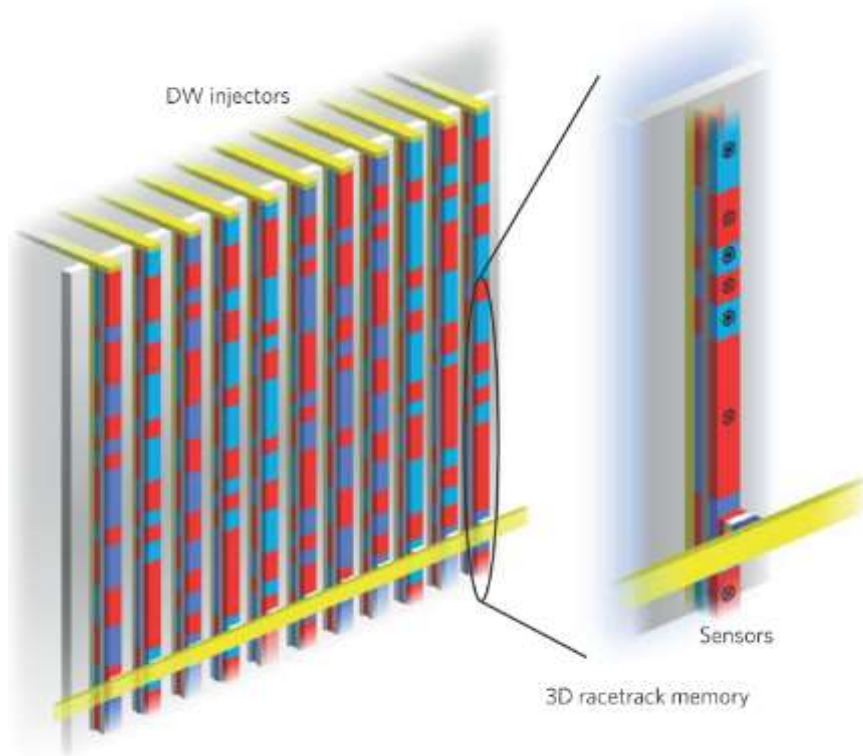
J. Sampaio *et al*, *Nat. Nanotech.* **8**, 839 (2013)

2013-2016, from numerical simulations to actual experiments:

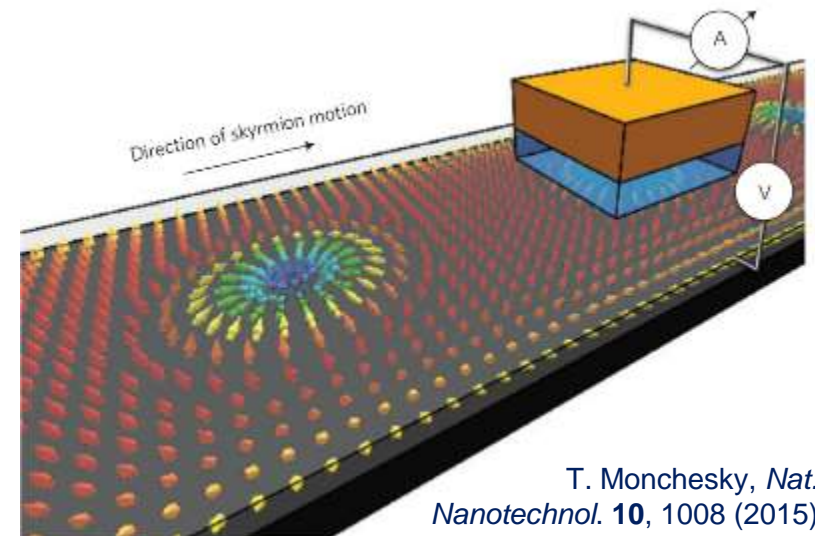


C. Moreau-Luchaire *et al*, *Nat. Nanotech.* **11**, 444 (2016)

Racetrack-memory... a shift register memory



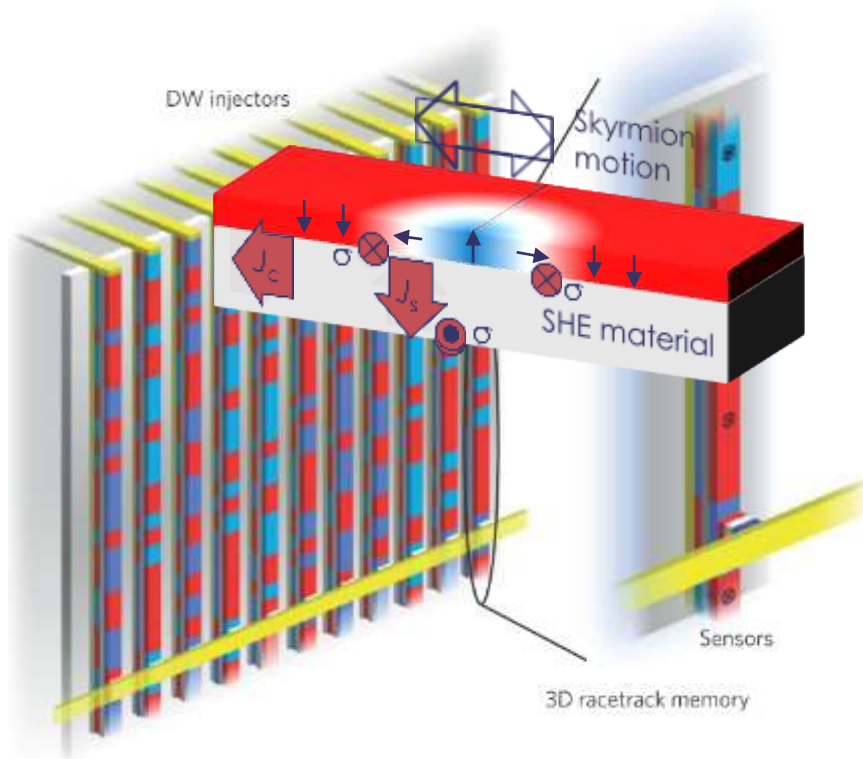
- Hard disk on a chip, no moving parts
- Resistant against vibrations, radiations, etc.
- Simple lithography in 2D
- Possibility of 3D architecture → huge information density
- Speed between HDD and DRAM.



S. Parkin, M. Hayashi, L. Thomas, *Science* **320**, 190 (2008)
S. Parkin, S.-H. Yang, *Nat. Nanotechnol.* **10**, 195 (2015)

T. Monchesky, *Nat. Nanotechnol.* **10**, 1008 (2015)

Racetrack-memory... domains versus skyrmions

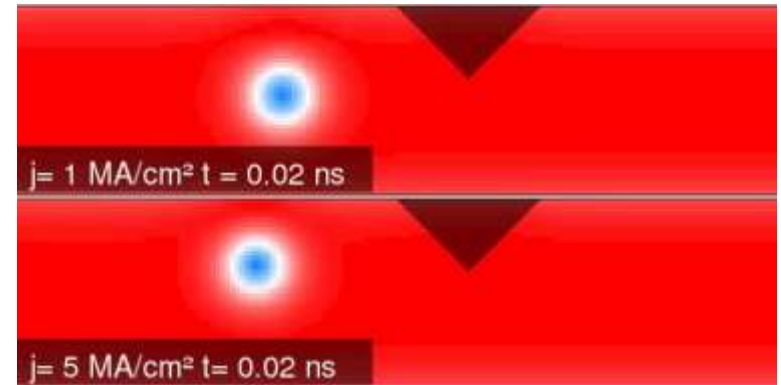


S. Parkin, M. Hayashi, L. Thomas, *Science* **320**, 190 (2008)

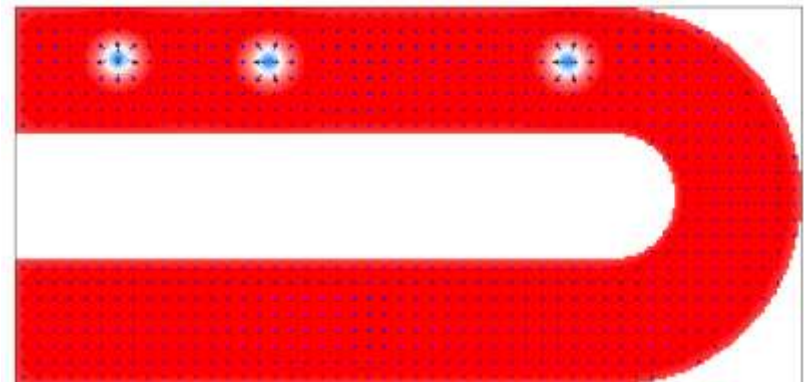
S. Parkin, S.-H. Yang, *Nat. Nanotechnol.* **10**, 195 (2015)

J. Sampaio *et al*, *Nat. Nanotechnol.* **8**, 839 (2013)

➤ Less sensitive to edge defects



➤ Better behavior around sharp turns



Other Type of Devices

Multiple states memory

- Increase memory density.

Logical operation

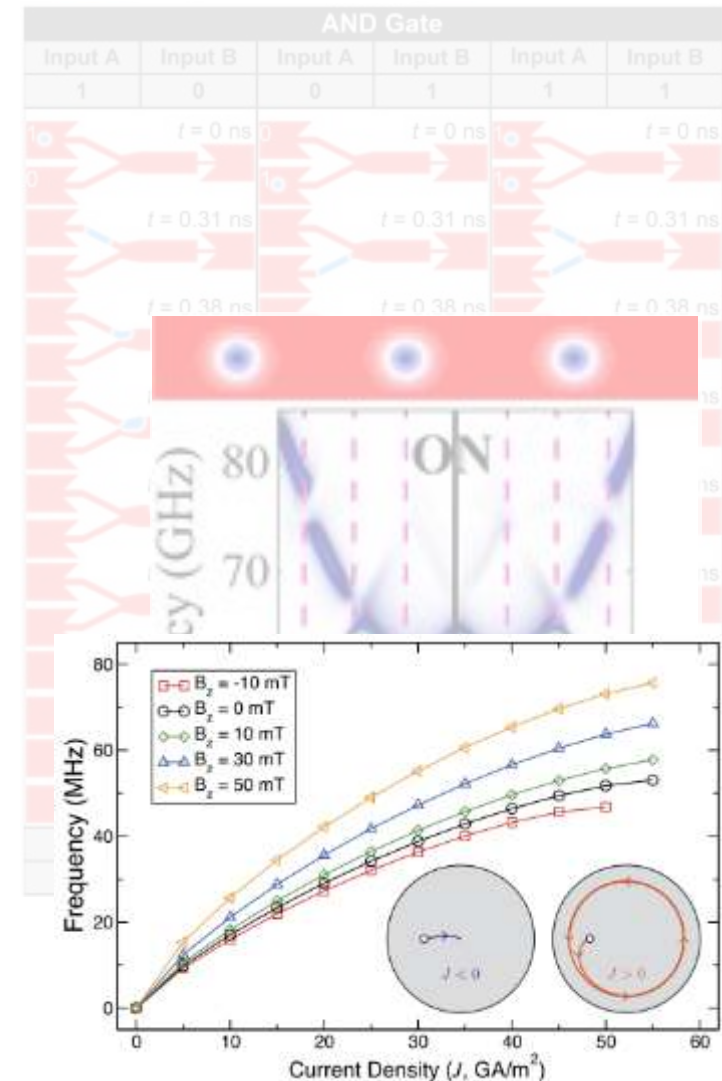
- OR and AND gates are numerically “demonstrated” using skyrmion-domain wall transformations.

Reconfigurable magnonic crystals

- A skyrmion lattice acts as a magnon filter.

Rf sources

- Peculiar modes of excitations.



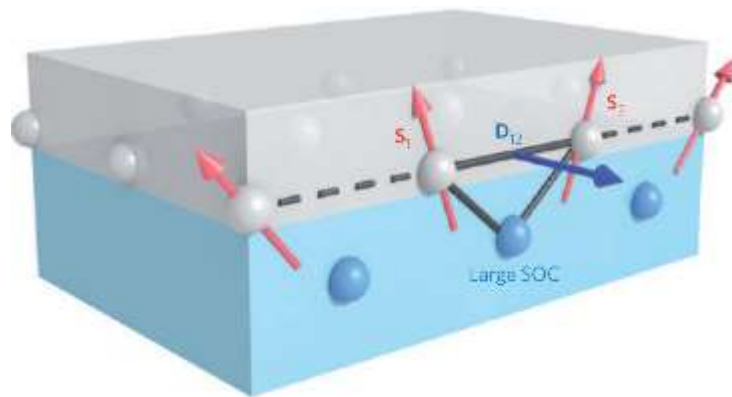
F. Garcia-Sanchez *et al*, *New J. Phys.* **18**, 075011 (2016)

**Technical
means: How to
make them?
How to
observe them?**

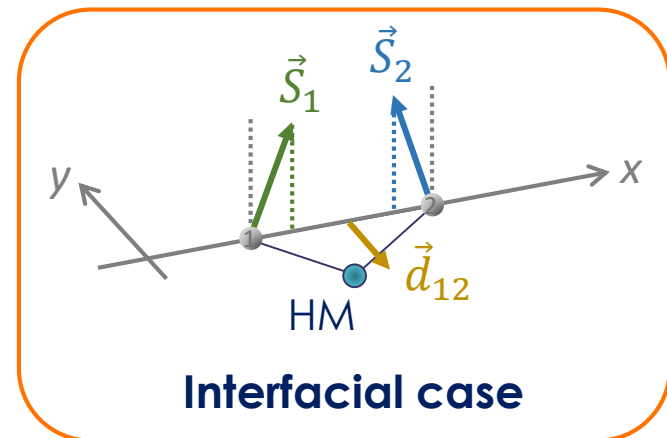
Dzyaloshinskii-Moriya Interaction in Bilayers

How to obtain DMI?

- Spin-orbit interaction
- Break the inversion symmetry



A. Fert *et al*, *Nat. Nanotechnol.* **8**, 152 (2013)

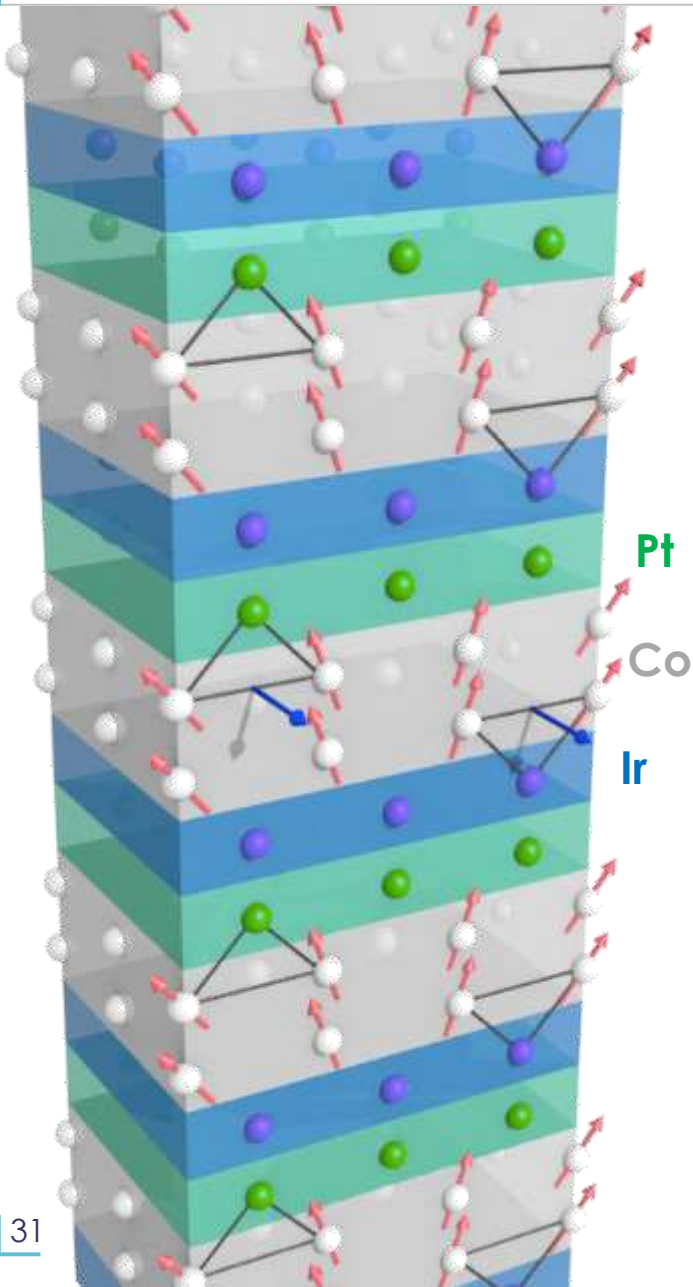


Interfacial case

A. Fert, *Mater. Sci. Forum* **59-60**, 439 (1990)

How to increase room stability against thermal fluctuations?

Design of Magnetic Multilayers (an example)



From bilayer to multilayers:

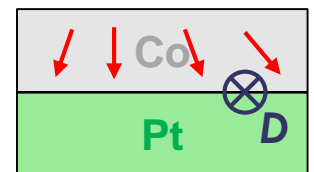
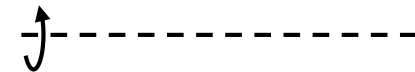
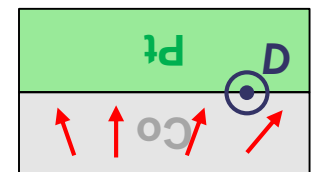
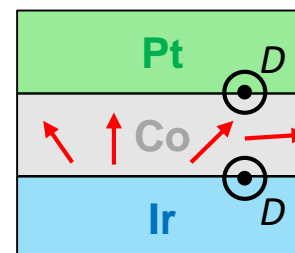
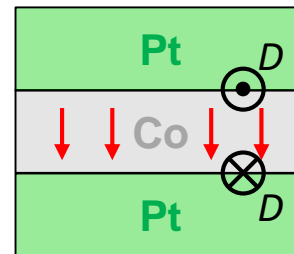
- Increase of the thermal stability
- Increase magnetic contrast in imaging experiments

Different top and bottom interfaces around the ferromagnetic layers: control of the amplitude of the DMI

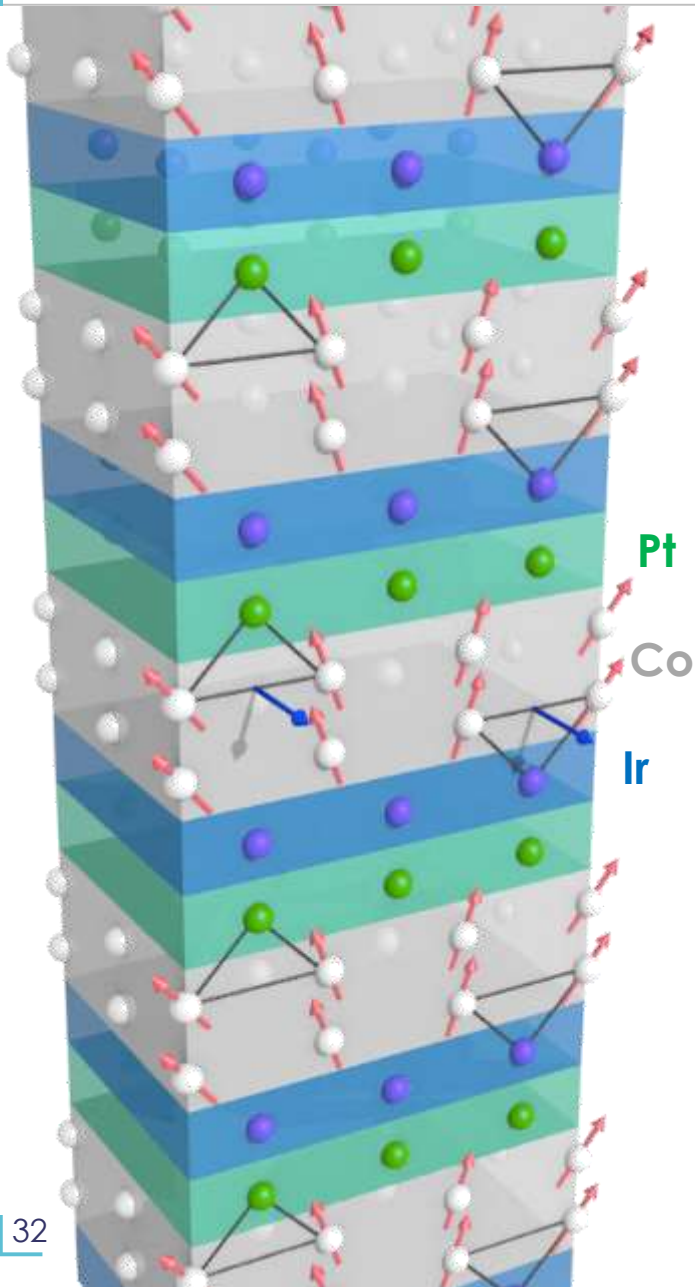
- Use of materials with opposite DMI sign to add up the effects, e.g:

$$\parallel \text{Pt}_{10} \mid (\text{Ir}_1 \mid \text{Co}_{0.8} \mid \text{Pt}_1)_n \mid \text{Pt}_3$$

$$D_{\text{eff}} \approx 0$$



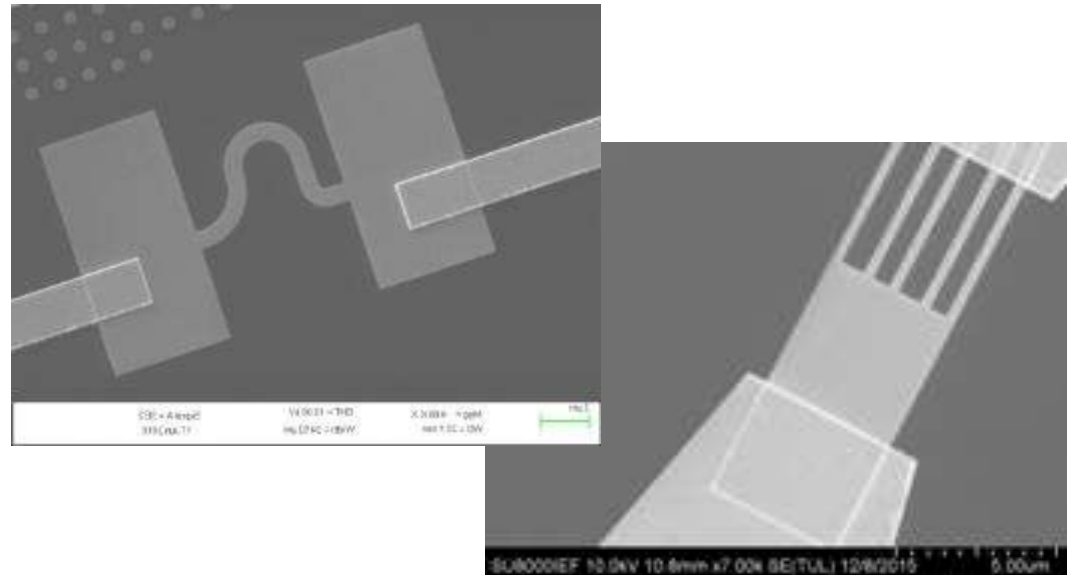
Growth and Patterning of Multilayers



Growth and patterning

- Sputtering growth at room temperature
- SiO₂/Si wafer substrates
- Si₃N₄ membranes for STXM or TEM imaging
- Textured polycrystalline films (rc FWHM ~8°)

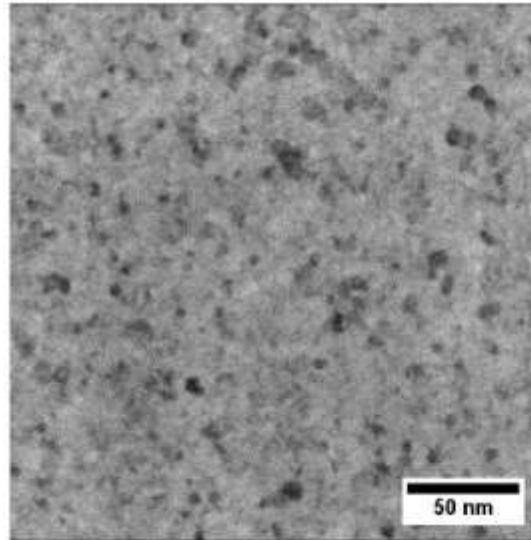
e-beam patterning hard mask, IBE (SIMS)



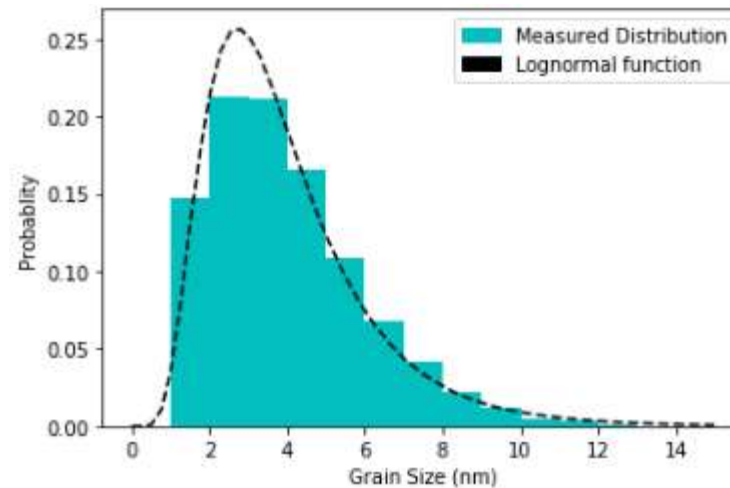
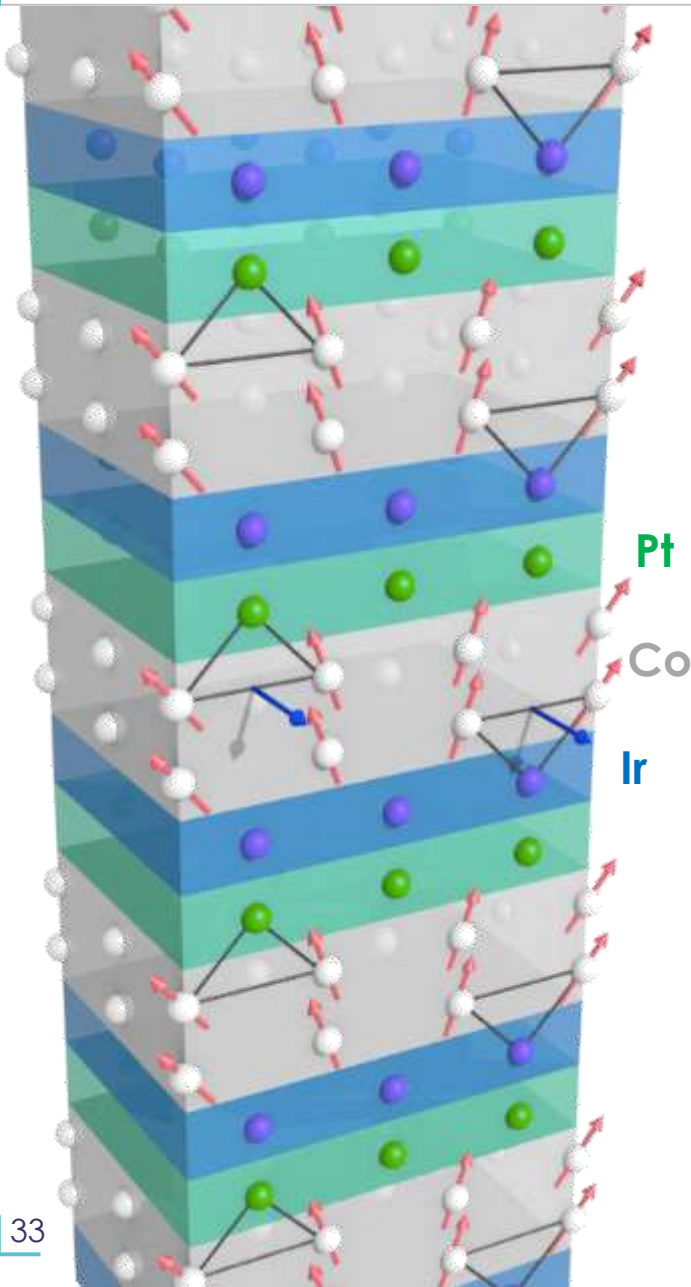
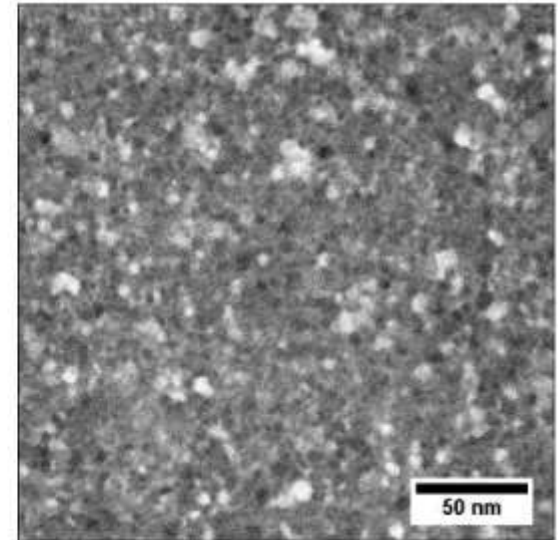
Growth of Multilayers – Grains from out-of-Plane TEM

Presence of grains

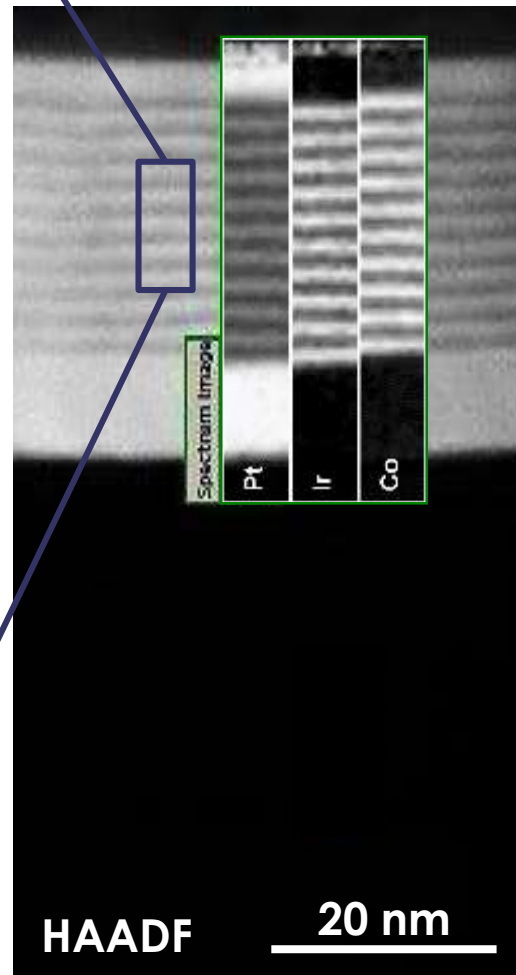
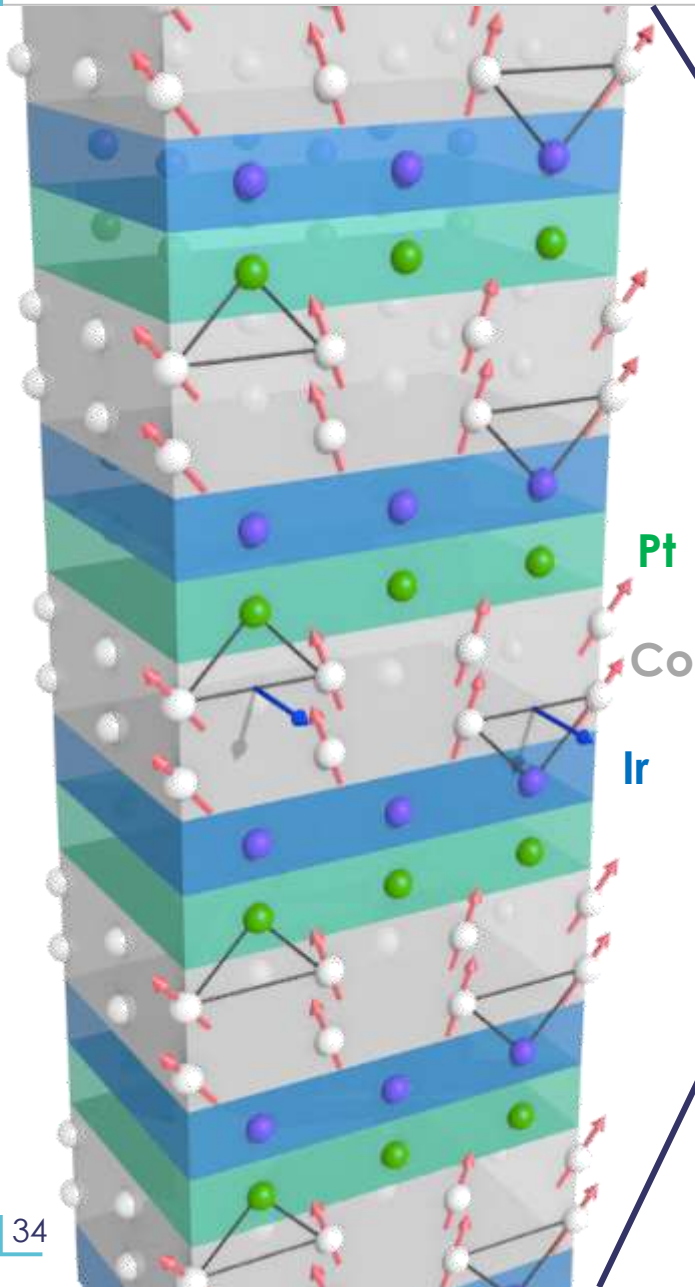
Dark field



HAADF



Growth of Multilayers – Cross-Section TEM



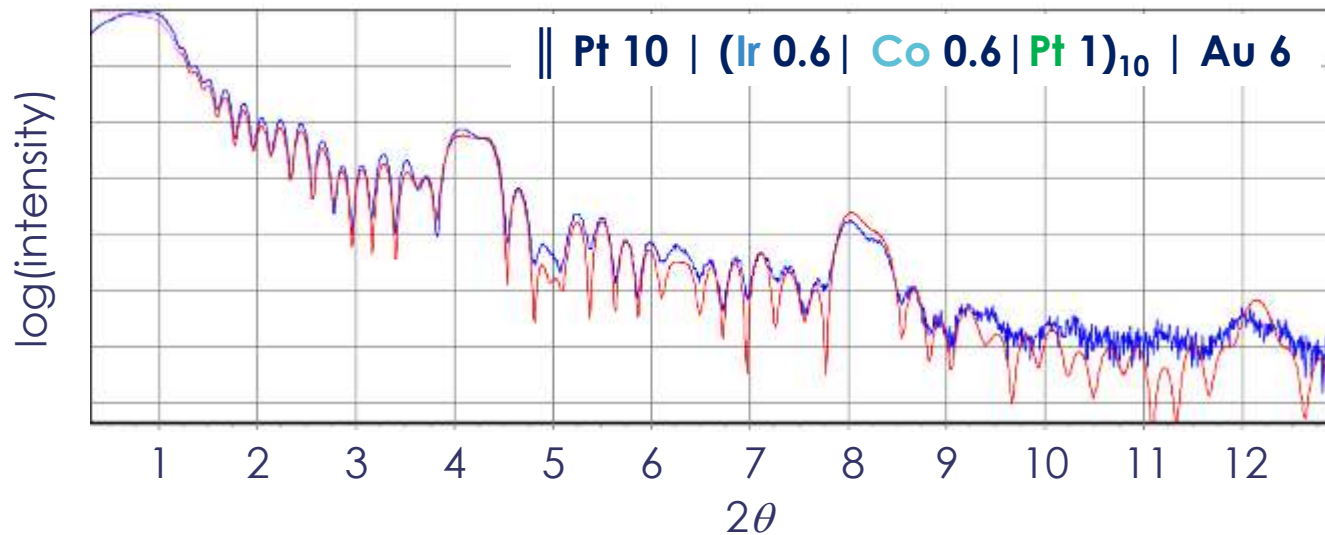
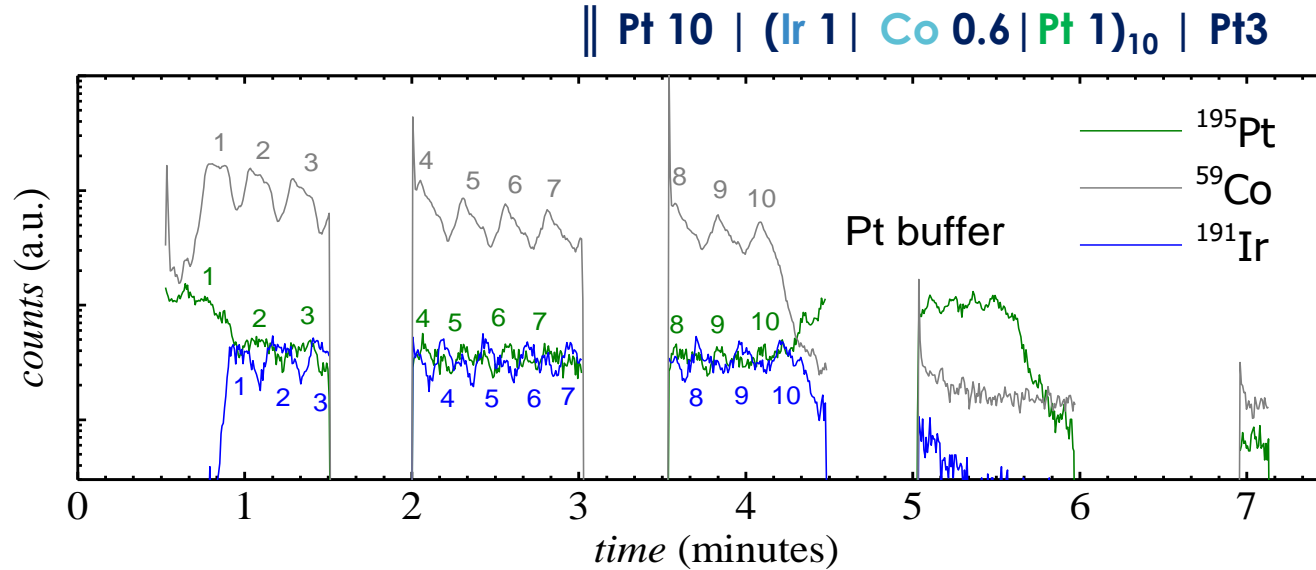
capping layer

MML ($n = 10$)

buffer

SiO₂/Si wafer

Growth of Multilayers – SIMS, x-rays, ...

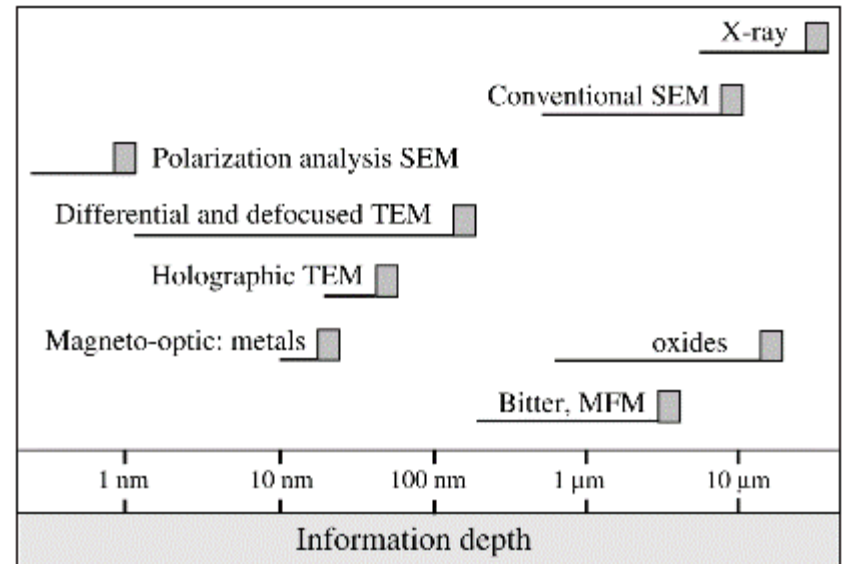
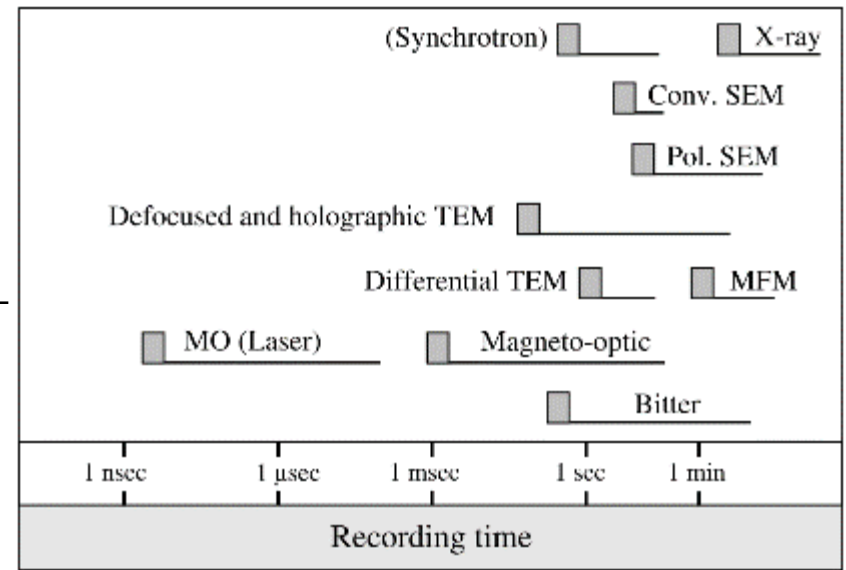
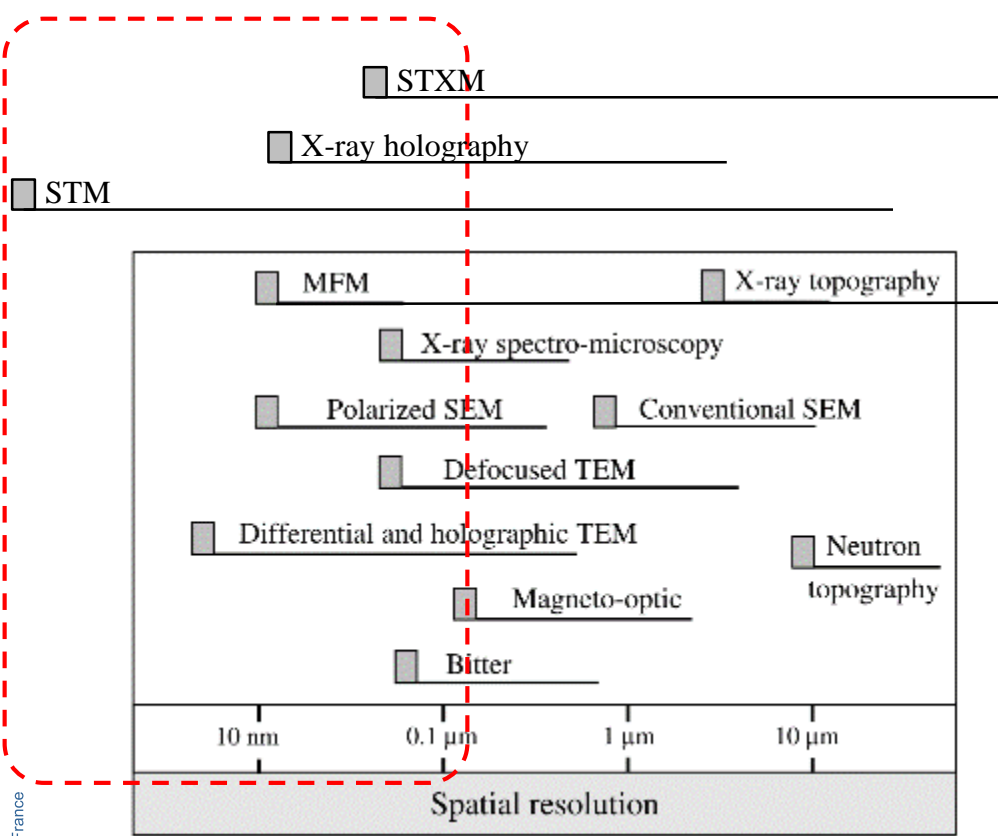


$t_{Pt} = 0.95$ nm
 $r_{Pt} = 0.10$ nm

$t_{Co} = 0.64$ nm
 $r_{Co} = 0.31$ nm

$t_{Ir} = 0.61$ nm
 $r_{Ir} = 0.33$ nm

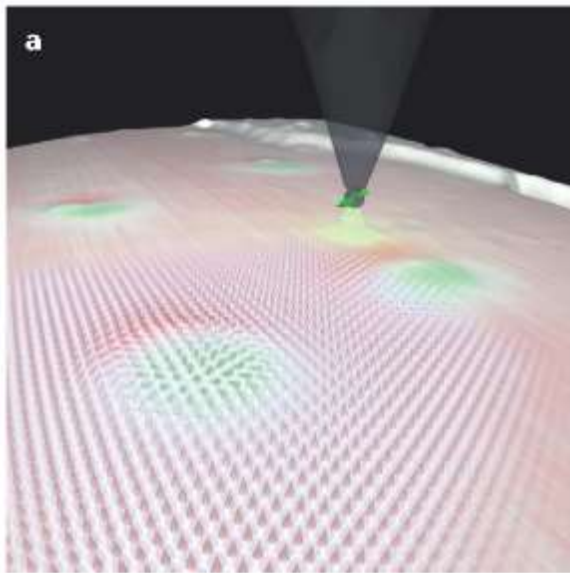
How to Observe Isolated sub-100nm-diameter Skyrmions?



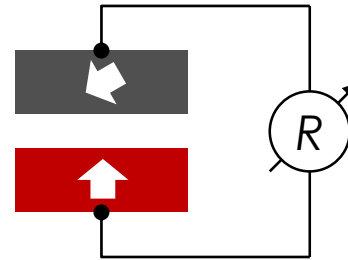
How to Observe Isolated sub-100nm-diameter Skyrmions?

(Spin-Polarized) Scanning Tunneling Microscopy (SP-STM)

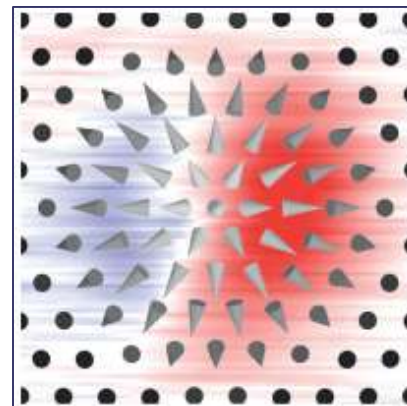
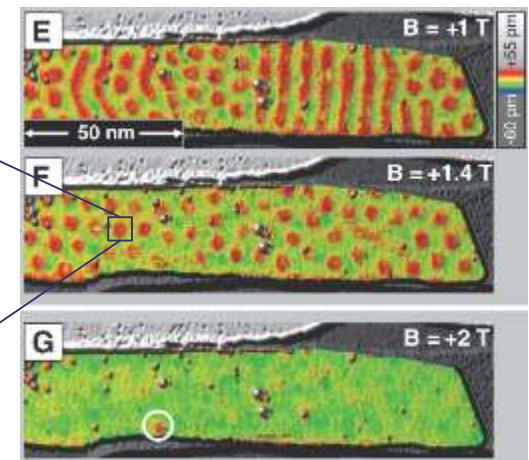
- “Ultimate” resolution (atomic) ☺
- Need clean surface (no capping) ☹



R. Wiesendanger, *Nat. Rev. Mater.* **1**, 16044 (2016)



TMR measurement:
Resistance (or tunnel current at fixed voltage) depends on the relative orientation of the magnetization.

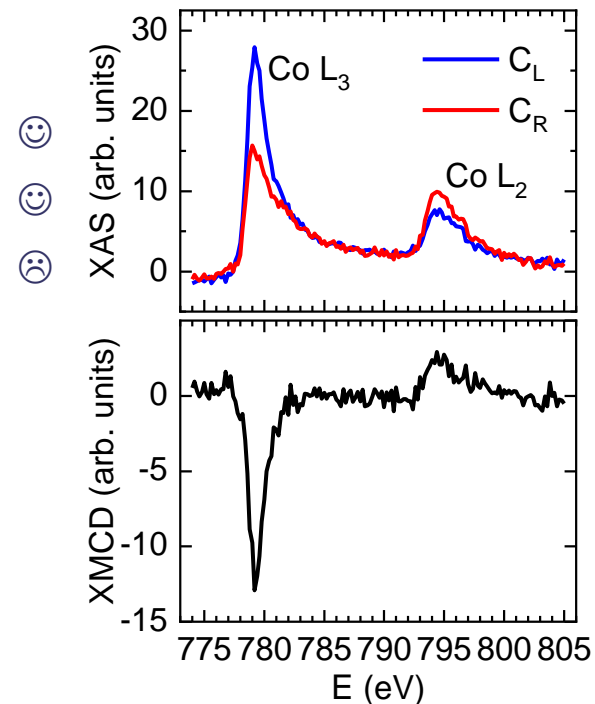
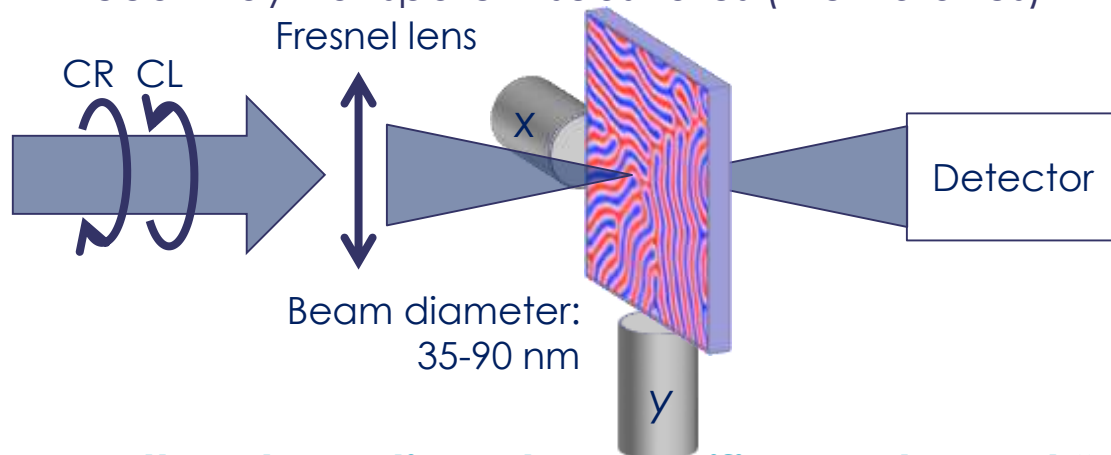


- Using “TXMR” or “NCMR” a non-magnetic tip can be used.

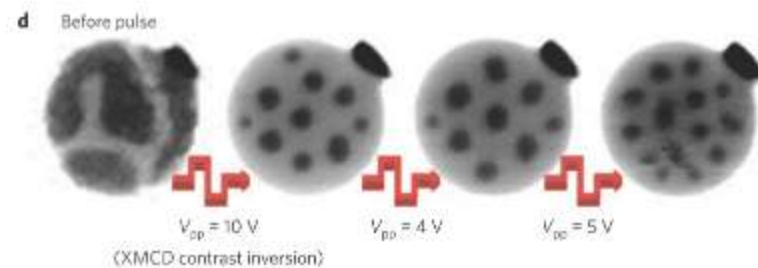
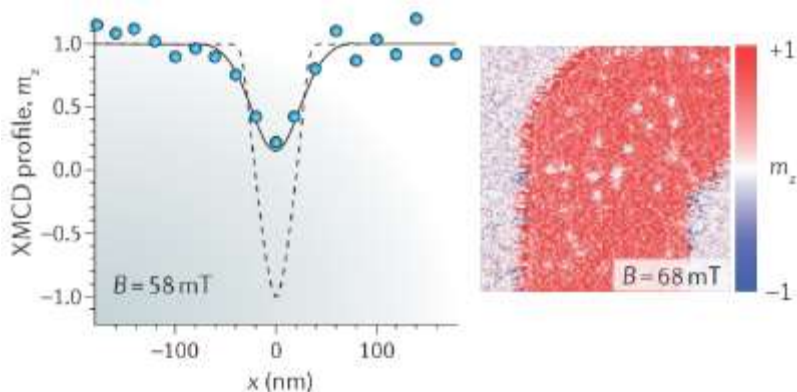
How to Observe Isolated sub-100nm-diameter Skyrmions?

Scanning Transmission X-ray Microscopy

- Element specific, probe through capping layers, etc. 😊
- External fields, currents, etc. can be applied 😊
- Need x-ray transparent substrates (membranes) 😞



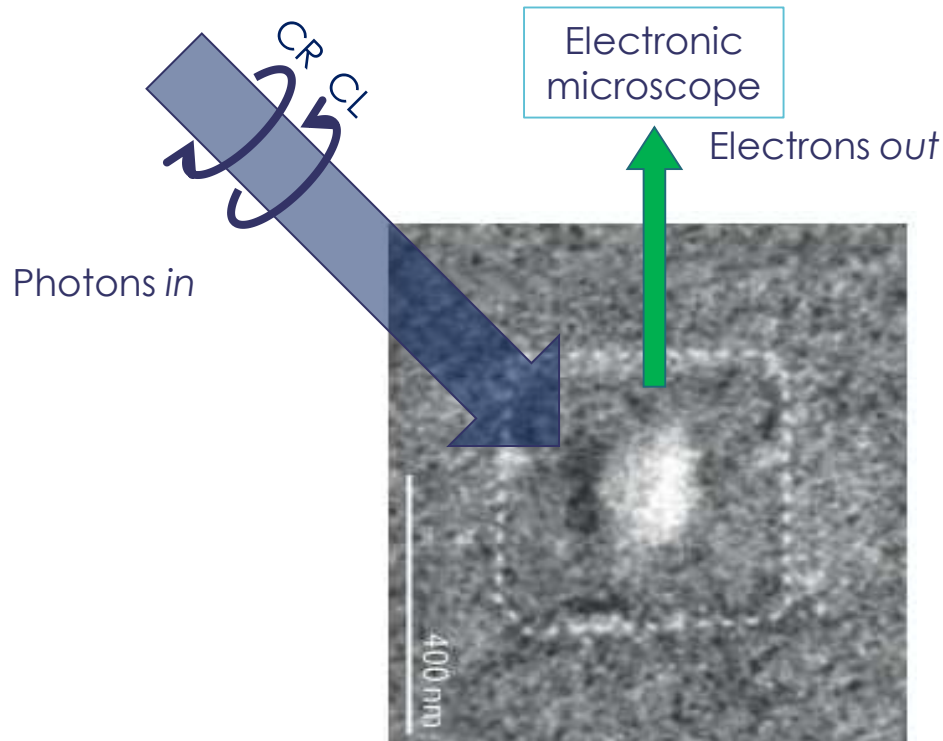
Map the absorption at a specific FM element "edge"



How to Observe Isolated sub-100nm-diameter Skyrmions?

X-ray magnetic circular dichroism photoemission electron microscopy (XMCD-PEEM)

- Element specific ☺
- Need magnetic layer very close to surface ☹
- Limited magnetic field ☹



O. Boulle *et al*, *Nat. Nanotechnol.* **11**, 449 (2016)

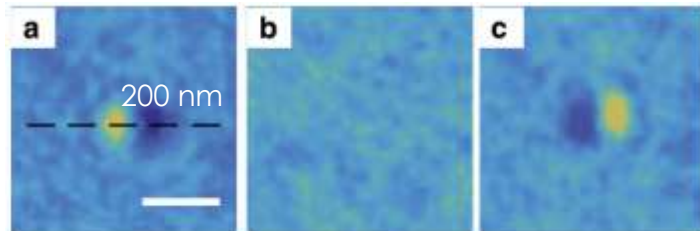
How to Observe Isolated sub-100nm-diameter Skyrmions?

Lorentz-TEM, Differential Phase Contrast, Electron holography, etc.

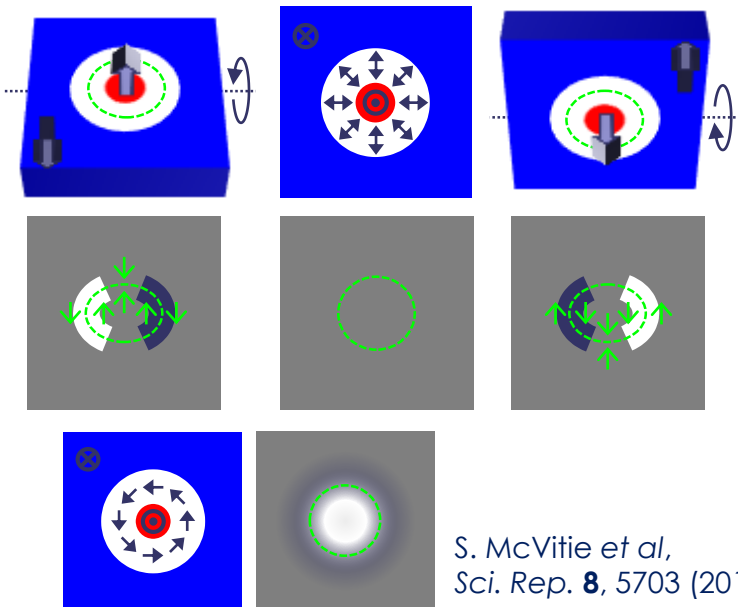
➤ Probe magnetization ☺

Only probe the surface ☹

Lorentz transmission electron microscopy (L-TEM)

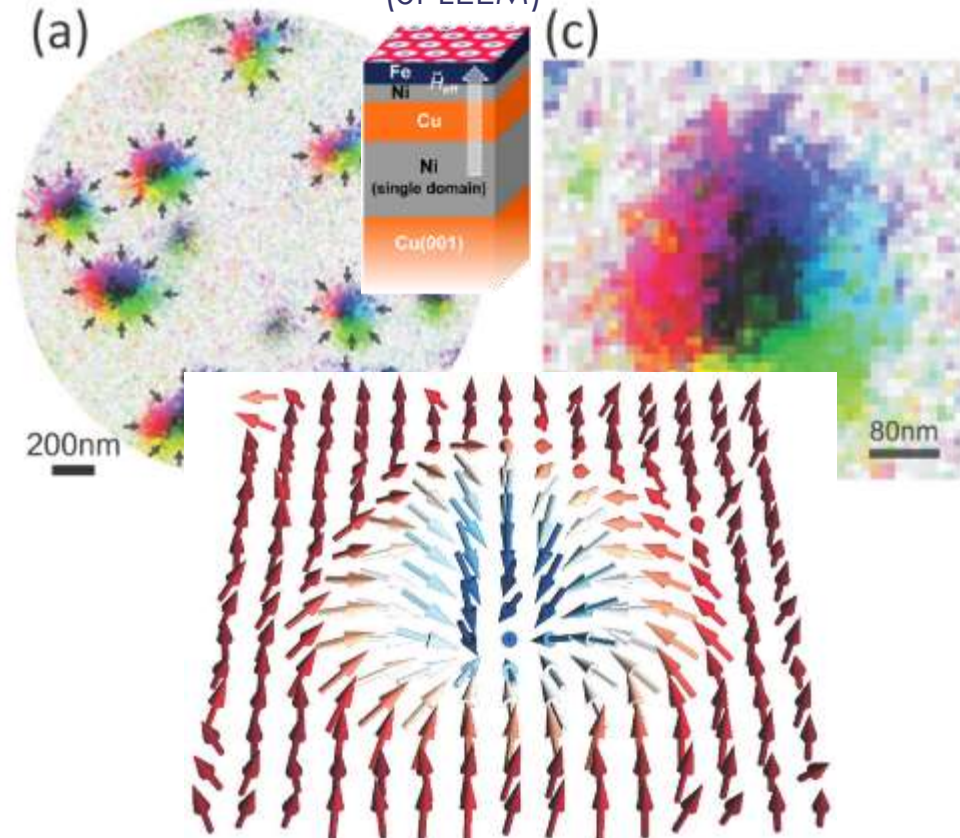


S. D. Pollarde *et al*, *Nat. Commun.* **8**, 14761 (2017)



S. McVitie *et al*, *Sci. Rep.* **8**, 5703 (2018)

Spin polarized low-energy electron microscopy (SPLEEM)

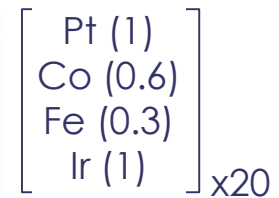
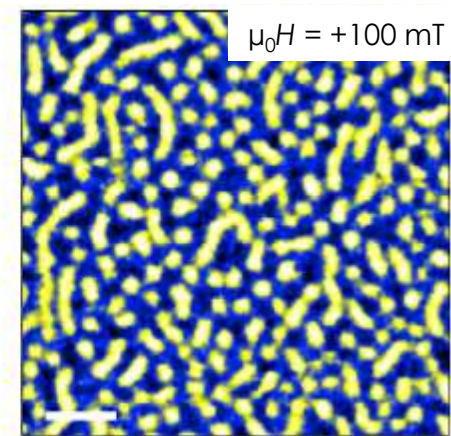
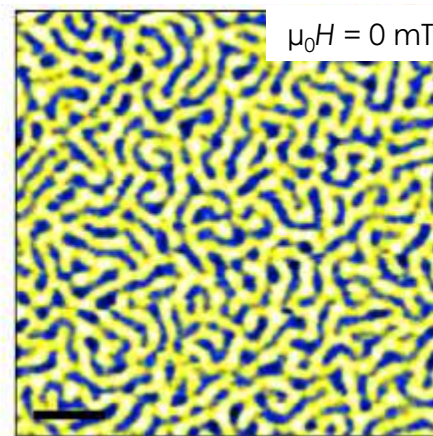
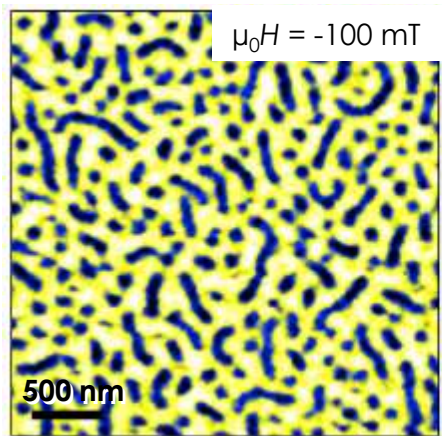
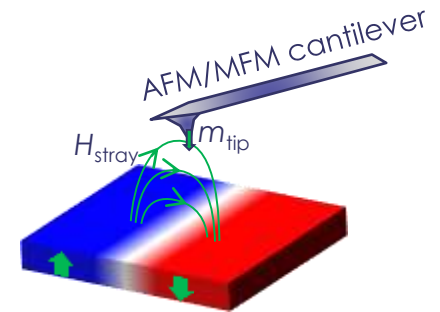


G. Chen *et al*, *Appl. Phys. Lett.* **106**, 242404 (2015)

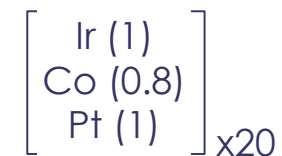
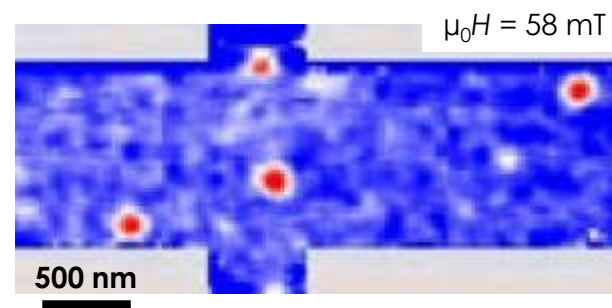
How to Observe Isolated sub-100nm-diameter Skyrmions?

Magnetic Force Microscopy (MFM)

- Tabletop laboratory technique
- Measure (mostly) stray fields (of buried layer)
- Measure (mostly) stray fields



A. Soumyanarayanan *et al*, *Nat. Mater.* **16**, 898 (2017)



D. Maccariello *et al*, *Nat. Nanotechnol.* **13**, 233 (2018)

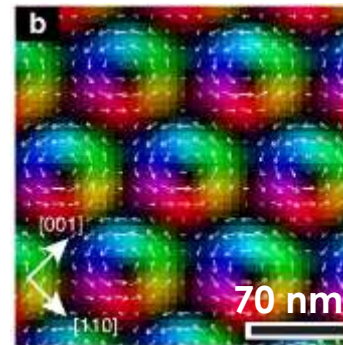


Skymion
stability,
nucleation,
motion...

Field-Temperature Phase Diagram in B20 materials

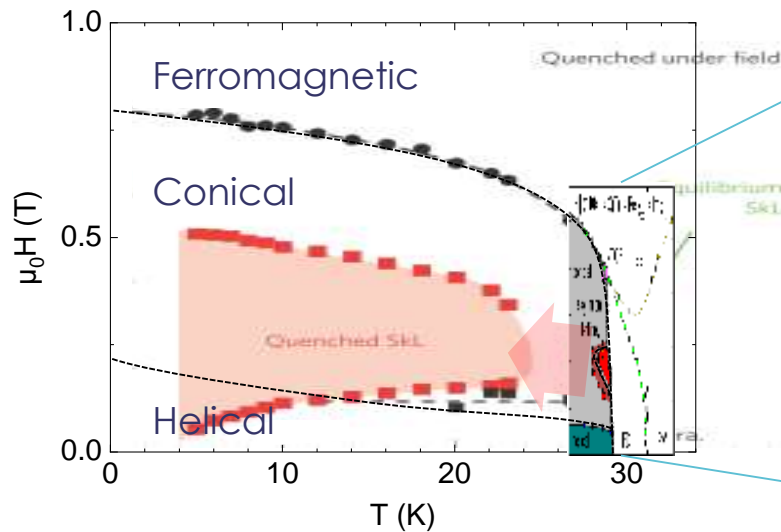
In B20-types of materials

- Narrow range of stability
- Ground state → skyrmion array

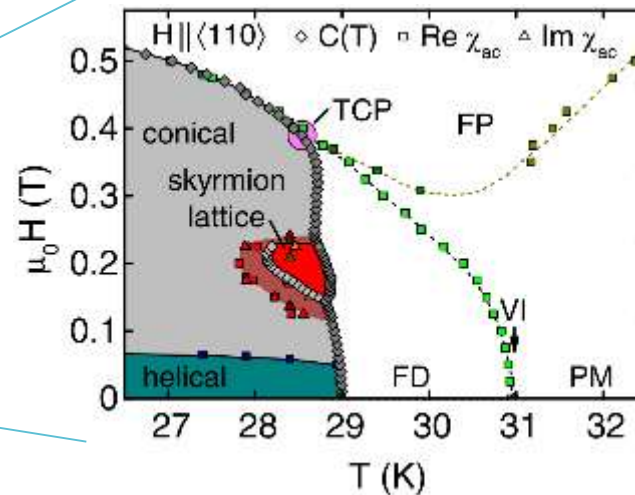


Skyrmion lattice in FeGe

X. Z. Yu *et al*, *Nat. Commun.* **3**, 988 (2012)



H. Oike *et al*, *Nat. Phys.* **12**, 62 (2016)



A. Bauer *et al*, *Phys. Rev. Lett.* **110**, 177207 (2013)

Metastable skyrmions

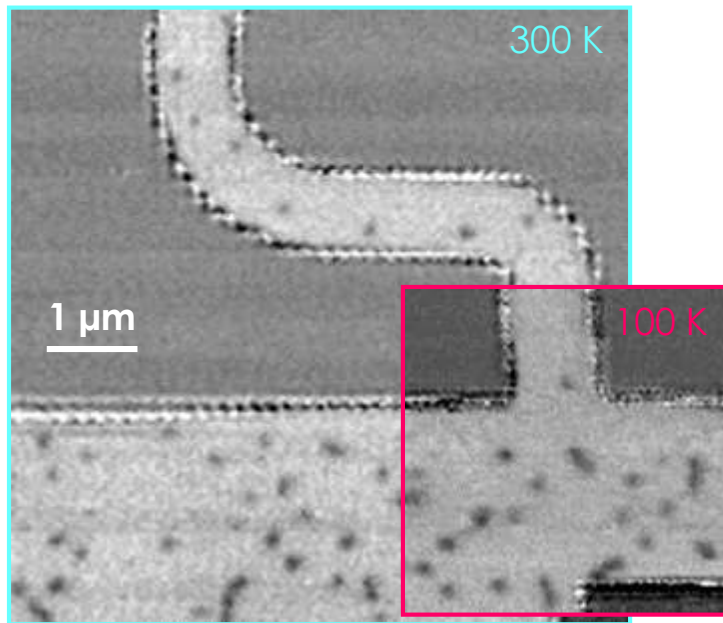
- Obtained by temperature quench from the lattice phase

H-T Phase Diagram for Metallic Multilayers

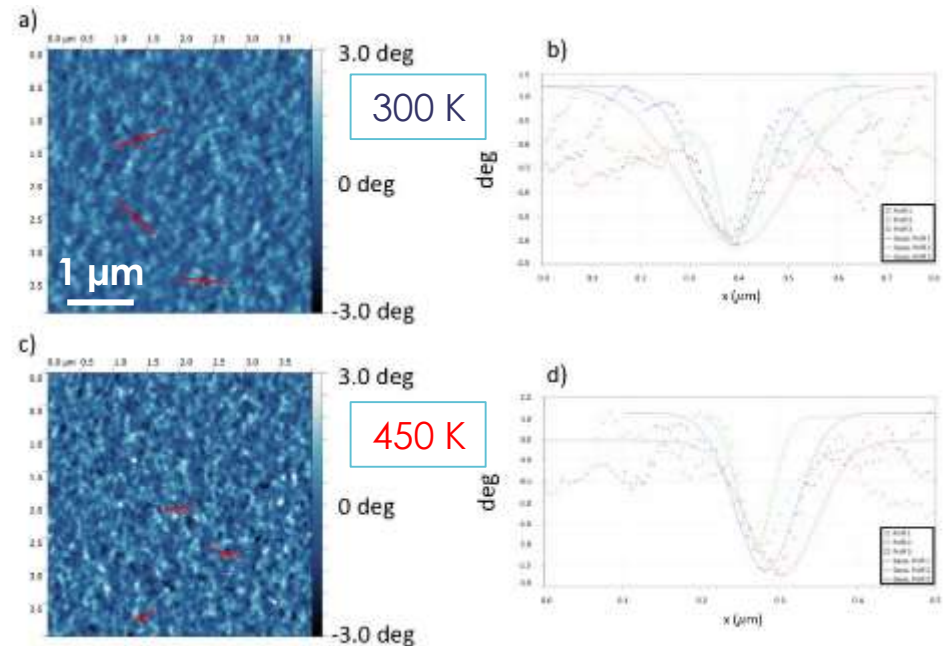
■ No real phase diagram published (yet)?

■ Metastability → isolated skyrmions

➤ For Pt | Co system, isolated skyrmions are observed (at least) in the temperature range 100 - 400 K, and $|\mu_0 H| < 200$ mT (typical value...).



STXM

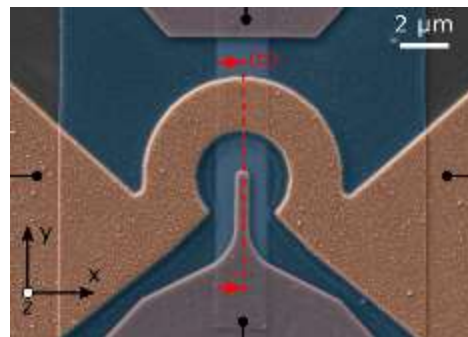


MFM

Means of Nucleation

Field and temperature sweeps

- Possibility to apply rather local fields



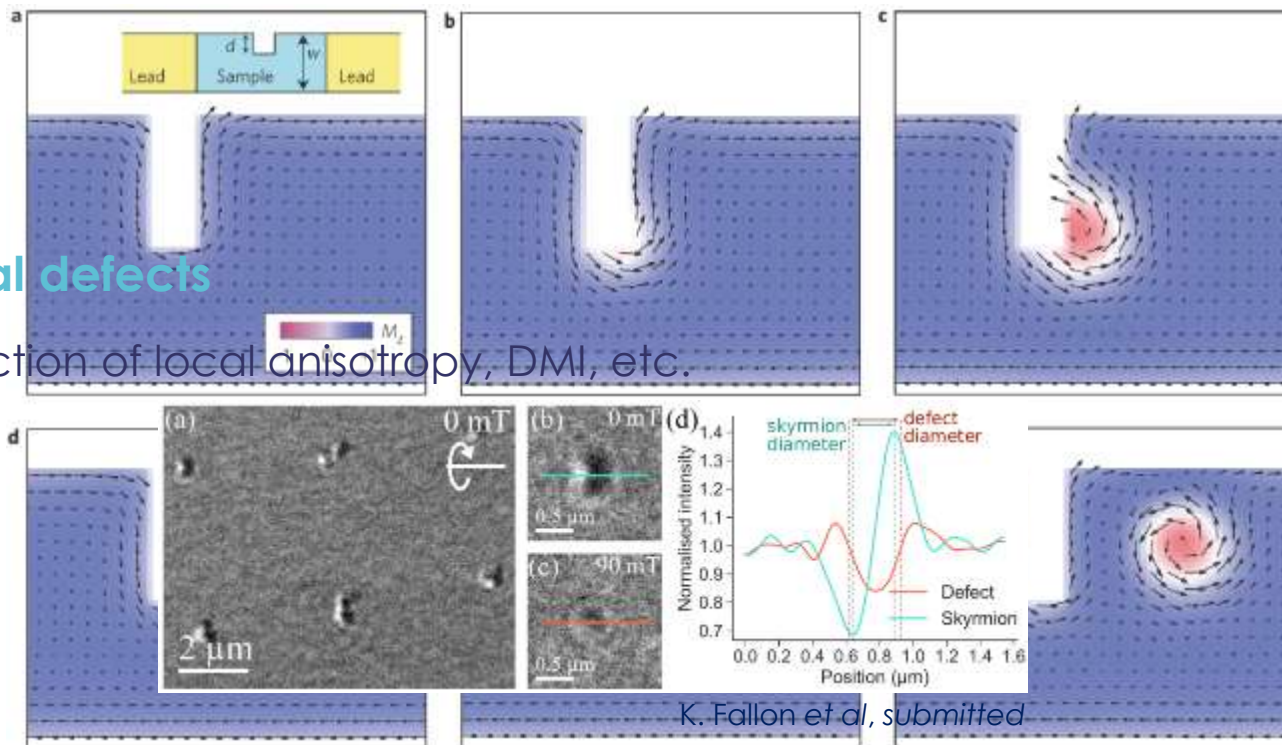
S. Finizio *et al*,
arxiv: **1902.10435**

Use of the geometrical boundaries

- Boundary “breaks” the topological protection

Artificial defects

- Reduction of local anisotropy, DMI, etc.



K. Fallon *et al*, submitted

J. Iwasaki *et al*, *Nat. Nanotechnol.* **8**, 742 (2013)

Current-induced Skyrmion Nucleation in a Track

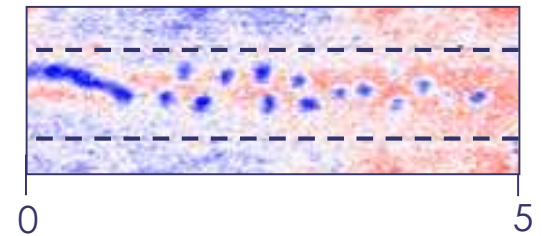
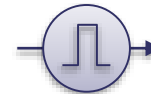
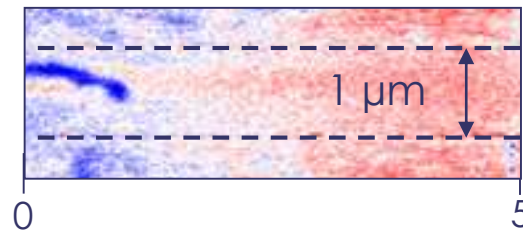
Sputtered samples structure – difficult field nucleation

- #1: || Ta 15 | Co 0.6 | (Pt 1 | Ir 1 | Co 0.6)_{x10} | Pt 3
- #2: || Ta 15 | Co 0.8 | (Pt 1 | Ir 1 | Co 0.8)_{x10} | Pt 3
- #3: || Ta 15 | Co 1.0 | (Pt 1 | Ir 1 | Co 1.0)_{x10} | Pt 3

1000 pulses of 200ns

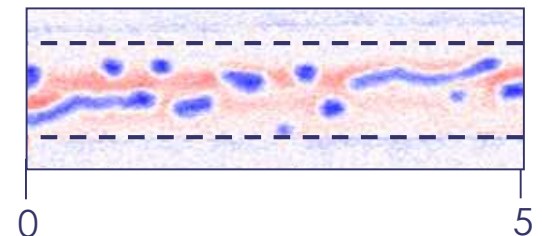
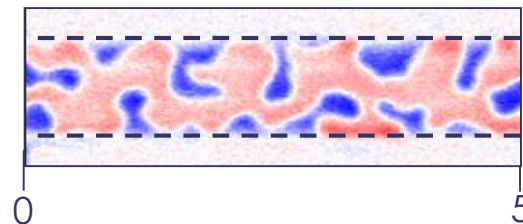
#1 (0.6 nm Co)

$$J_n = \pm 1.43 \cdot 10^{11} \text{ A m}^{-2}$$



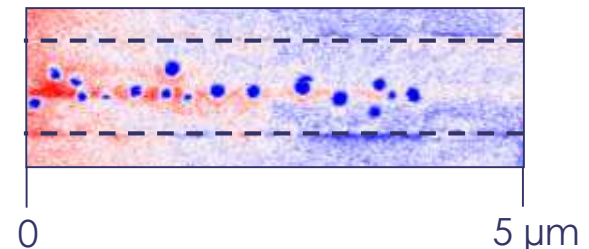
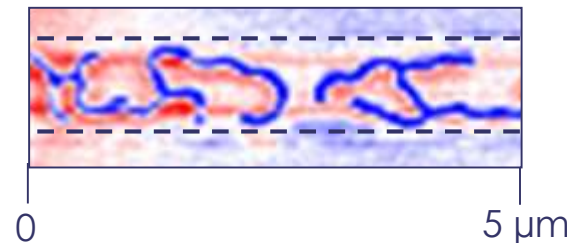
#2 (0.8 nm Co)

$$J_n = \pm 2.38 \cdot 10^{11} \text{ A m}^{-2}$$



#3 (1.0 nm Co)

$$J_n = \pm 2.96 \cdot 10^{11} \text{ A m}^{-2}$$

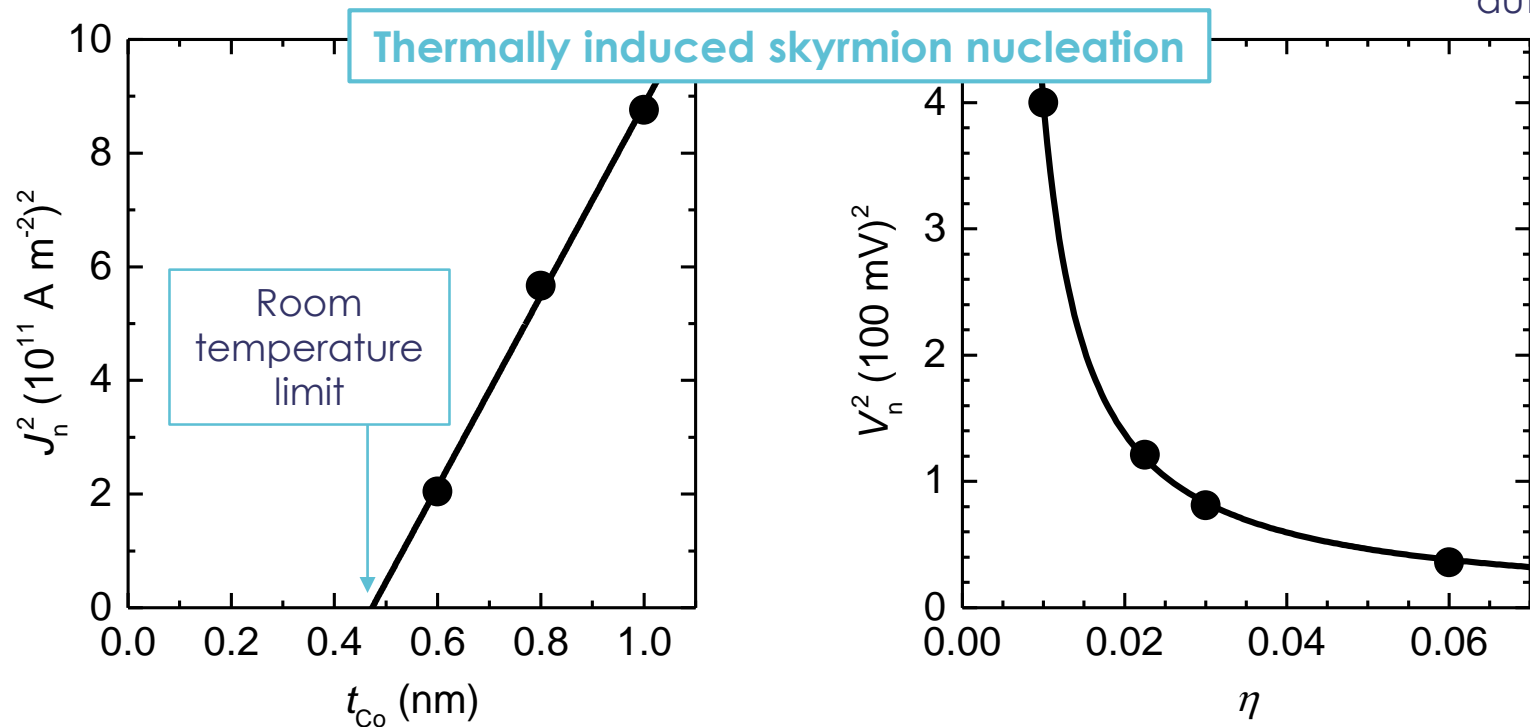


(Mainly) Thermal Origin of the Nucleation

Hypothesis of the thermal nucleation

- Stability of domains proportional to magnetic volume => Co thickness t_{Co}
- Joule heating proportional to J^2
- Role of room temperature: minimum thickness for stabilization
- Temperature elevation ~ Joule power: $\Delta T_n \propto P_n \propto \eta V_n^2(\eta) \Rightarrow V_n^2(\eta) \propto \frac{1}{\eta}$

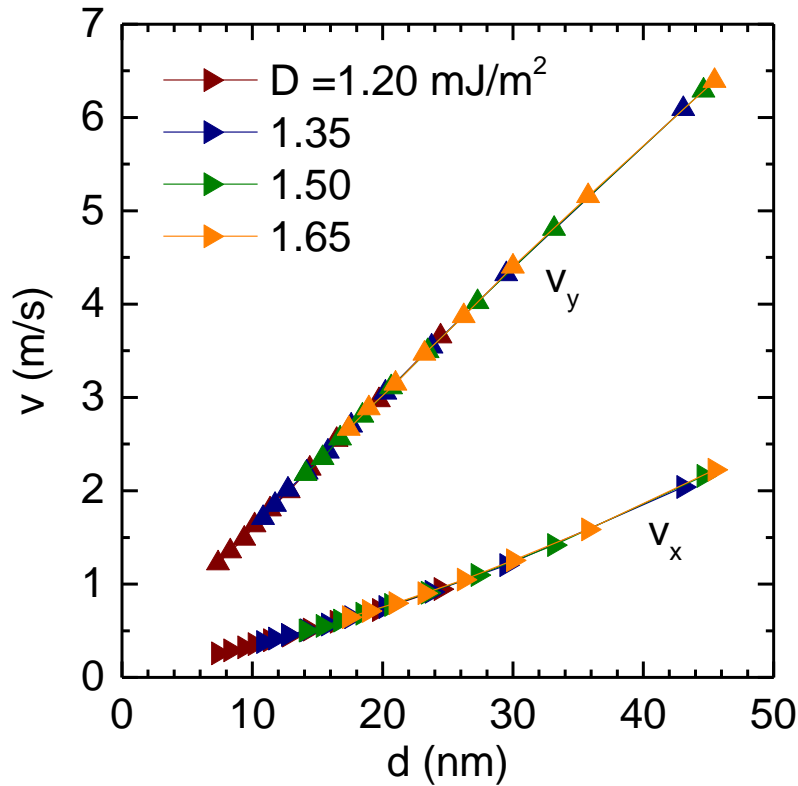
duty cycle



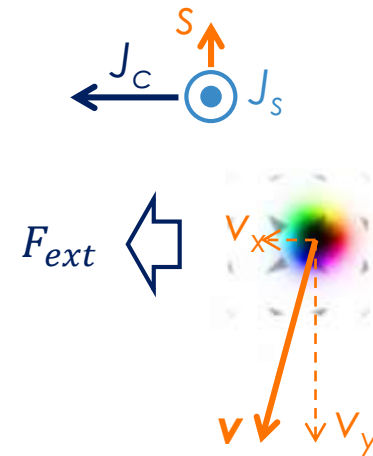
Velocity and Diameter in “Plain Films”

The velocity of a “compact skyrmion” depends on its size

- Micromagnetic simulations for $J = 67 \text{ GA/m}^2$
- $M_s = 956 \text{ kA/m}$; $K_U = 717 \text{ kJ/m}^3$; $A = 10 \text{ pJ/m}$; $\alpha = 0.2$; $\theta_{\text{SHE}} = 0.06$
- various D and H_z



Without confinement
30 mT, $D = 1.35 \text{ mJ/m}^2$



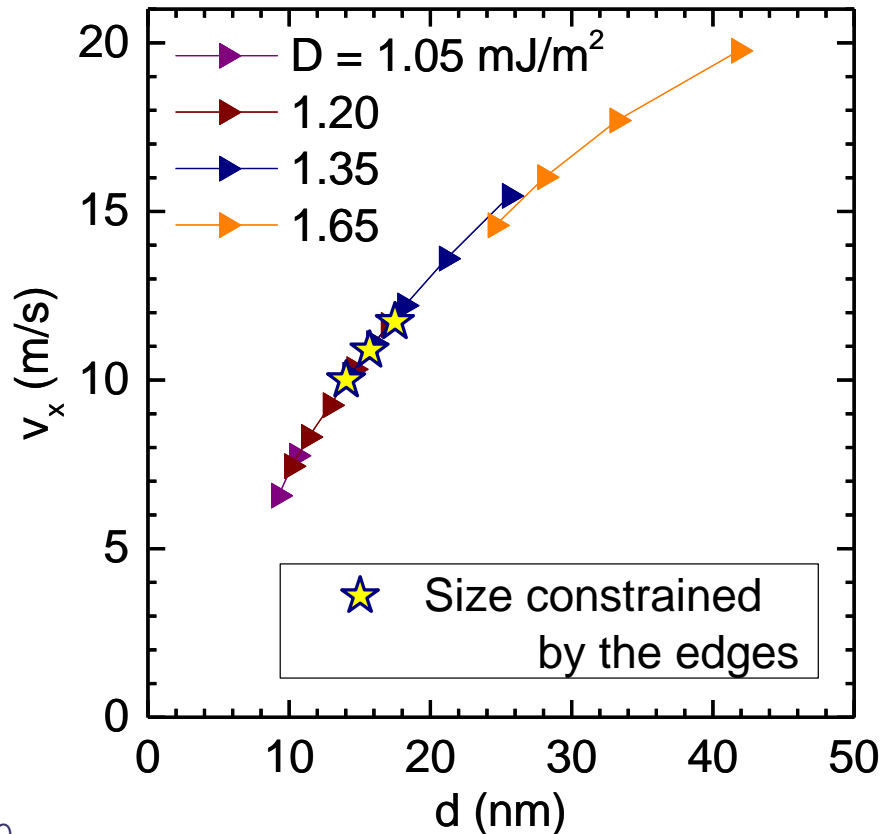
$$\mathbf{G} \wedge \mathbf{v} + \alpha D \mathbf{v} + \mathbf{F}_{\text{ext}} = 0$$

gyrovector damping SHE

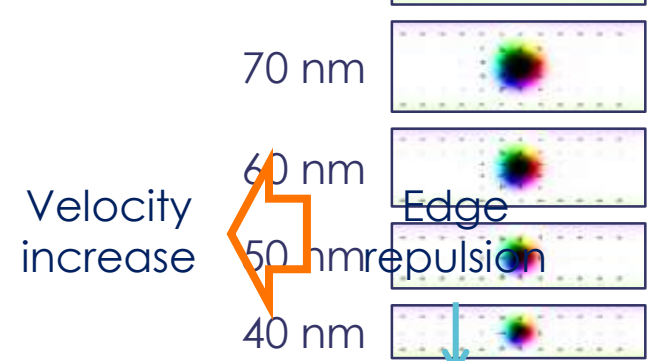
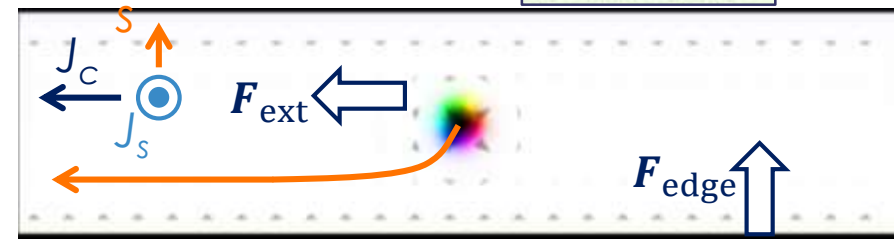
Velocities in Track: Still Proportional to Diameter

The velocity of a “compact skyrmion” depends on its size

- Micromagnetic simulations for $J = 67 \text{ GA/m}^2$
- $M_s = 956 \text{ kA/m}$; $K_U = 717 \text{ kJ/m}^3$; $A = 10 \text{ pJ/m}$; $\alpha = 0.2$; $\theta_{\text{SHE}} = 0.06$
- various D and H_z + Track width!



In a track
 30 mT , $D = 1.35 \text{ mJ/m}^2$, track width = 120 nm



$$\mathbf{G} \wedge \mathbf{v} + \alpha D \mathbf{v} + \mathbf{F}_{\text{ext}} = 0$$

gyrovector → damping → SHE

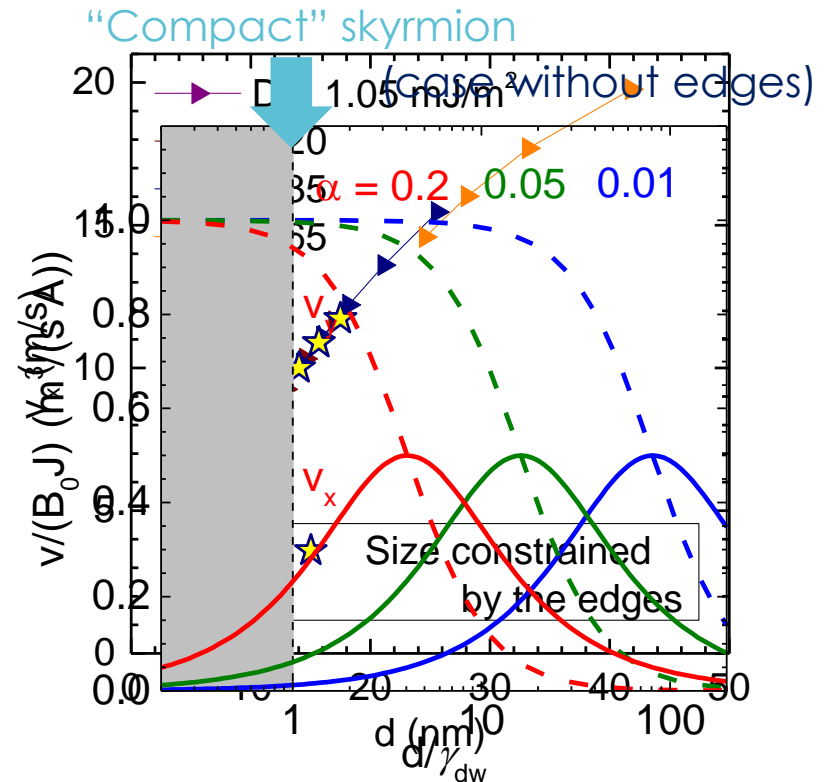
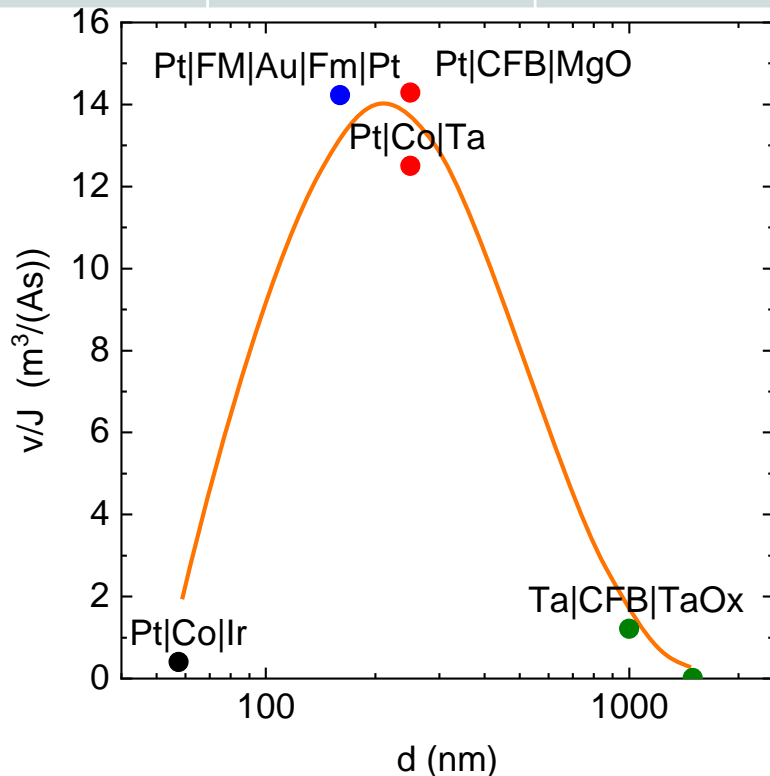
Velocities and Sizes Reported in the Literature

Composition	Laboratory	Skyrmion diameter d (nm)
Pt Co Ir	CNRS/Thales...	35 to 80
Pt CoFeB MgO	MIT+Mainz+...	250
Pt Co Ta	MIT+Mainz+...	250
Pt FM Au FM Pt	LPS+...	160
Ta CoFeB TaO _x	ANL+...	~1000 700 to 2000

Thiele equation developed by Tomasello *et al*, and also used in Jiang *et al*:

$$\begin{cases} v_x = \frac{\alpha \mathcal{D}}{1 + \alpha^2 \mathcal{D}^2} B_0 J_x, & \text{with } \mathcal{D} = \frac{\pi^2}{8} \frac{d}{\gamma_{DW}} \\ v_y = \frac{1}{1 + \alpha^2 \mathcal{D}^2} B_0 J_x. \end{cases}$$

R. Tomasello *et al*, *Sci. Rep.* **4**, 6784 (2014)
W. Jiang *et al*, *Nat. Phys.* **13**, 162 (2017)



Moving Skyrmions using Electrical Current

Series of MFM images after electrical pulses

200 ns; $J \approx 2 \cdot 10^{11}$ A/m²; $\mu_0 H = 35$ mT; $T = 300$ K

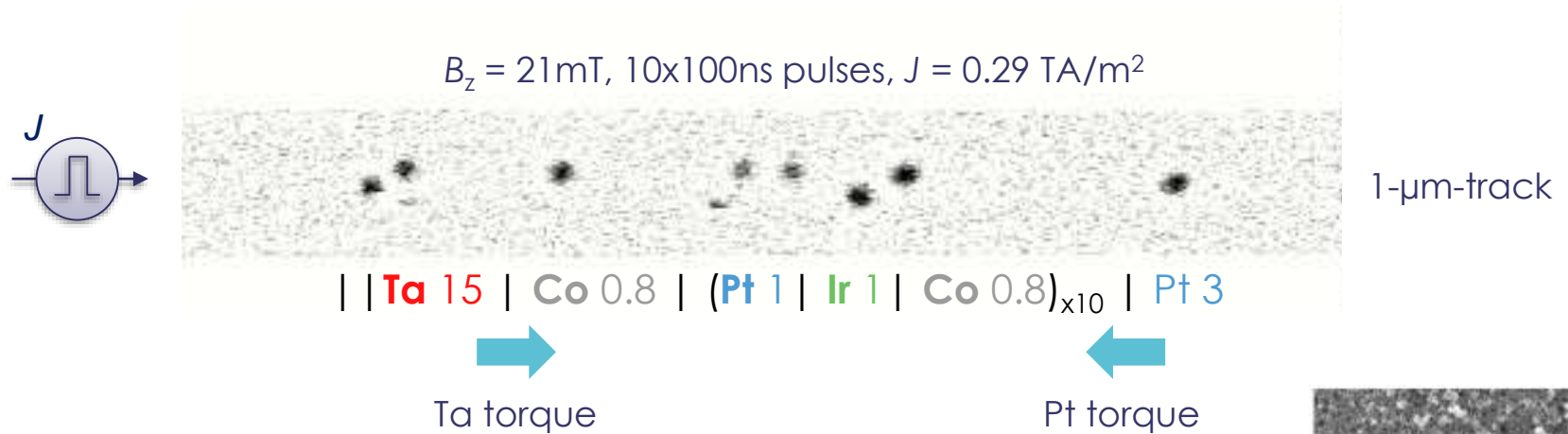


What is the origin of their
“chaotic” motion?

Skyrmion Motion under Current Pulses

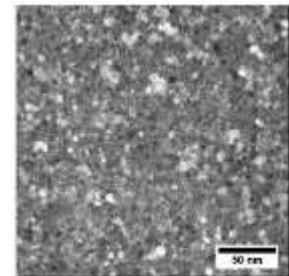
Motion is observed using short pulses just below nucleation threshold

- No clear skyrmion Hall effect (in any of our sample)
- Low velocity (typically 50 nm/s, up to 0.5 m/s)
- Disordered motion against the electron flow



Presence of grains with different properties?

- Grains observed by TEM
- Variation of the properties reported by quantitative MFM (Bacani *et al*, arXiv:1609.01615)



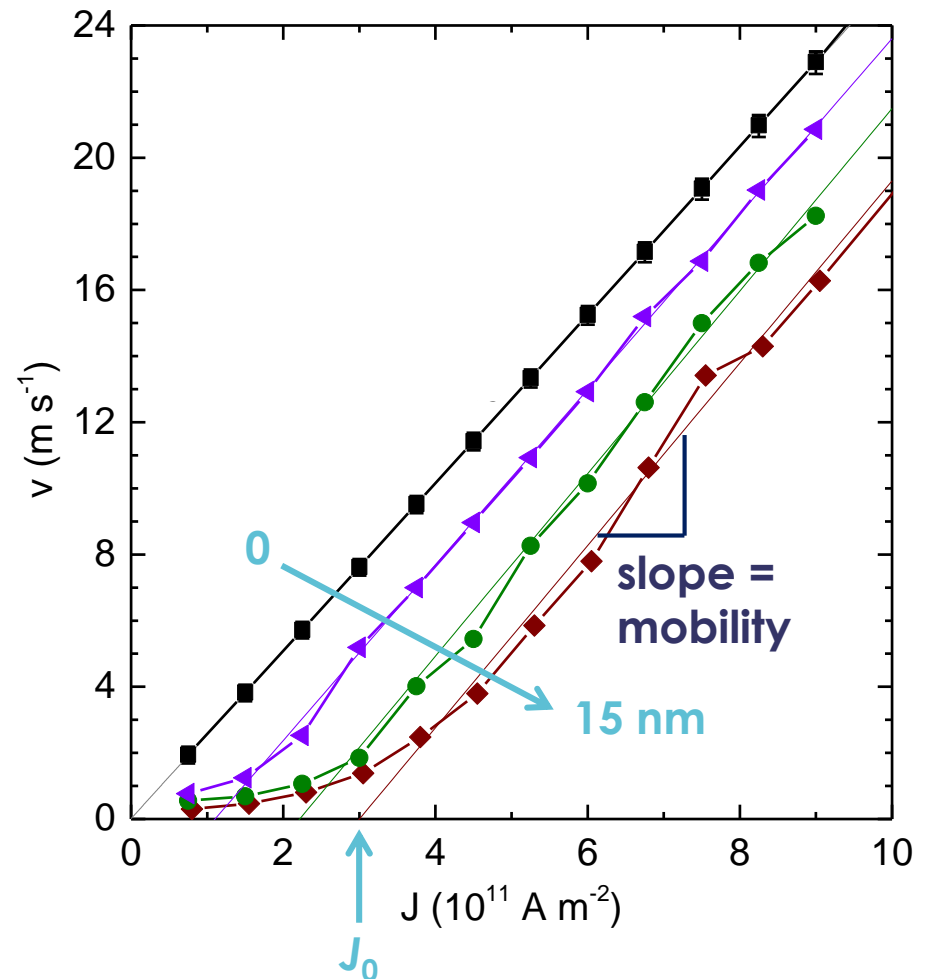
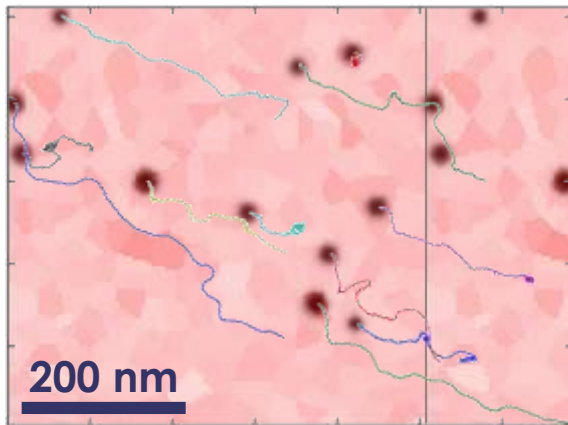
Creep-Like Regime

Existence of a “mobility edge” and a “depinning current”

- Due to the distribution of grains properties => existence of a potential barrier at grain boundaries
- As grain size is increased the “depinning current” increases...

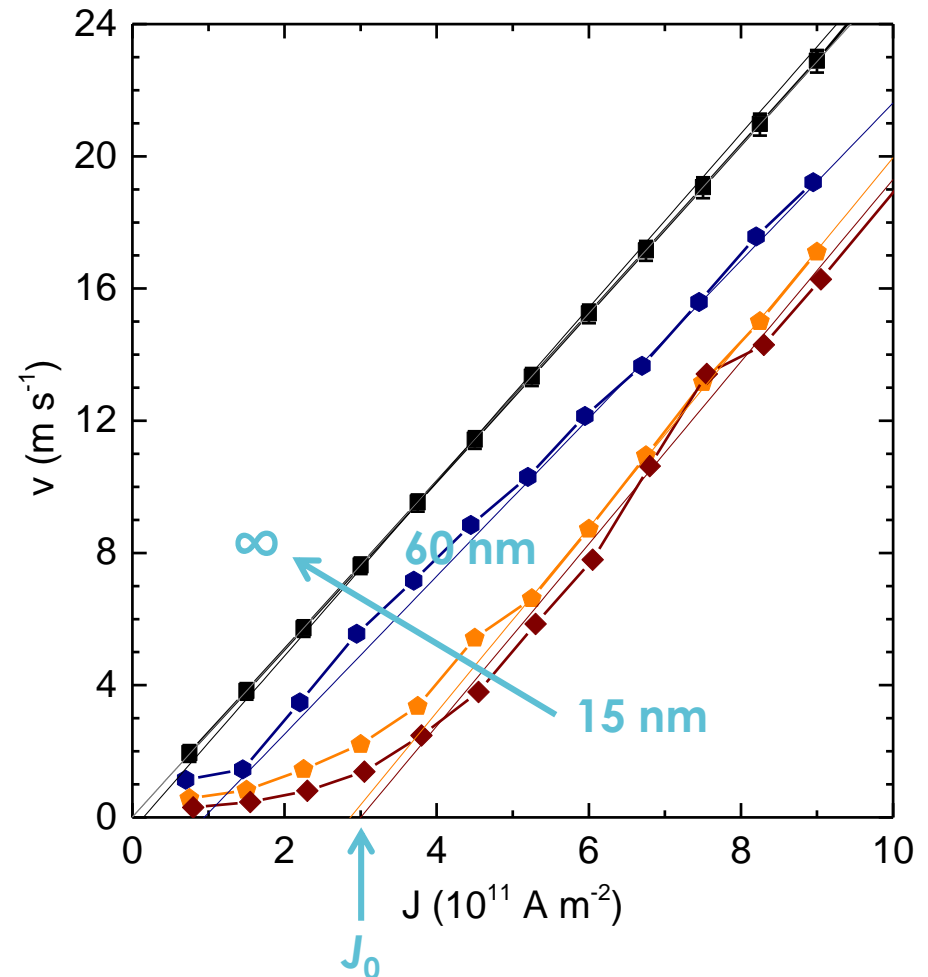
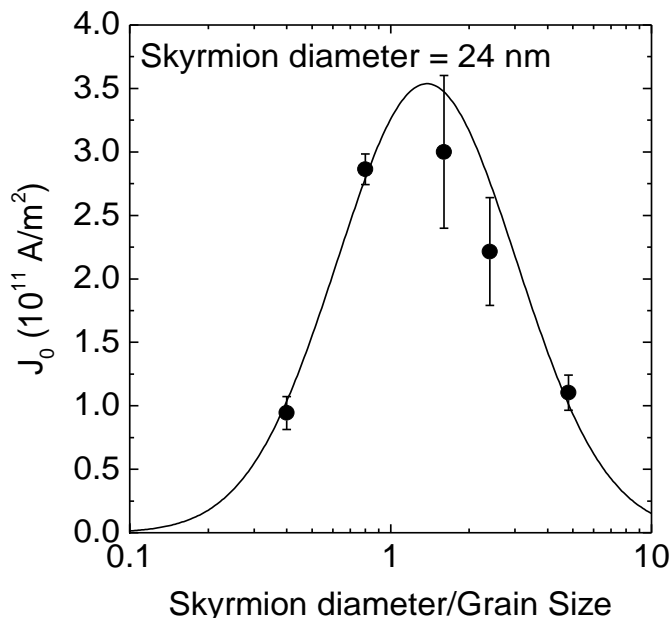
- ▶ the velocity is never recovered
- ▶ the mobility is recovered above J_0

10% D variation



Existence of a “mobility edge” and a “depinning current”

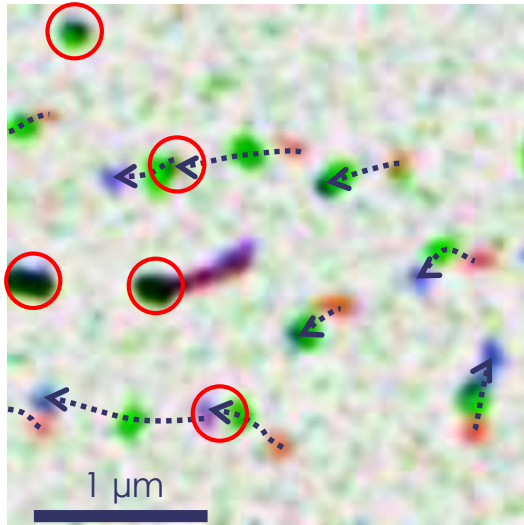
- Due to the distribution of grains properties => existence of a potential barrier at grain boundaries.
- As grain size is increased the “depinning current” increases...
- ... and decreases again once the grains sizes largely exceed the skyrmions sizes.



Skyrmion velocity (and data rate)

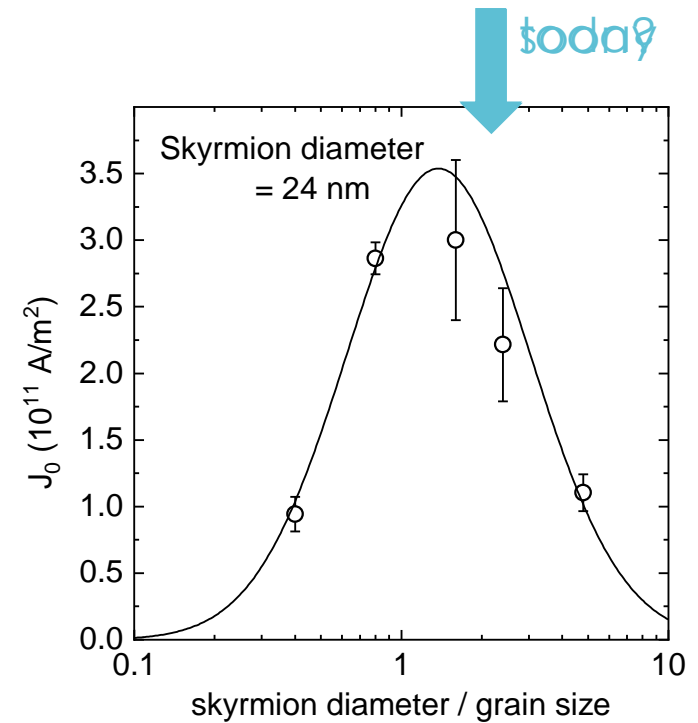
Improve of design: increased velocity

Pinning points



|Ta10|Pt8|(Co1.4|Ru1.2|Pt0.6)x3|Pt2.4
 $7 \times 10^{11} \text{ A/m}^2$ pulses of 12 ns

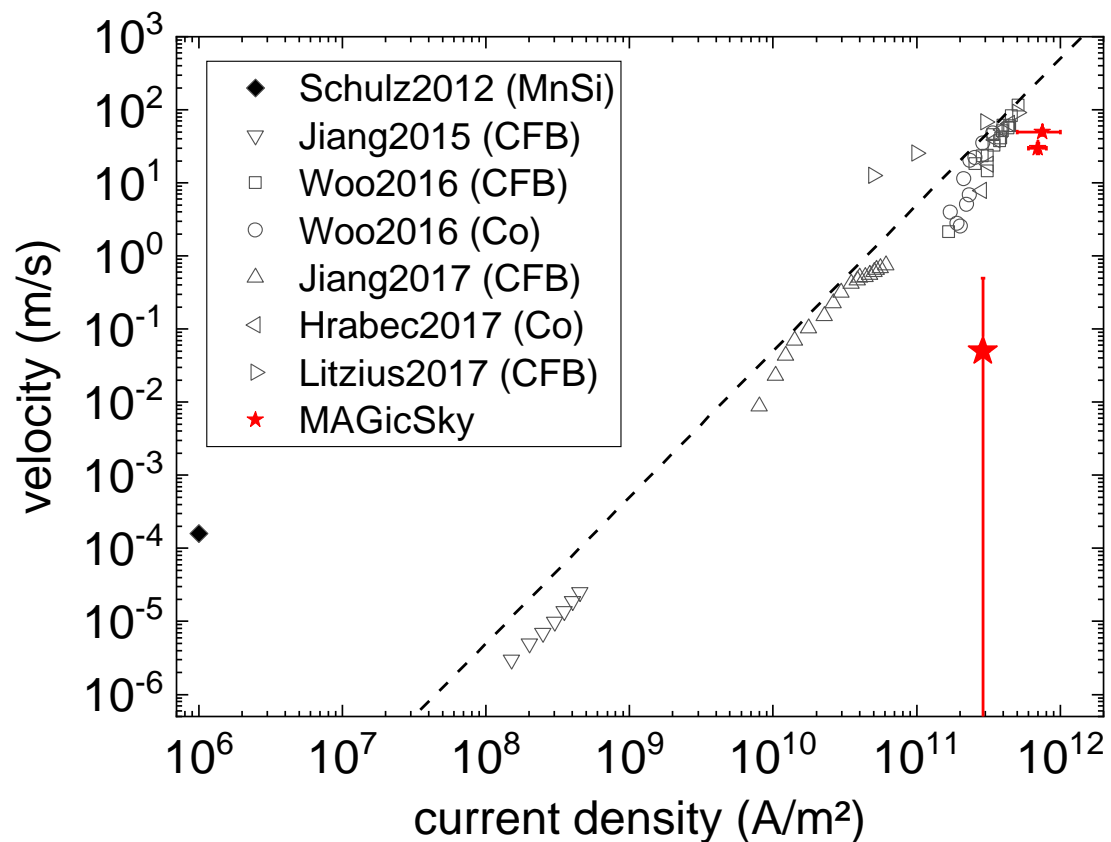
$v \approx 30\text{-}40 \text{ m/s}$



W. Legrand *et al*, *Nano Letters* **17**, 2703 (2017)

J.-V. Kim & M.-W. Yoo, *Appl. Phys. Lett.* **110**, 132404 (2017)

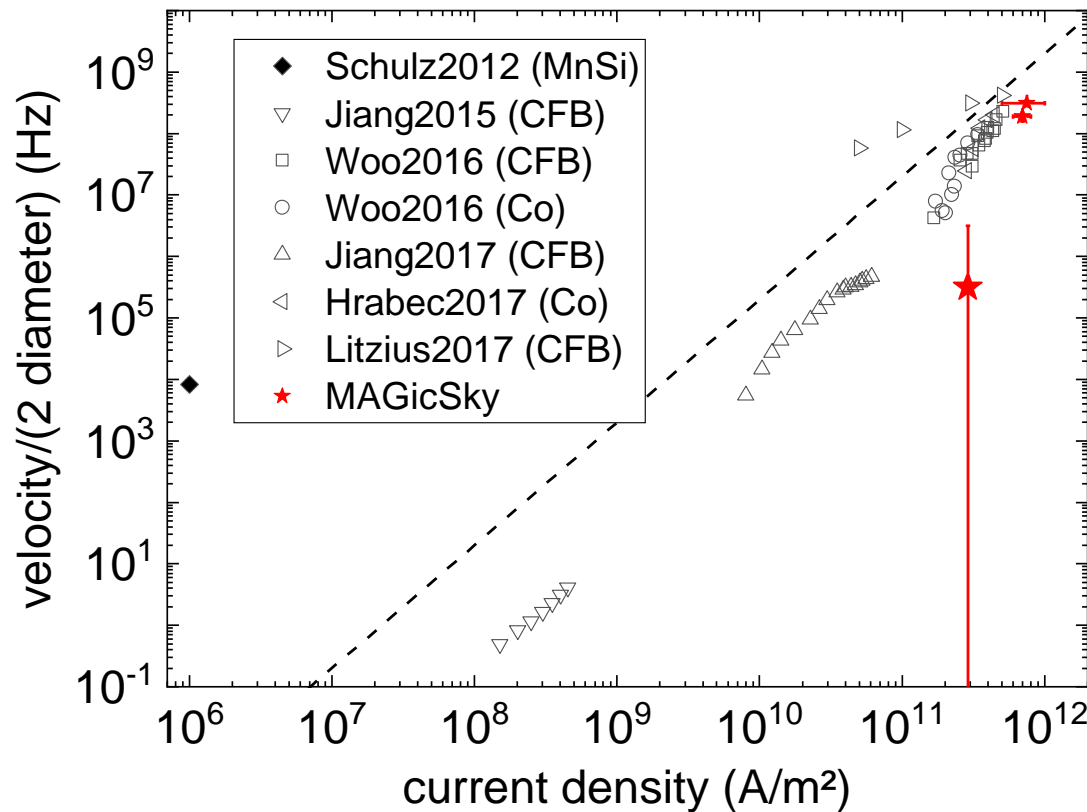
Velocity as a function of the current density in tracks



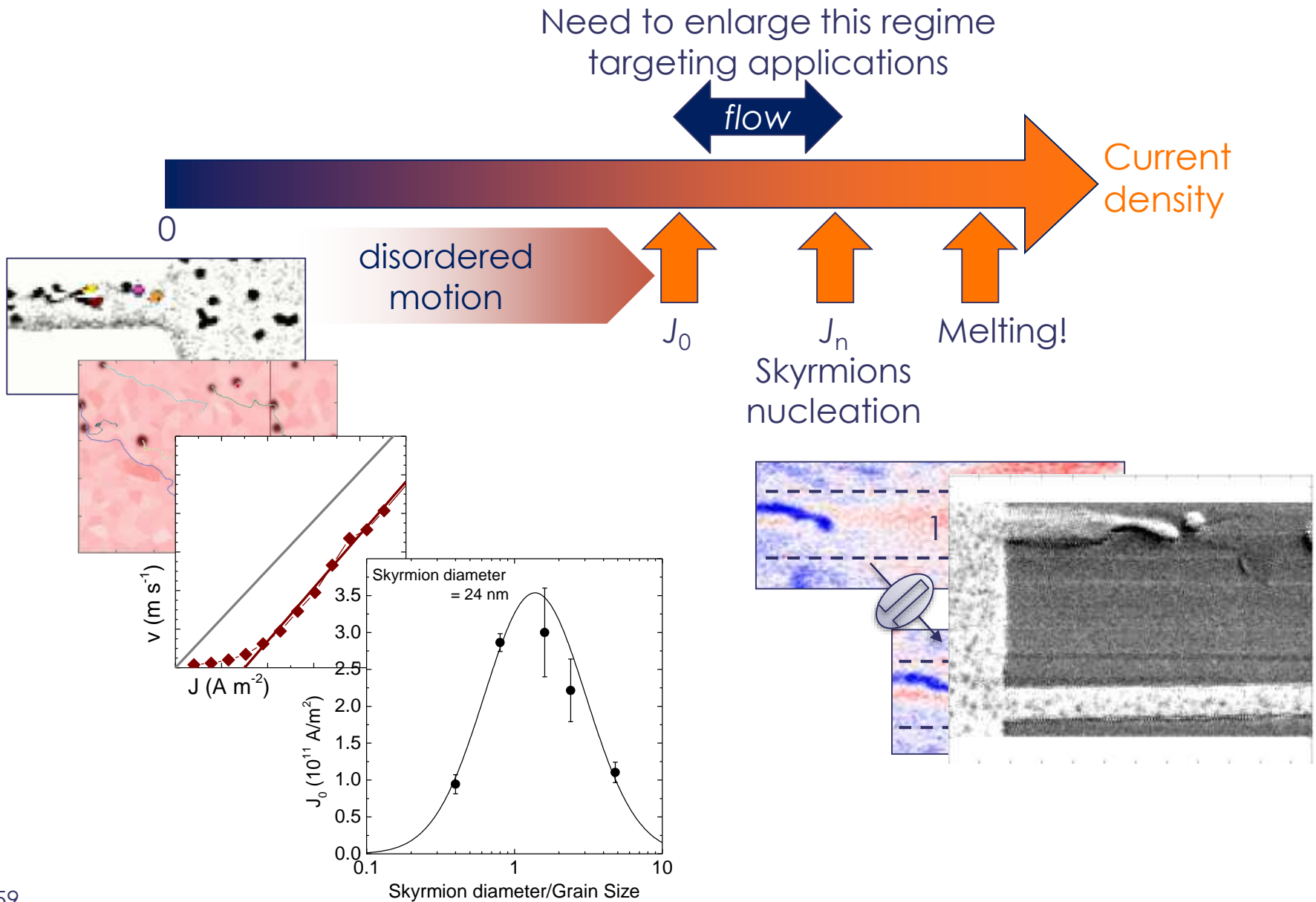
Skyrmion Velocity: State of the Art

Velocity/diameter as a function of the current density in tracks

- Proper figure of merit is the bit rate: how many skyrmions are read per unit of time

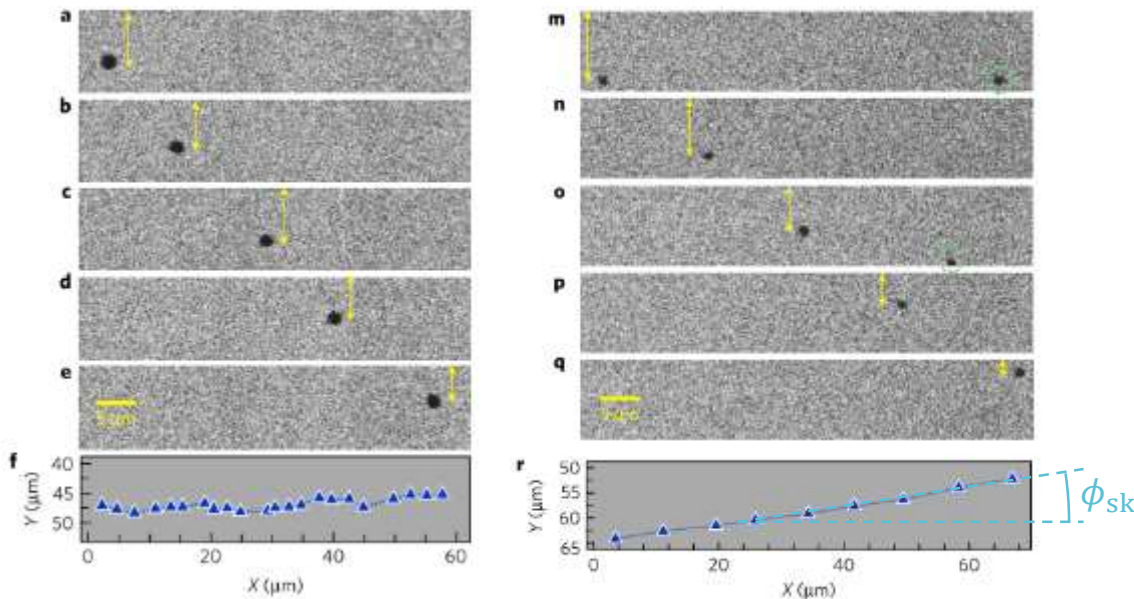


Summary of the Current-induced Phenomena



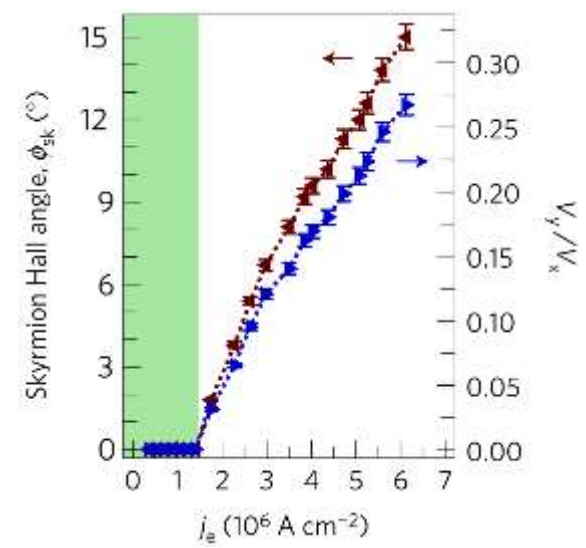
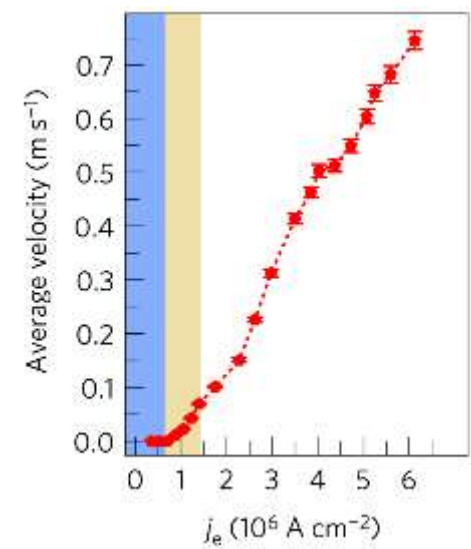
Observation of the Skyrmion Hall Effect

- Chiral Néel bubble in Ta(5)/Co₂₀Fe₆₀B₂₀(1.1)/TaO_x(3)
- Observed by optical Kerr microscopy



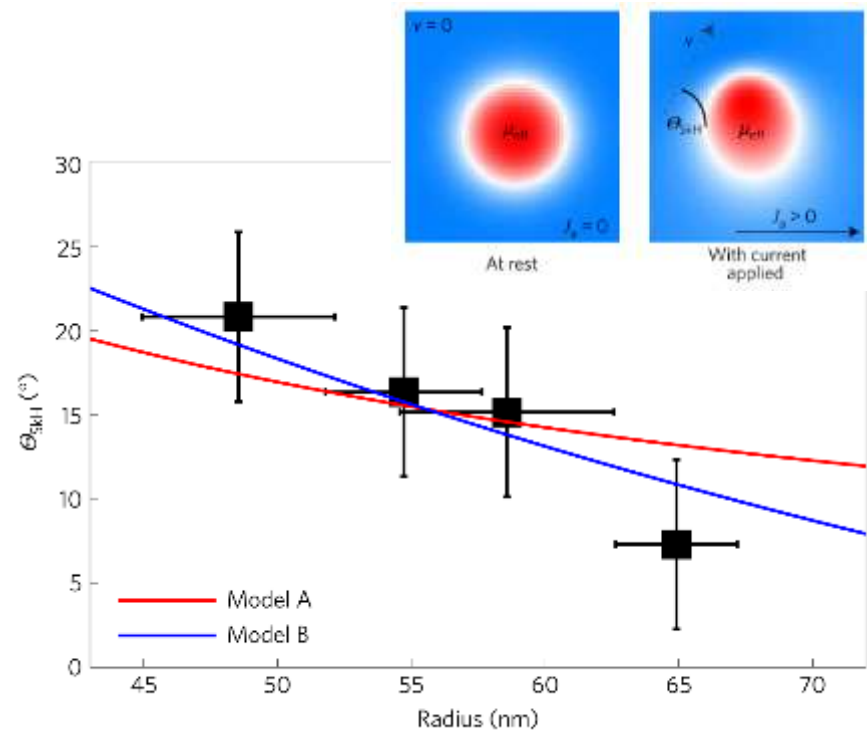
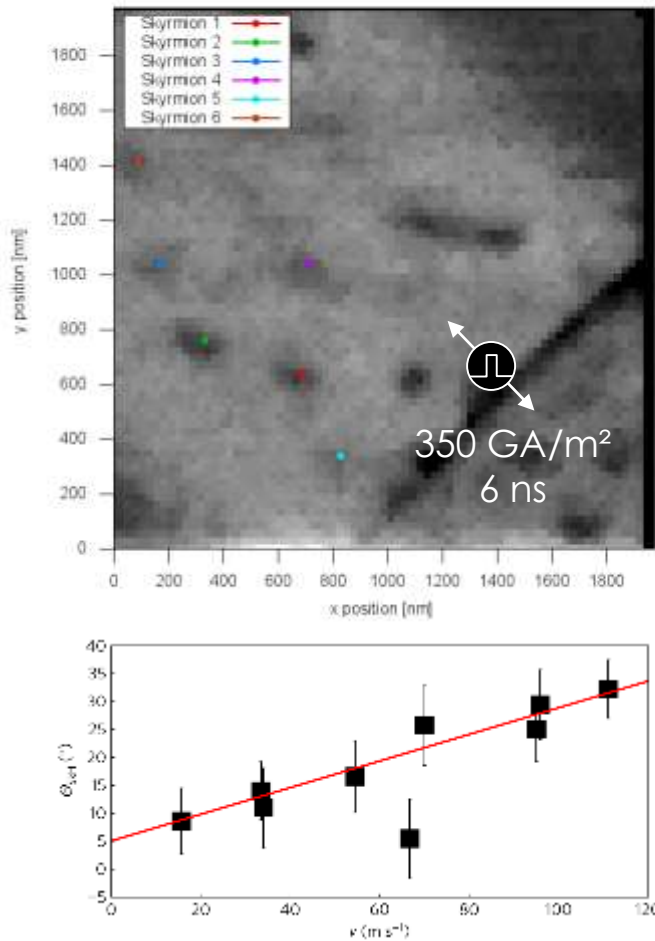

 13 GA/m²
 50 μs


 28 GA/m²
 50 μs



Observation of the Skyrmion Hall Effect

- Skyrmions in $[\text{Pt}(3.2)/\text{CoFeB}(0.7)/\text{MgO}(1.4)]_{15}$
- Observed by “pump-probed” STXM



Deformation of the skyrmion during its motion

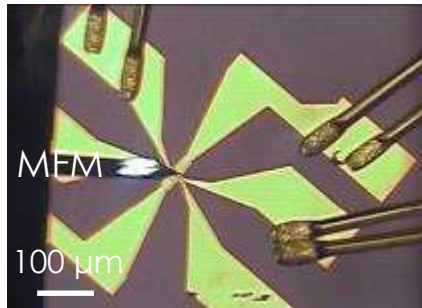
→ modify the dynamics.



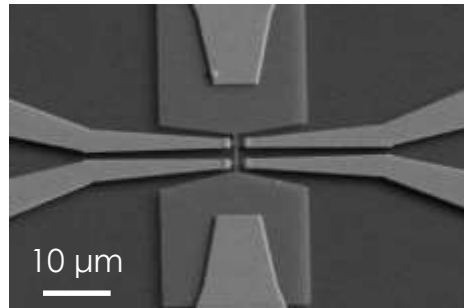
Combining MFM and Transport Measurements

Combined magnetic field and current pulses can be used to control skyrmion density in tracks, 200-nm to 1- μm wide:

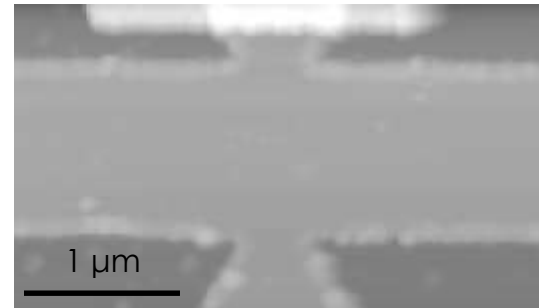
Optical



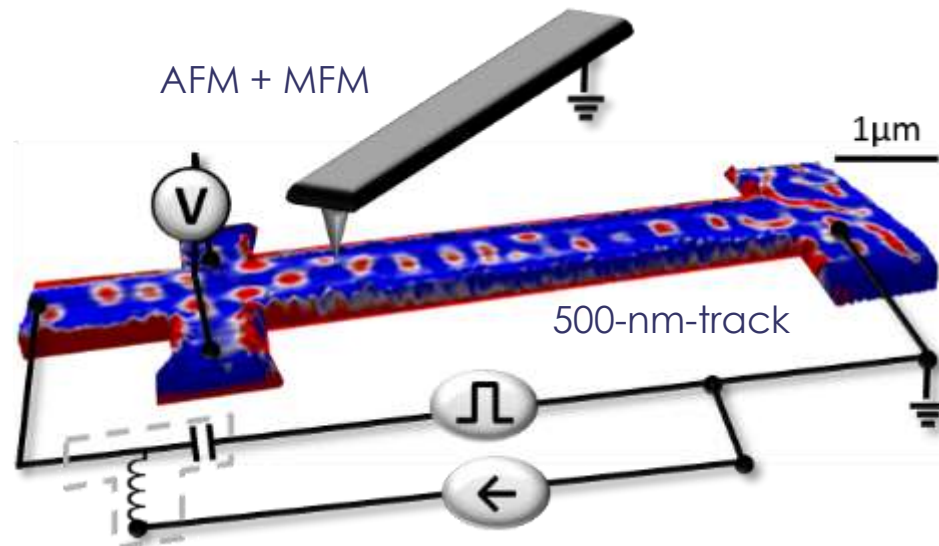
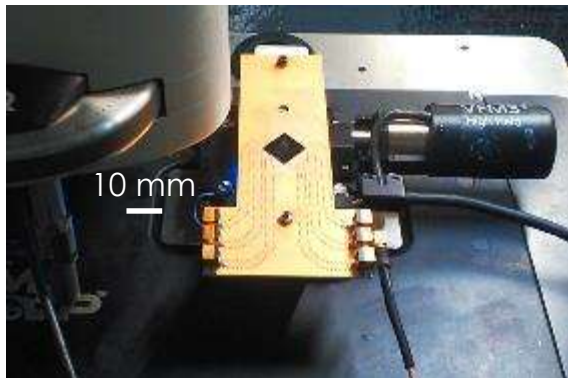
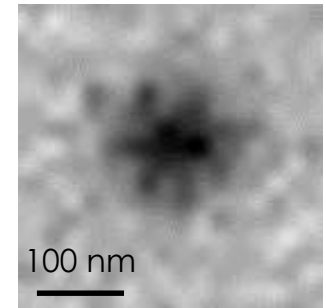
SEM



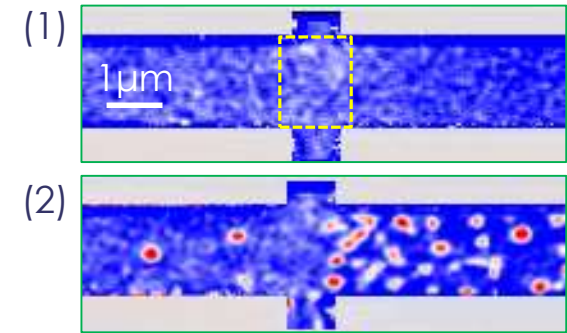
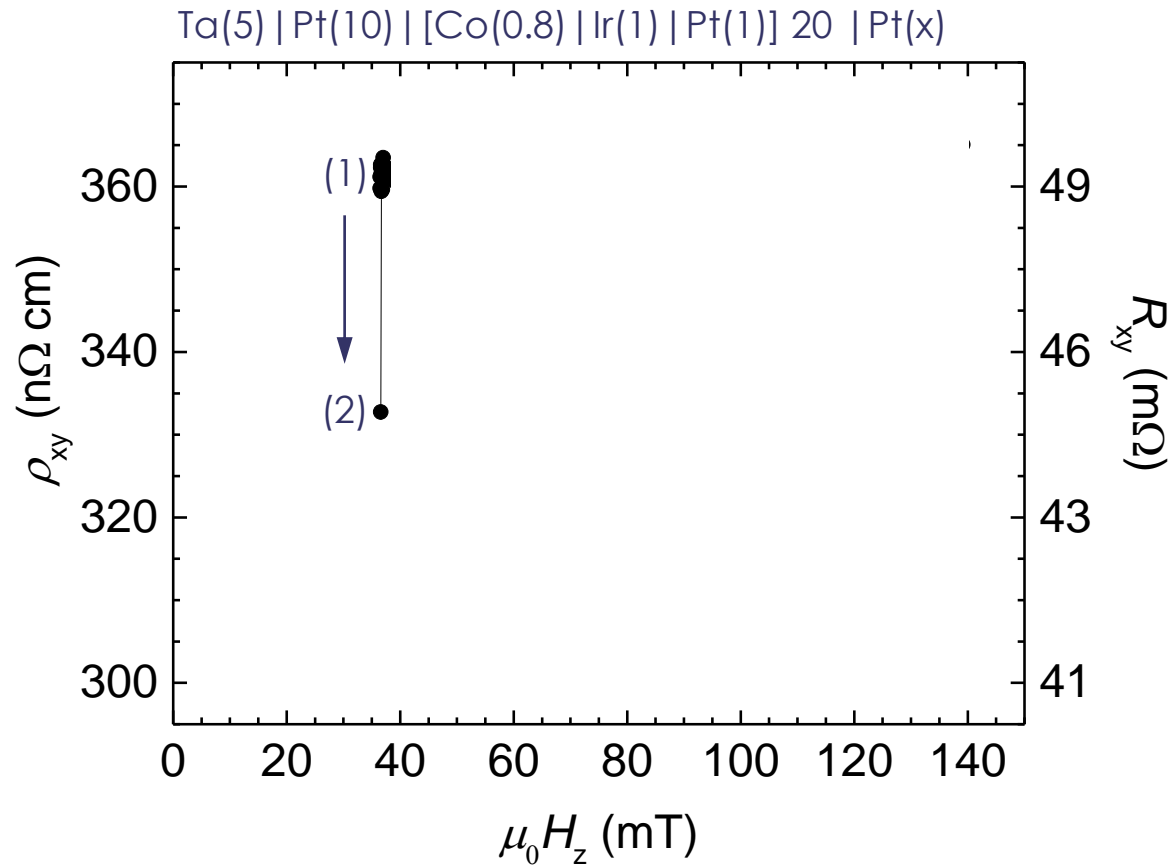
AFM



STXM



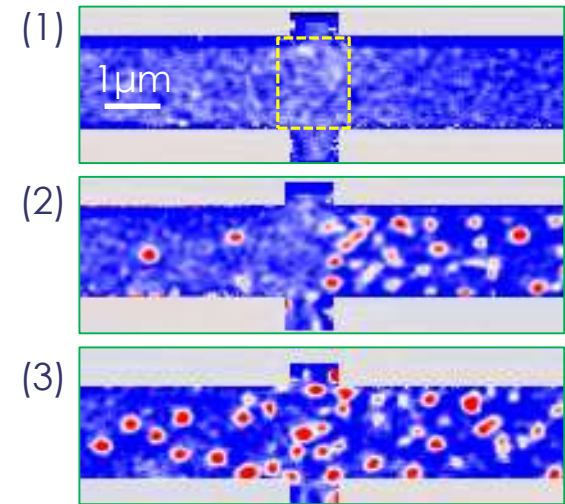
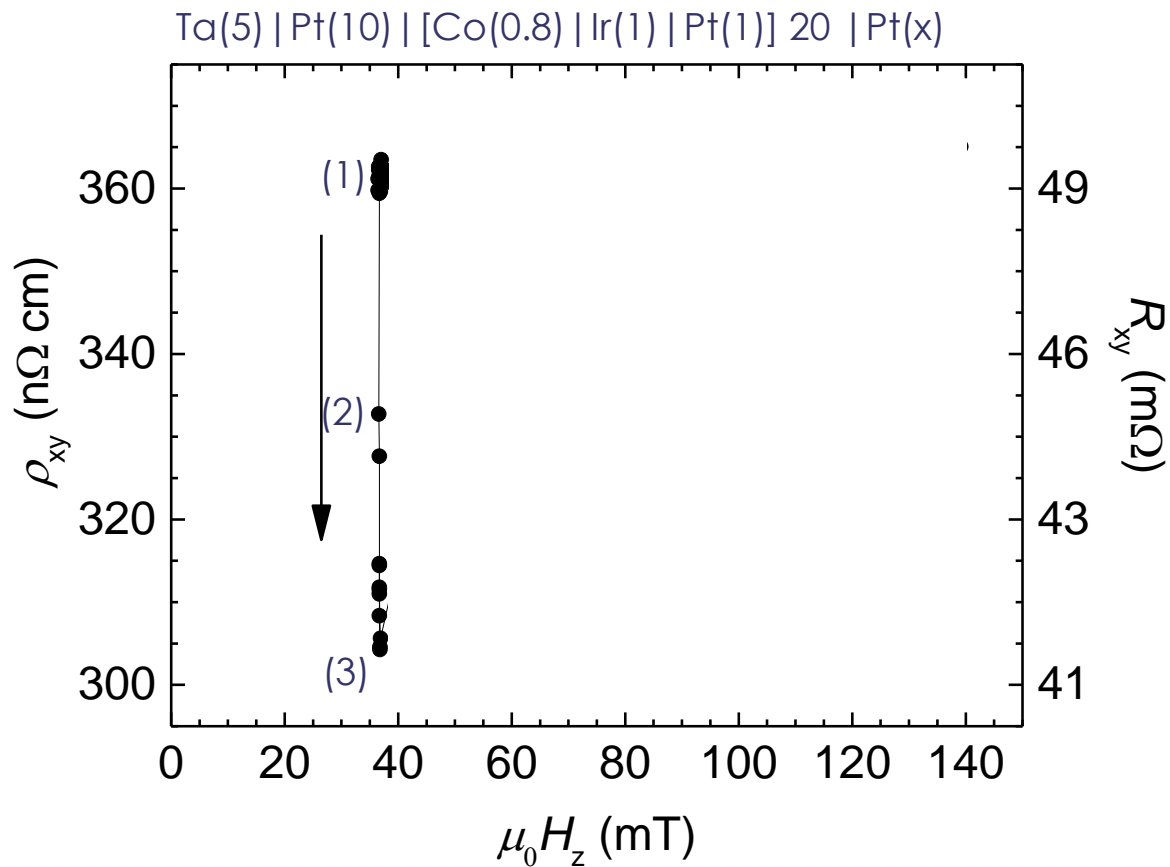
Electrical Signal from Skyrmions



Nucleation by current pulses

- 20 pulses 100-ns-long, $J = 2 \times 10^{11}$ A/m².

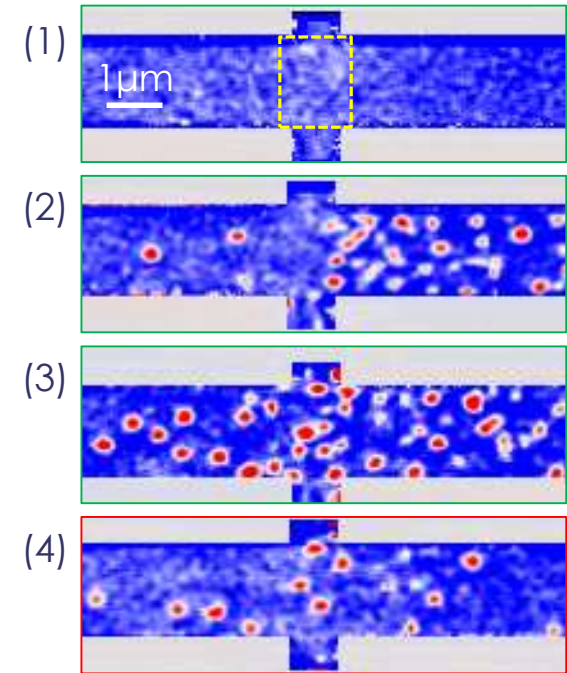
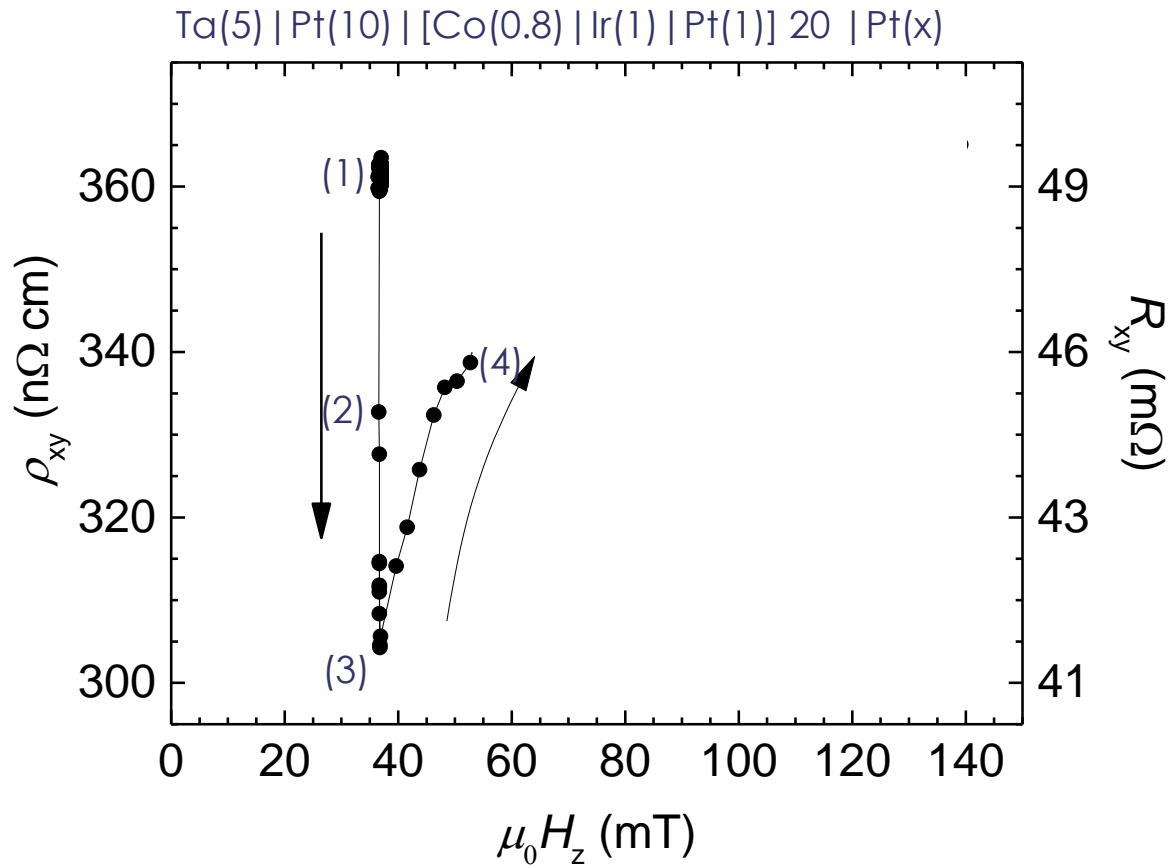
Electrical Signal from Skyrmions



Nucleation by current pulses

- 20 pulses 100-ns-long, $J = 2 \times 10^{11} \text{ A/m}^2$.
- Maximum density for given magnetic field.

Electrical Signal from Skyrmions



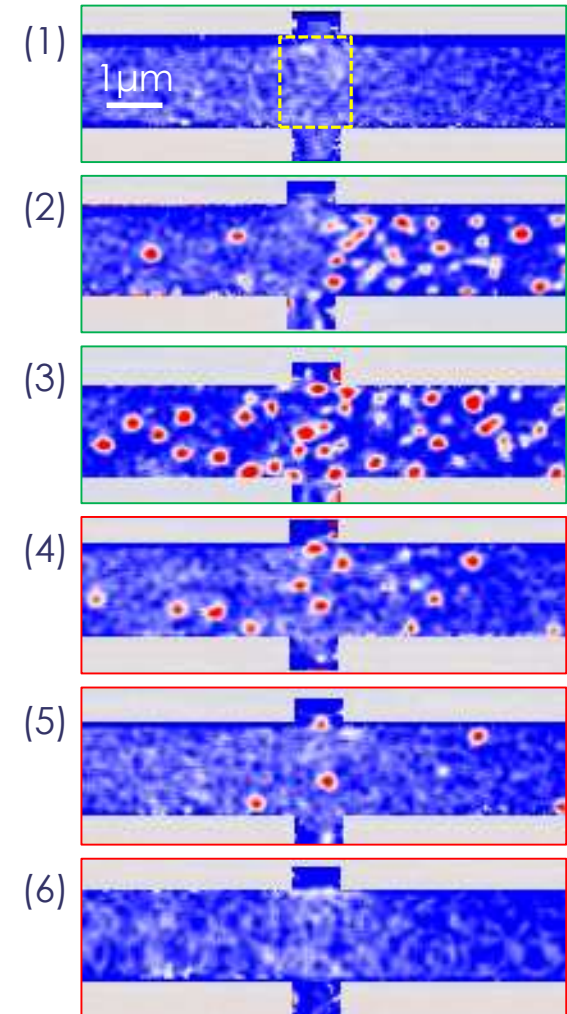
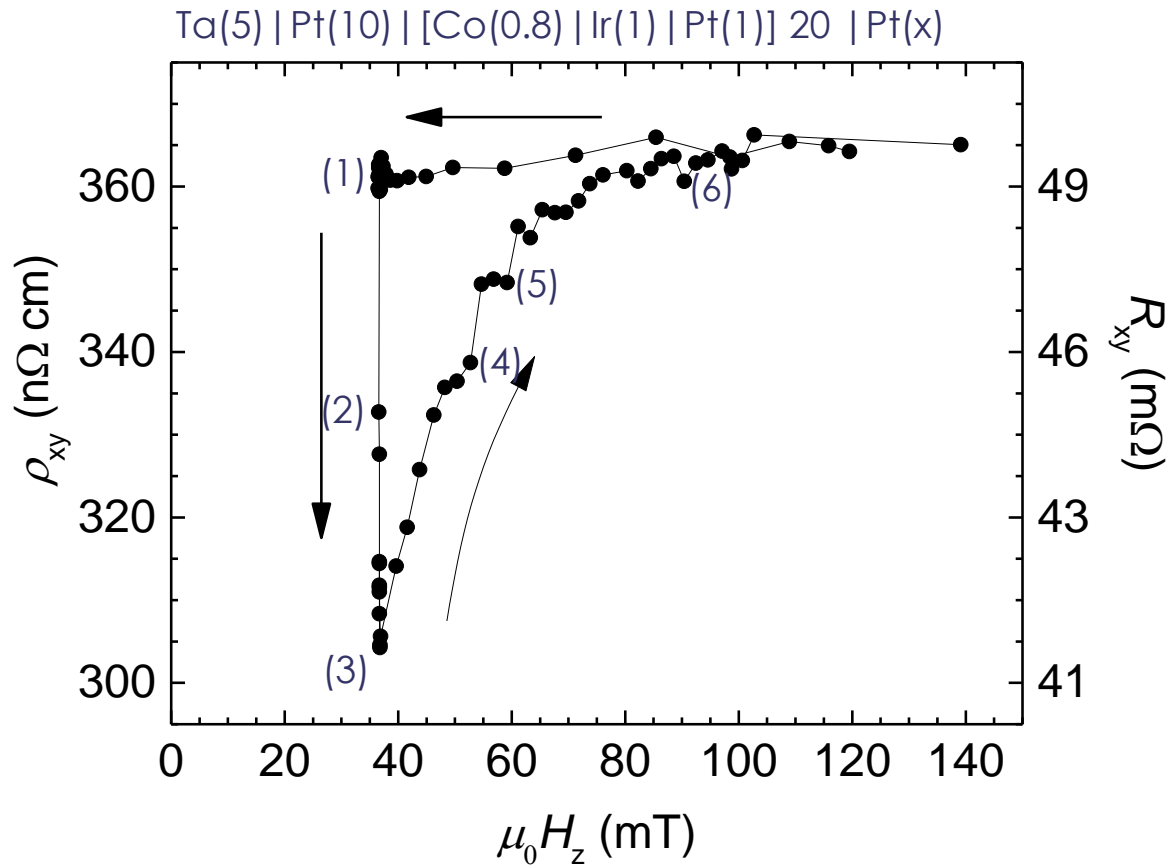
Nucleation by current pulses

- 20 pulses 100-ns-long, $J = 2 \times 10^{11}$ A/m². Maximum density for given magnetic field.

Annihilation with magnetic field and current pulses

- 20 pulses 100-ns-long, $J = 2 \times 10^{11}$ A/m², $\mu_0 H$ increasing...

Electrical Signal from Skyrmions



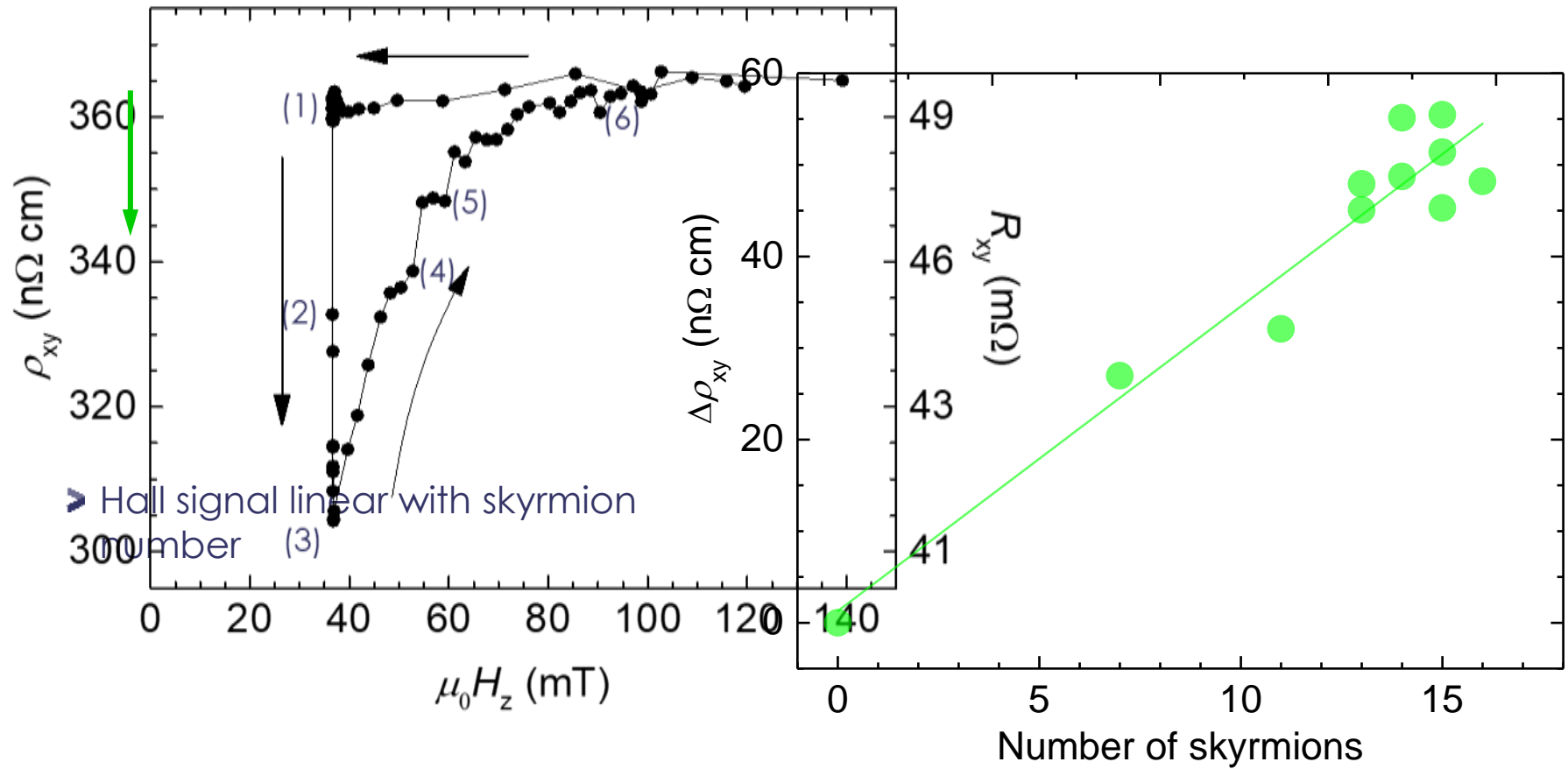
Nucleation by current pulses

- 20 pulses 100-ns-long, $J = 2 \times 10^{11} \text{ A/m}^2$.

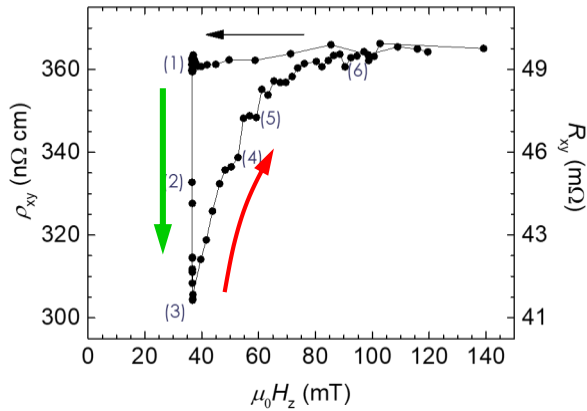
Annihilation with magnetic field and current pulses

- 20 pulses 100-ns-long, $J = 2 \times 10^{11} \text{ A/m}^2$, $\mu_0 H$ increasing...

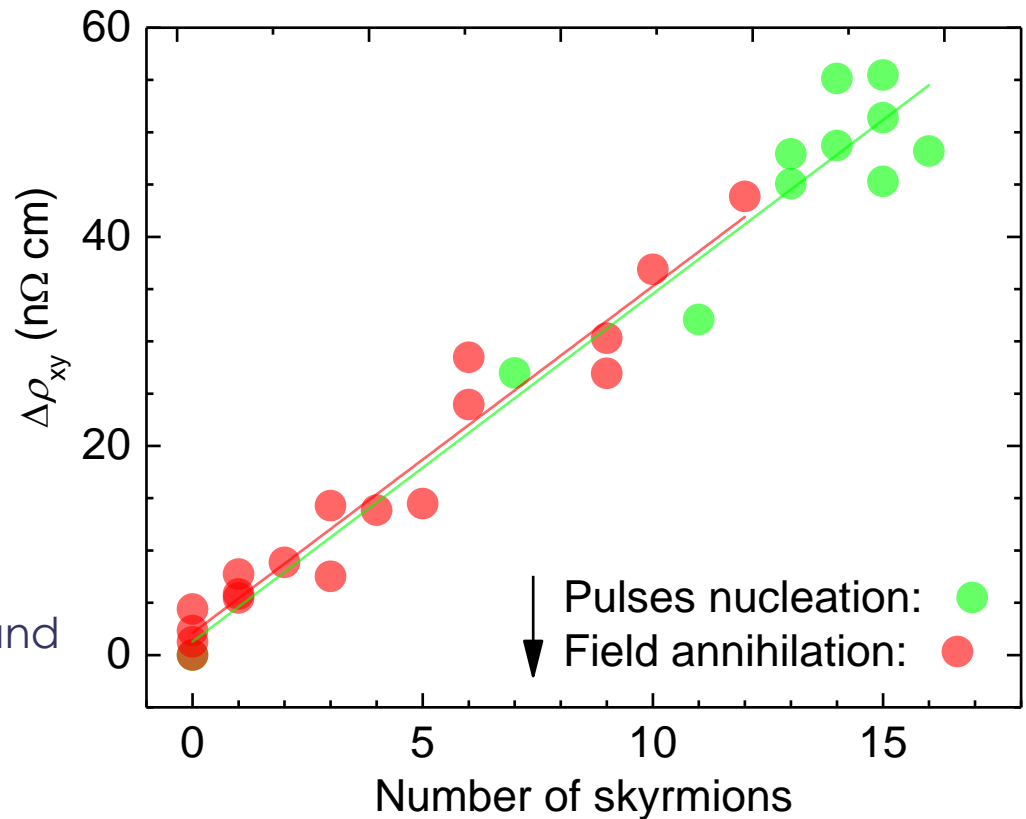
Electrical Signal from Skyrmions



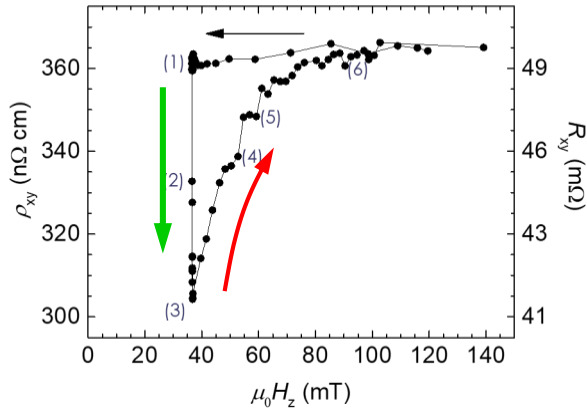
Electrical Signal from Skyrmions



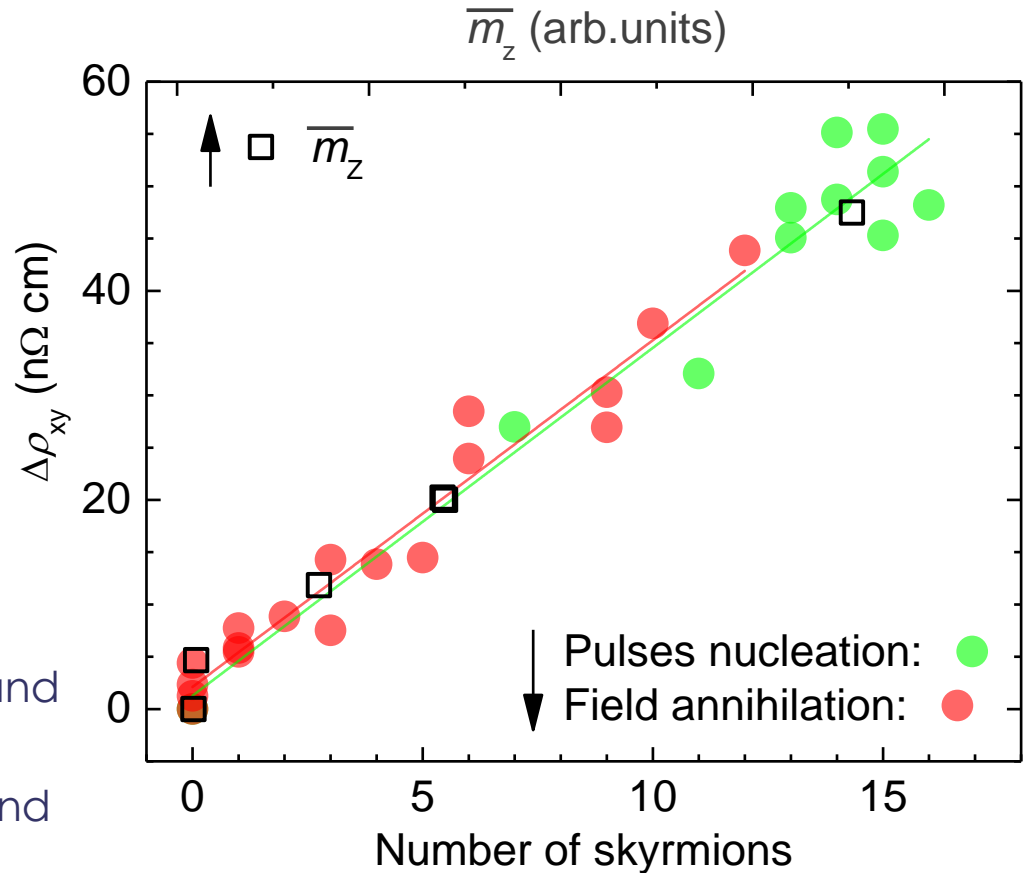
- Hall signal linear with skyrmion number
- Same behavior for nucleation and annihilation



Electrical Signal from Skyrmions



- Hall signal linear with skyrmion number
- Same behavior for nucleation and annihilation
- Correspondence of mean m_z and skyrmion number

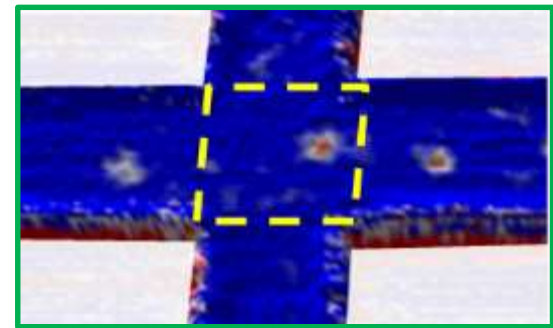
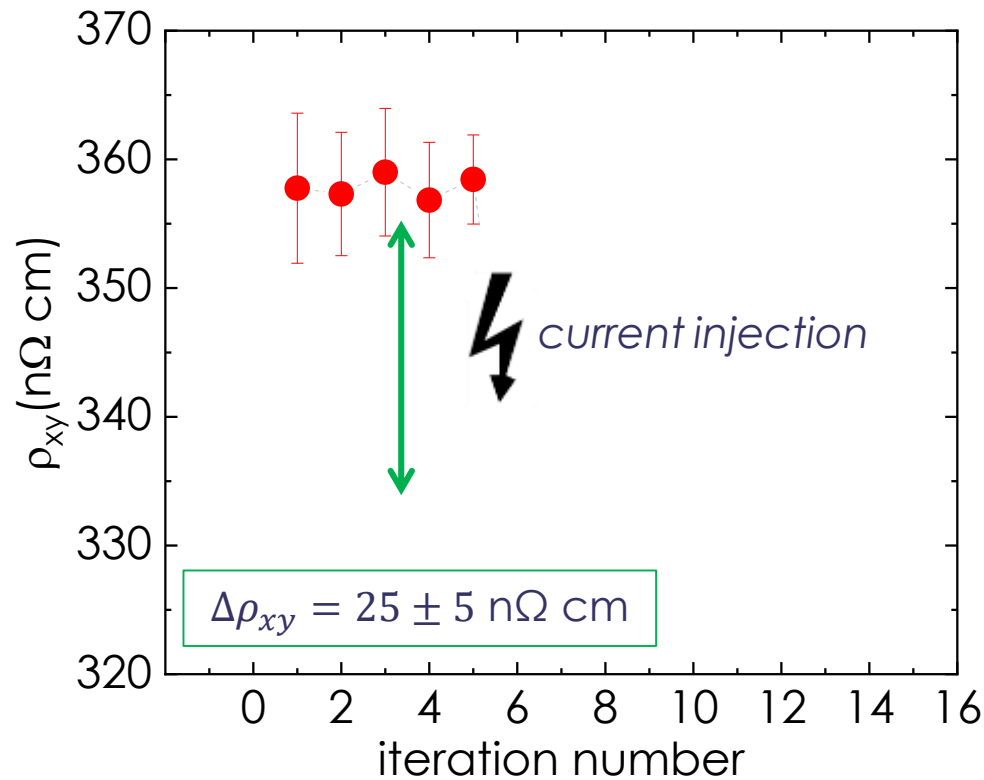


Experimental transverse resistivity of the single skyrmion: $\Delta\rho_{xy} = 3.5 \pm 0.5$ n Ω cm

Electrical Detection of a Single Skyrmion

The AHE signal increases as the track width decreases

- Signal is proportional to ratio “skyrmion area” over “track area”



What is the Origin of the Hall Signal?

Estimation of the anomalous Hall effect (AHE):

➤ Proportional to mean m_z (from STXM). For a single skyrmion, the change in ρ_{xy} is:

$$\overline{m_z} = \frac{1}{S} \int_S m_z ds \approx 0.5$$

$$\Delta\rho_{\text{AHE}} = \rho_{\text{AHE}} \frac{\overline{m_z} \pi d_{\text{sk}}^2}{a_{\text{cross}}} \approx \rho_{\text{AHE}} \frac{1}{2} \frac{a_{\text{sk}}}{a_{\text{cross}}} = 23 \pm 3 \text{ n}\Omega \text{ cm}$$

From STXM:
 $d_{\text{sk}} = 85 \pm 10 \text{ nm}$

What about the topological Hall effect (THE)?

➤ Most optimistic approach for THE is 1 flux quantum per skyrmion area:

$$\Delta\rho_{\text{THE}} = P\rho_{\text{OHE}} \frac{\Phi_0}{a_{\text{sk}}} \frac{a_{\text{sk}}}{a_{\text{cross}}} \leq \rho_{\text{OHE}} \frac{\Phi_0}{a_{\text{cross}}} \approx 1 \cdot 10^{-2} \text{ n}\Omega \text{ cm}$$

There are theories to address the non-adiabatic cases:

e.g. K. S. Denisov, I. V. Rozhansky *et al*, *Sci. Rep.* **7**, 17204 (2017)

AHE is enough to explain the experimental observation, THE is orders of magnitude weaker.

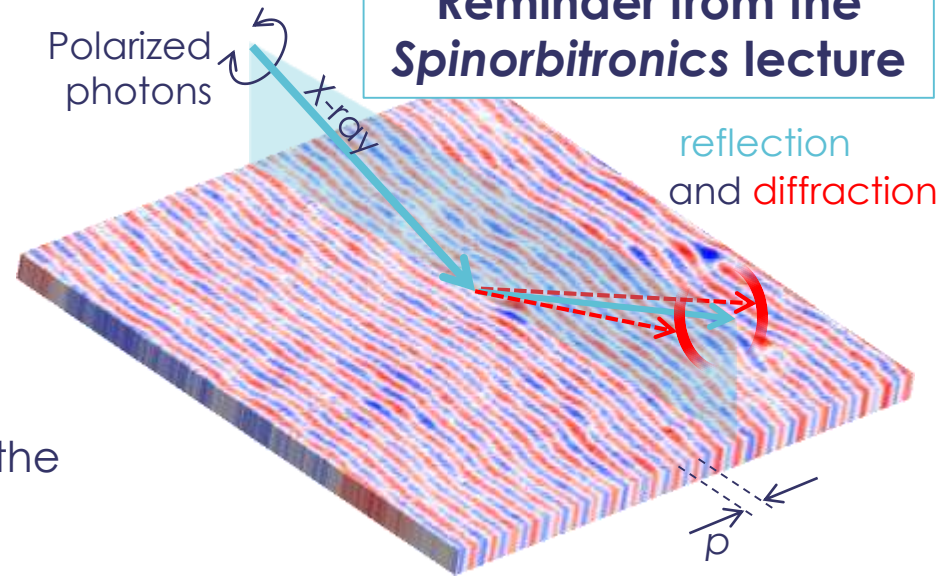
Experimental transverse resistivity of the single skyrmion is detected and corresponds to the expected AHE

X-ray Resonant Magnetic Scattering probes the Wall Structures

Reminder from the Spinorbitronics lecture

Synchrotron technique: probe magnetism using photons at the Co L_3 -edge energy

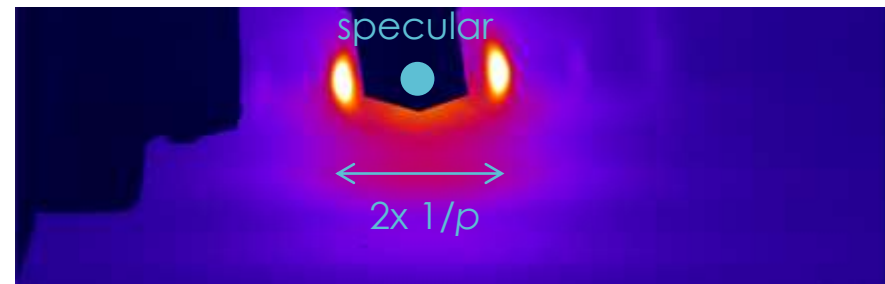
- 2D detector on SEXTANTS beamline at Synchrotron SOLEIL: get real-space periodicity of the domains
- Circular dichroism: get the chirality of the structure



$(CL-CR)/(CL+CR)$



CCD signal (CL+CR)



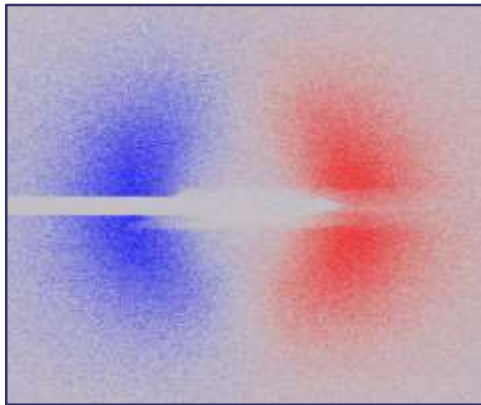
Strong circular dichroism of the XRMS diffraction peaks in our multilayers

Definite Determination of the Chirality of the Multilayers

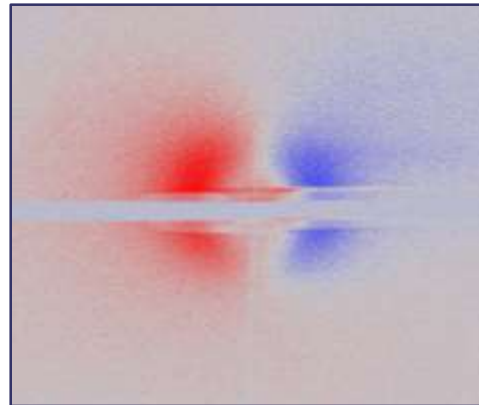
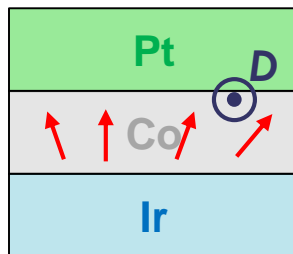
Reminder from the
Spinorbitronics lecture

Inversion of the multilayer stack

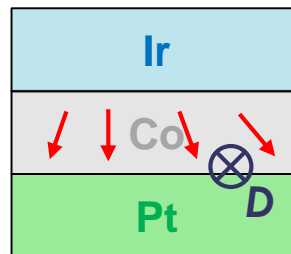
- Pure Néel walls in both case
- Inverted chirality: CCW for Co on top of Pt, CW for Pt on top of Co



$[\text{Ir}(1) | \text{Co}(0.8) | \text{Pt}(1)]_{\times 5}$



$[\text{Pt}(1) | \text{Co}(0.8) | \text{Ir}(1)]_{\times 5}$



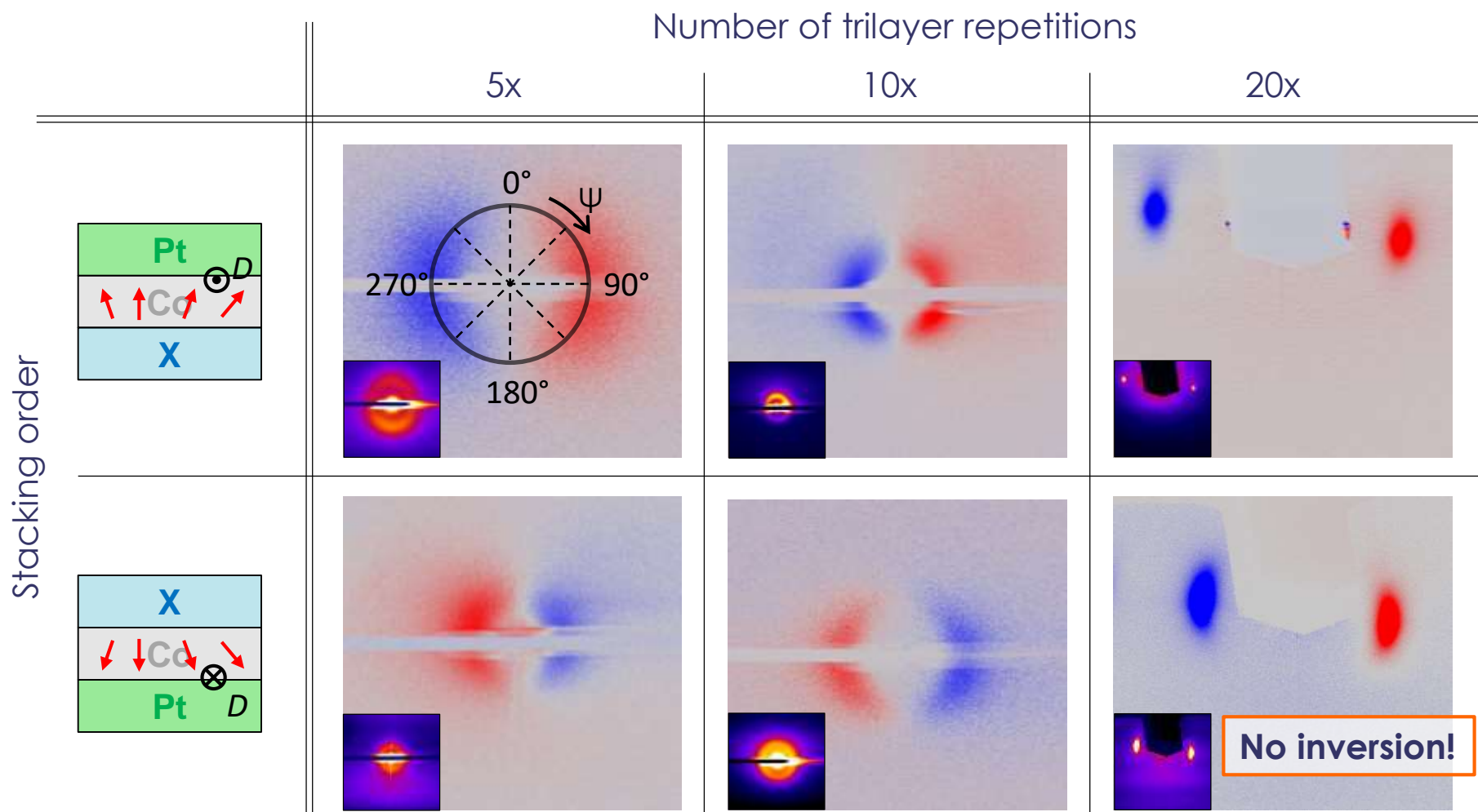
**Just looking at a couple of
XRMS images without
analysis directly reveals the
domain structure!**

- Fast (10 minutes)
- No need to pattern
- No parameter to know
- Probe under a capping layers
- Sensitive to few nm of magnetic materials
- No effect on magnetization
- Possibility to apply field
- Possibility to probe insulating sample (BiFeO_3)
- ...

So, we understood everything?

Reminder from the Spinorbitronics lecture

Something happens at large repetition number...



W. Legrand *et al*, *Science Adv.* **4**, eaat0415 (2018)

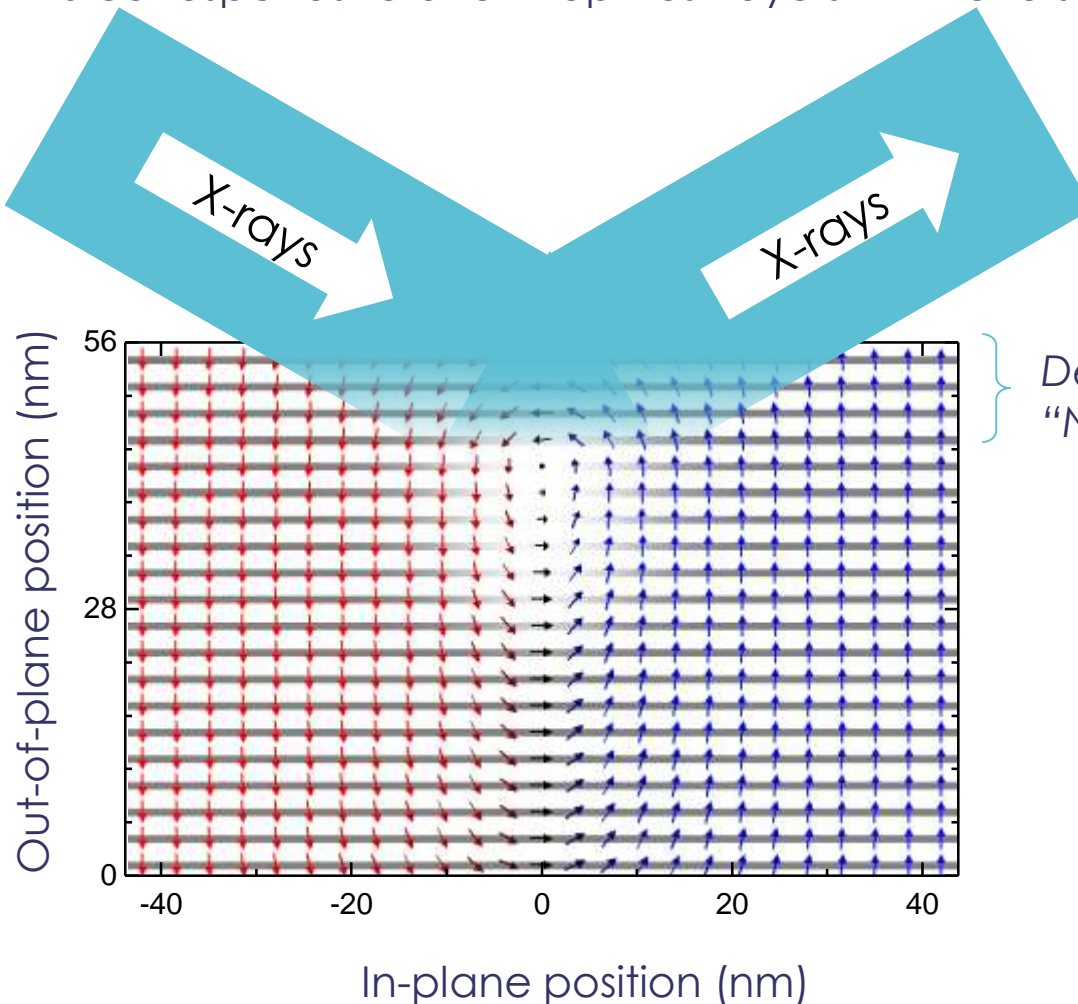
Recently reproduced in W. Li *et al*, *Adv. Mater.* **31**, 1807683 (2019)

Explanation of the XRMS

Resonant X-rays at Co L₃ edge penetrate only the first nm

➤ XRMS corresponds to a few topmost layers with reversed chirality.

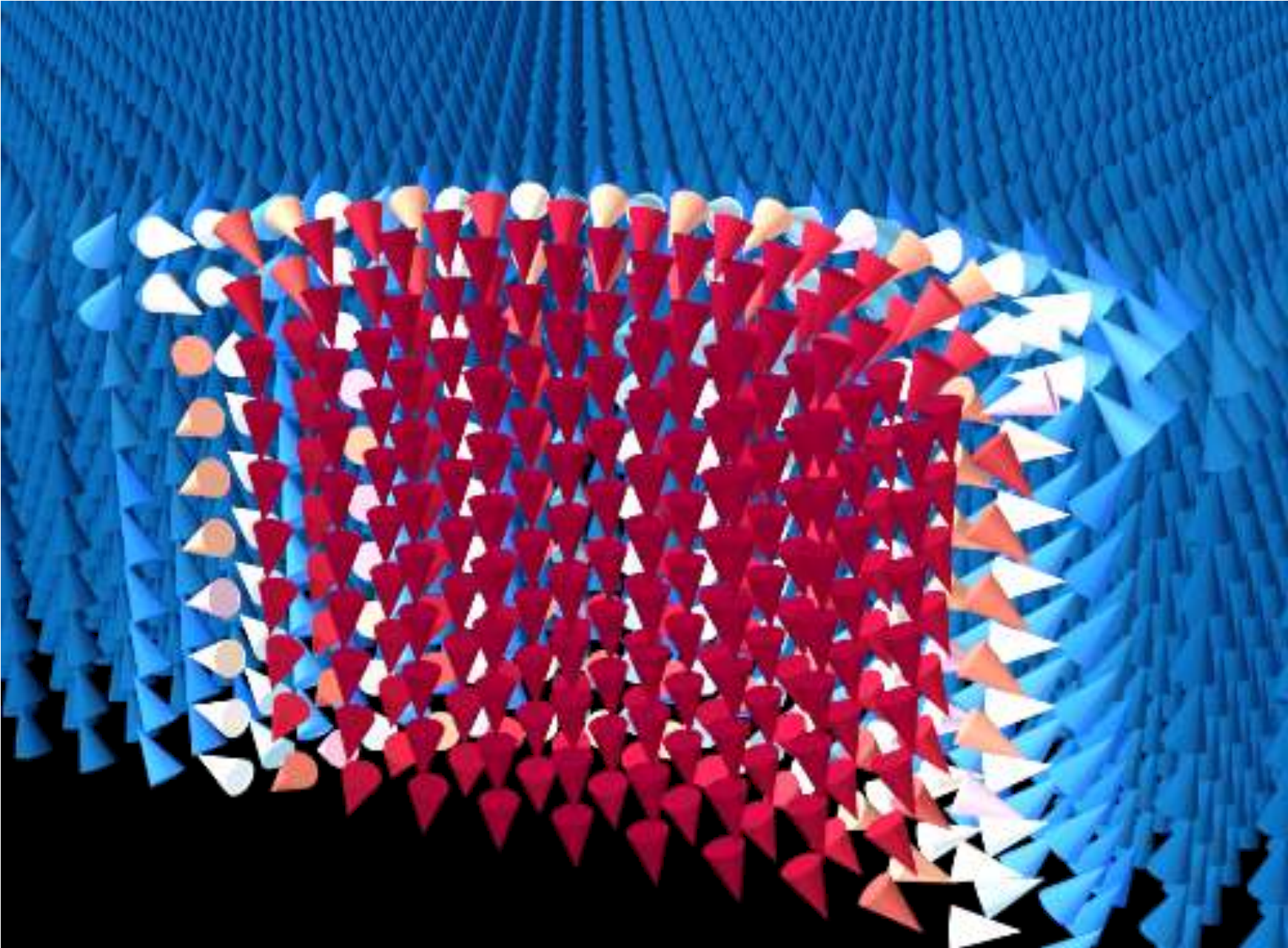
$$\begin{aligned}M_s &= 1370 \text{ kA/m} \\K_u &= 1430 \text{ kJ/m}^3 \\A &= 10 \text{ pJ/m} \\D &= 1.0 \text{ mJ/m}^2\end{aligned}$$



} Detection of the "Néel cap" only.

Domain wall texture (including chirality) changes through the different Co layers.

Skyrmions with hybrid chirality

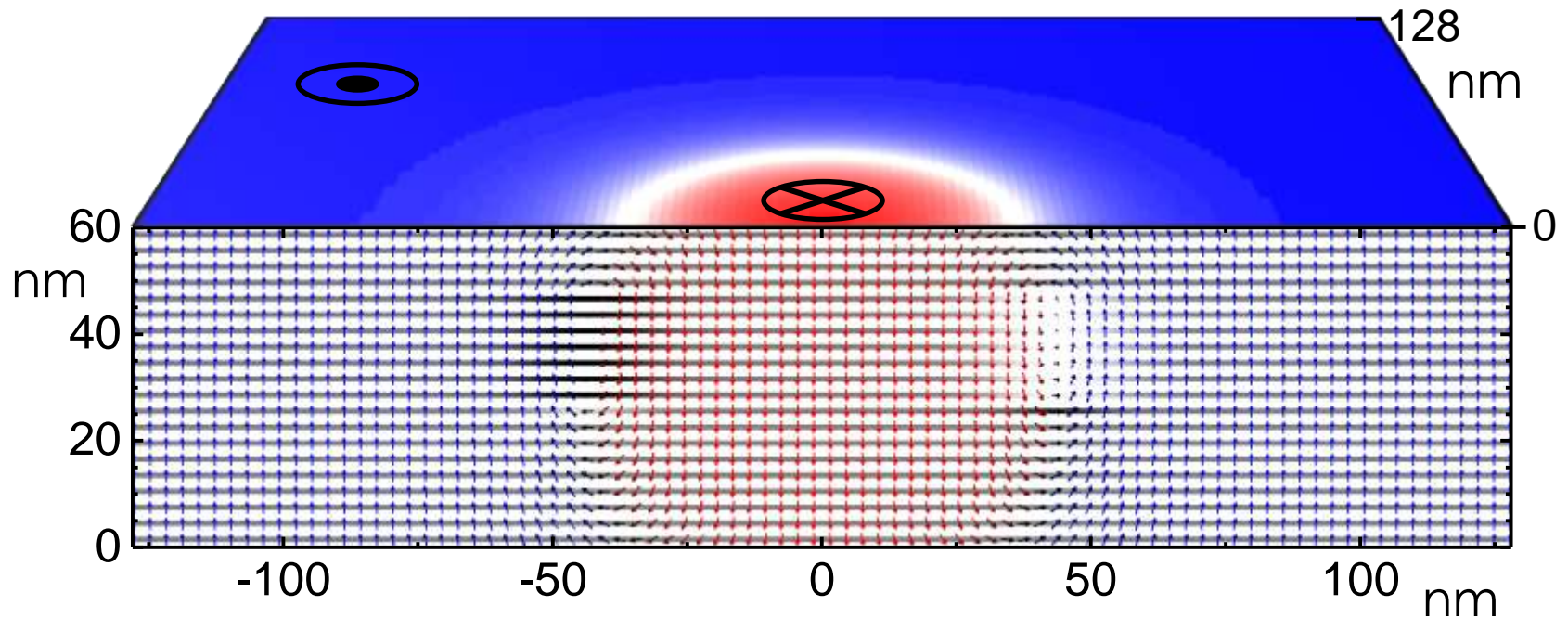


Consequences for Skyrmion Motion and SOT Engineering

Chirality depends on position in the stack

- Inverted chirality at the top and the bottom
- SOT must be adapted for more efficient motion

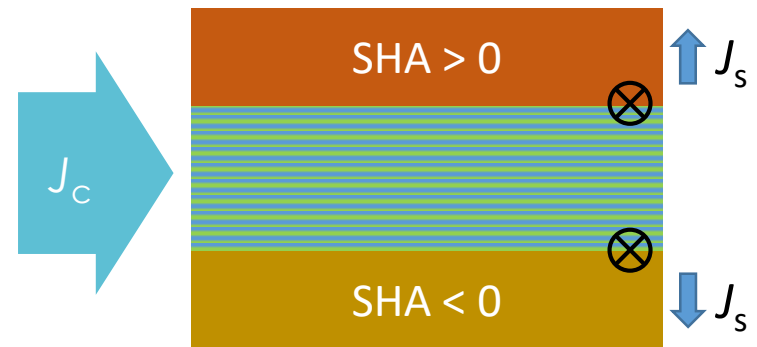
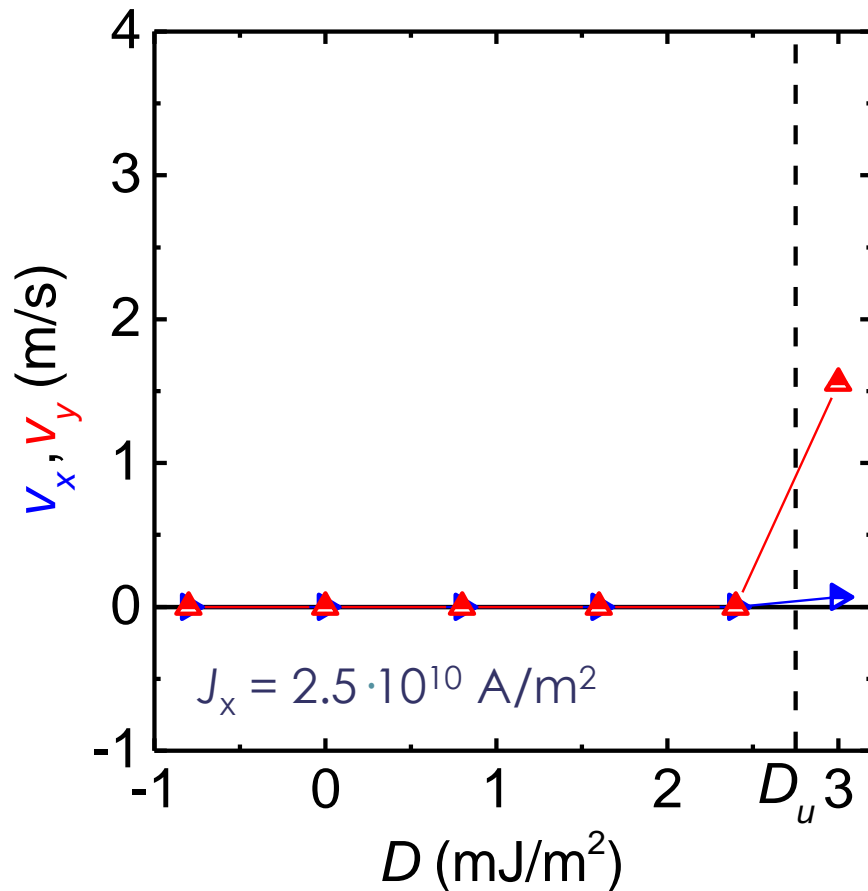
$$\begin{aligned}M_s &= 1306 \text{ kA/m} \\K_U &= 1230 \text{ kJ/m}^3 \\A &= 10 \text{ pJ/m} \\D &= 0.8 \text{ mJ/m}^2\end{aligned}$$



Torques from Buffer and Capping Layers

Opposite chirality for bottommost and topmost layer up to D_u

- Heavy metal layers with opposite spin Hall angles will result in opposite torques due to opposite chiralities

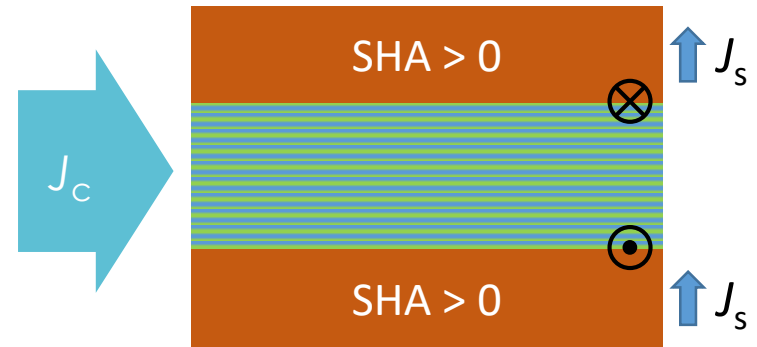
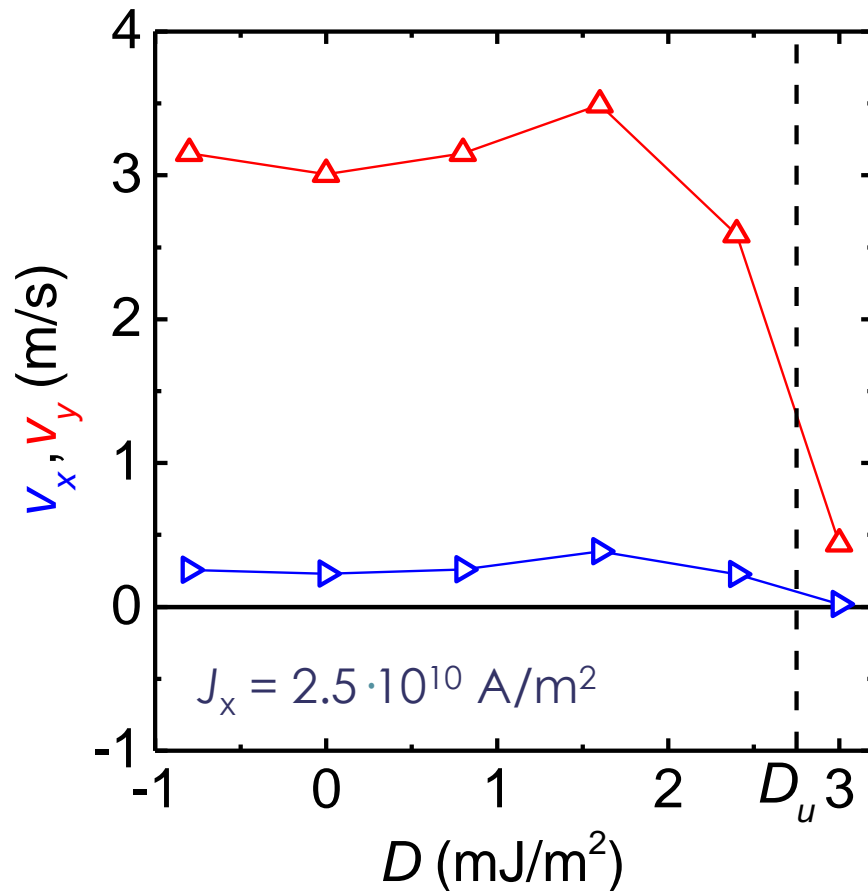


| Pt 8 | (Co 1 | Z 1 | X 1)_{x20} | Ta 10

Torques from Buffer and Capping Layers

Opposite chirality for bottommost and topmost layer up to D_u

- Heavy metal layers with identical spin Hall angles will result in additive torques due to opposite chiralities

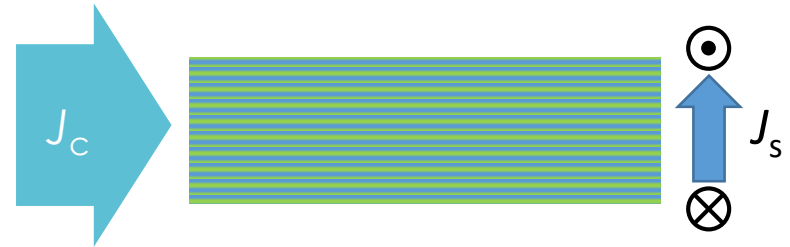
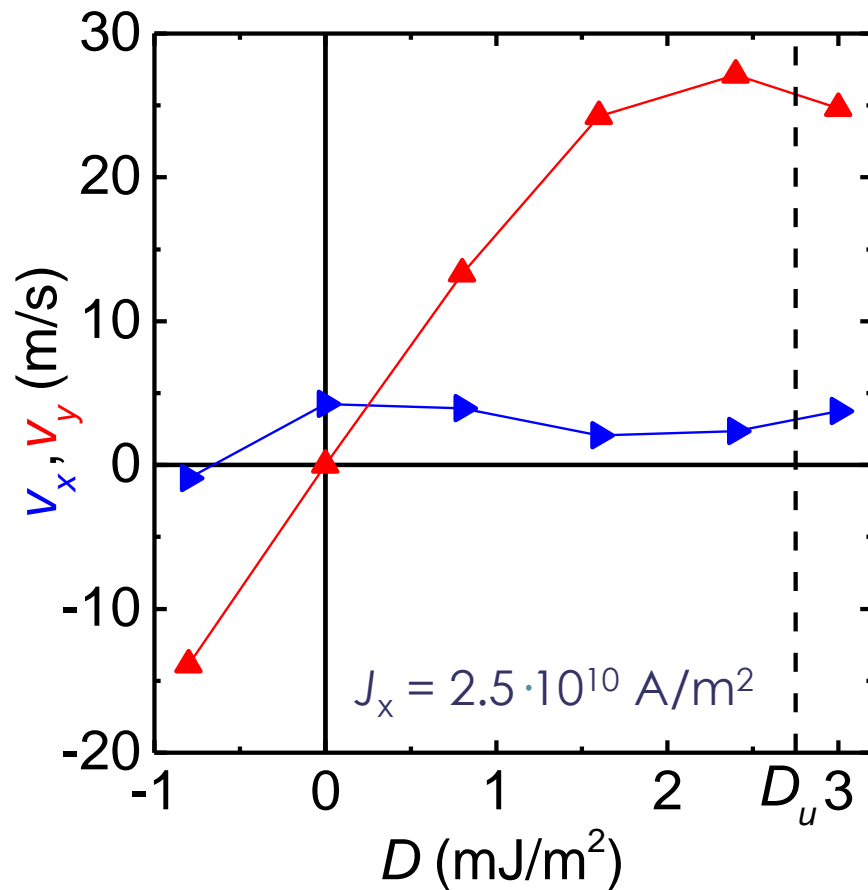


| Pt 8 | (Co 1 | Z 1 | X 1)_{x20} | Pt 8

Torques through All Layers

Opposite chirality for bottommost and topmost layer up to D_u

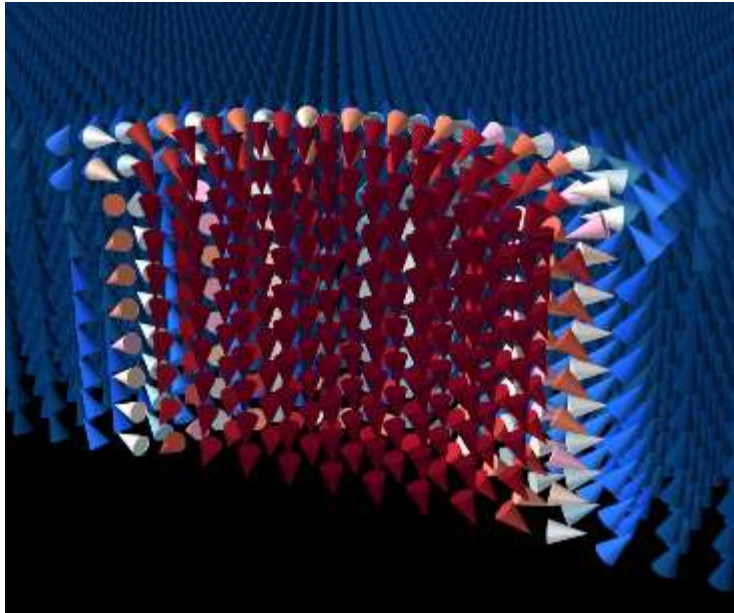
➤ Velocity determined by the ratio of the DW chiralities





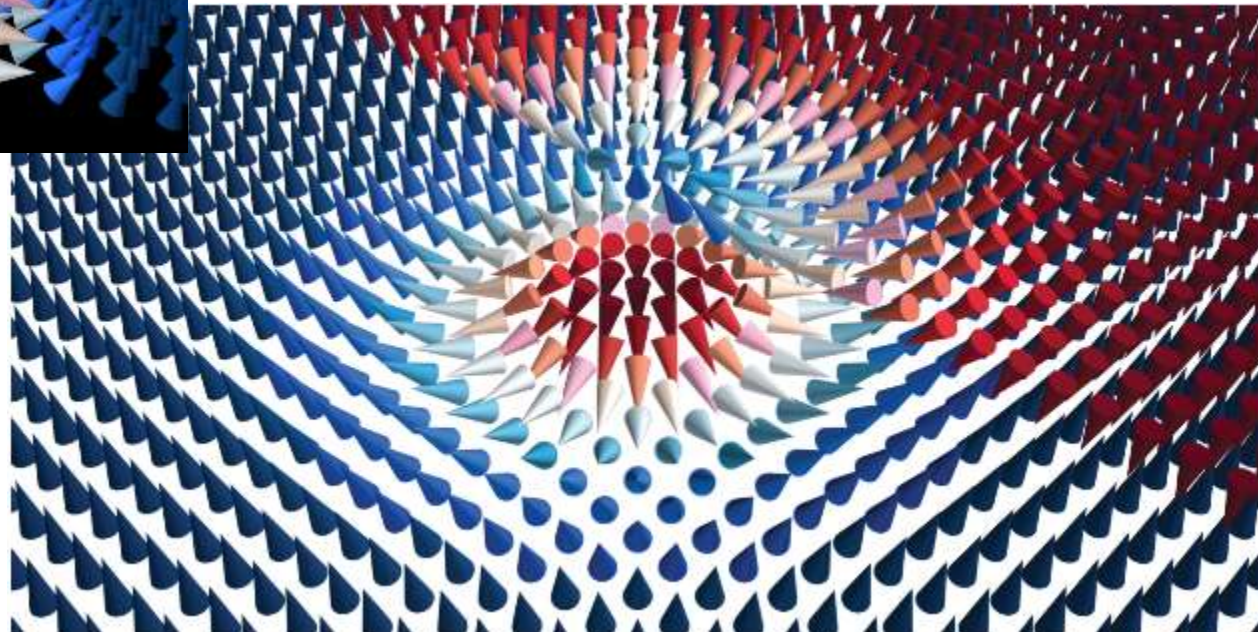
Conclusion

Increased complexity brings new “advantages” – still a lot to discover!



- C. Moreau-Luchaire, *Nature Nanotechnol.* **11**, 444 (2016)
W. Legrand *et al*, *Nano Lett.* **17**, 2703 (2017)
A. Fert *et al*, *Nature Review Materials* **2**, 17031 (2017)
D. Maccariello *et al*, *Nature Nanotechnol.* **13**, 233 (2018)
J.-Y. Chauleau *et al*, *Phys. Rev. Lett.* **120**, 037202 (2018)
S. McVitie *et al*, *Sci. Rep.* **8**, 5703 (2018)
W. Legrand *et al*, *Science Adv.* **4**, eaat0415 (2018)
W. Legrand *et al*, *Phys. Rev. Appl.* **10**, 064042 (2018)
K. Fallon *et al*, arXiv:1901.03652

... to be continued!



Thank you
for your
attention!